ANL-HEP-TR--91-05

DE91 012339

Argonne National Laboratory
9700 South Cass Avenue
Argonne, IL 60439

HIGH ENERGY PHYSICS DIVISION
SEMIANNUAL REPORT OF RESEARCH ACTIVITIES

July 1, 1990 - December 31, 1990

Prepared from information gathered
and edited by the Committee for
Publications and Information:

Members: E. Berger, Chairman
P. Moonier
E. May
J. Norem

February 1991

Table of Contents

High Energy Physics Division Semiannual Report of Research Activities
July 1, 1990 - December 31, 1990

ABSTRACT

A report is presented of research and development activities conducted in the High Energy Physics Division at Argonne National Laboratory during the six month period July 1 through December 31, 1990. Analyses of data from experiments performed by members of the Division are summarized, and the status of experiments taking data and of those being prepared is reviewed. Descriptions are included of research on theoretical and phenomenological topics in particle physics. Progress reports are provided on accelerator research and development, detector research and development, and experimental facilities research. Lists are presented of publications, of colloquia and conference talks, and of significant external community activities of members of the Division.

I. EXPERIMENTAL PROGRAM

A. Physics Results

1. Collider Detector at Fermilab

Analysis work has continued on the 1988-89 CDF data sample, and papers on a) the W mass, b) W and Z cross sections and production properties, c) electroweak asymmetries, d) inclusive QCD jet production, e) prompt photon production, and f) b-quark production, are completed or in various stages of preparation. Here we summarize recent results on W and Z production cross sections and on b-physics.

The cross section ratio, $\sigma(W)/\sigma(Z)$, is relatively insensitive to many (common) systematic errors, and the measured ratio, based on the inclusive electron sample, was used by CDF to establish the ratio of widths for the W and Z gauge bosons. In the more recent analyses, the inclusive electron sample was used to measure the absolute cross sections for W and Z production, and the transverse momentum (p_T) dependence of these cross sections. The main systematic uncertainty on these cross sections comes from the luminosity uncertainty. The latter has been reduced from the original estimate of ± 15% down to ± 6.8%, using an interlocked set of measurements on the nondiffractive total cross sections at UA4 (546 GeV) and at CDF (546 and 1800 GeV), combined with measurements of the beam bunch profiles and intensities at the Tevatron. The resulting W and Z production cross sections are plotted in Fig. 1, together with corresponding results from the recent UA2 run at the CERN collider and with theoretical predictions. To summarize the results, we obtain the following numbers:

$\sigma(W \to e\nu)$	$= 2.19 \pm 0.04$ (stat)	± 0.21 (sys)	nb.
$\sigma(Z \to e^+e^-)$	$= 0.209 \pm 0.013$	± 0.017	nb.
$\Gamma(W)$	$= 2.12 \pm 0.20$		GeV

The width parameter may be compared with the standard model prediction, $\Gamma(W) = 2.07$ GeV, which assumes $M(W) = 80.0$ GeV and $M(\text{top}) > M(W) - M(b)$.

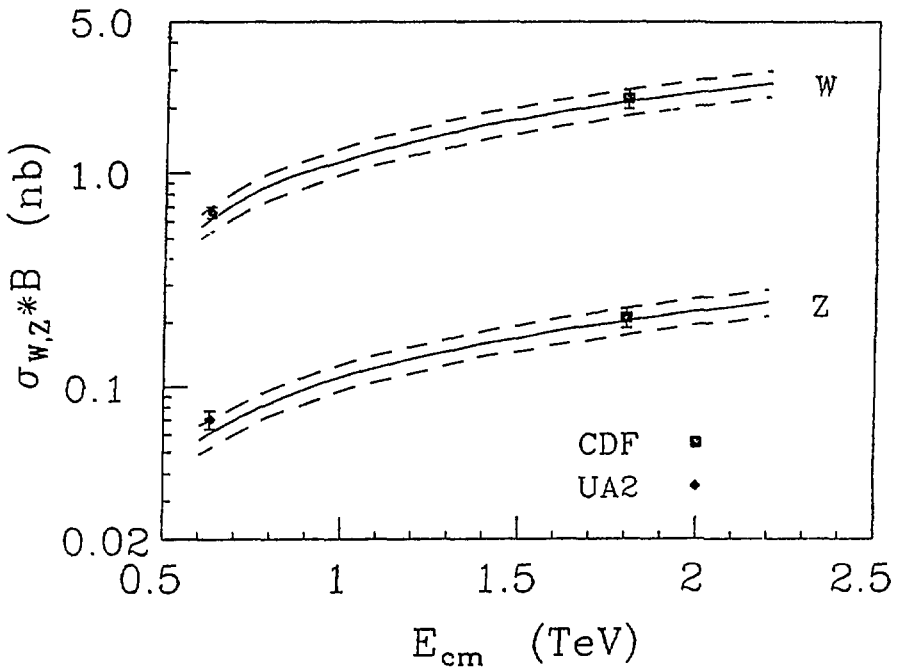

Fig. 1. Measured $W \to \ell\nu$ and $Z \to e^+e^-$ cross sections at 0.63 and 1.8 TeV, together with theoretical predictions (K. Ellis, Castiglione).

The spectrum of W and Z production at high p_T provides a sensitive test of next-to-leading order QCD calculations. In addition, deviations from the QCD predictions in the W or Z samples separately could serve as indicators of new physics. The p_T spectrum for Z's is measured directly using samples of 238 e^+e^- pairs and 106 $\mu^+\mu^-$ pairs. The p_T spectrum for W's must be reconstructed using the observed hadronic recoil energy in the CDF calorimeter. Since the calorimeter response is nonlinear, substantial care must be taken in modeling the calorimeter response; fortunately, the observed hadronic response in $Z \to e^+e^-$, $\mu^+\mu^-$ events can be used to check this modeling. The W sample used for this analysis consisted of 2496 events from the inclusive electron sample. The p_T spectra are shown in Figs. 2 and 3, compared with the next-to-leading order calculations by Arnold and Kauffman (an extension of earlier work by Arnold and Reno). The agreement between theory and experiment appears satisfactory.

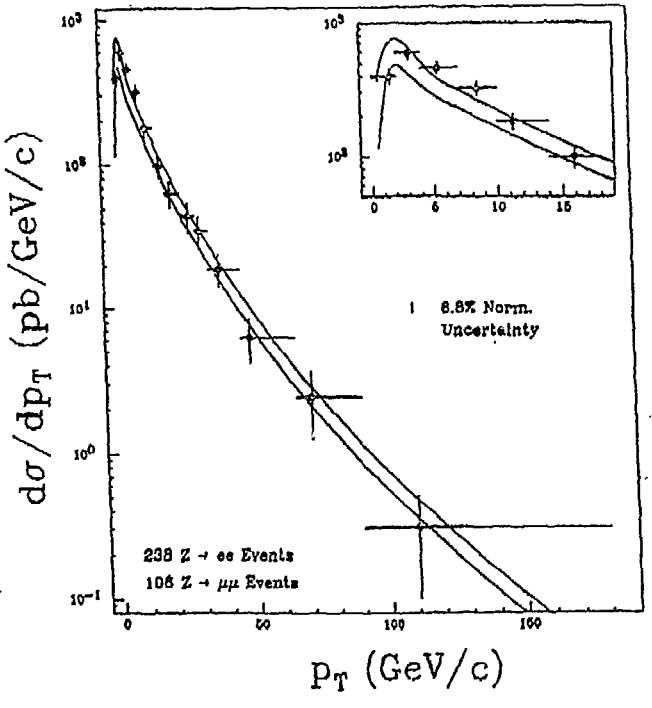

Fig. 2. Inclusive p_T spectrum for $Z \to \ell^+\ell^-$, together with next-to-leading order theoretical predictions.

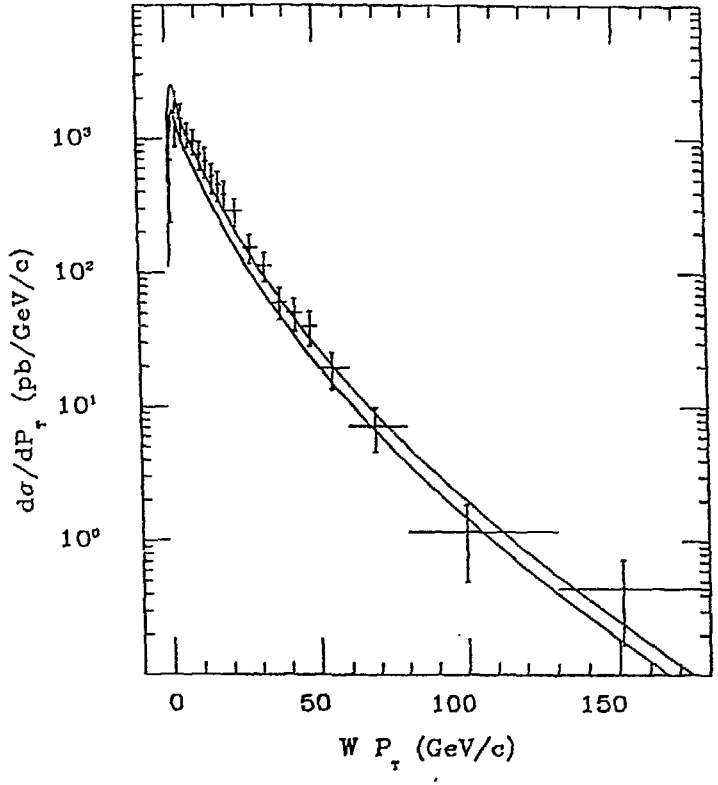

Fig. 3. Inclusive p_T spectrum for $W \to e\nu$, together with next-to-leading order theoretical predictions.

The bottom-quark cross section also provides a test of next-to-leading order QCD predictions, although at Tevatron energies the theoretical predictions are subject to large uncertainties, associated with the choice of low-x structure functions, b-quark mass, and renormalization scale. The CDF measurements involve reconstructing the bottom-hadron spectrum and then working back to the bottom-quark spectrum, using $b \rightarrow B$ fragmentation functions consistent with data from PEP, PETRA, and LEP. To obtain the bottom-hadron spectrum, we have used the following samples: a) inclusive semileptonic decays, $B \rightarrow e\,\nu X$; b) exclusive semileptonic decays, $B \rightarrow e\nu\, D^{\circ}\, X'$; and c) exclusive hadronic decays, $B \rightarrow J/\psi + K$. The inclusive semileptonic distribution gives the highest statistics, but requires detailed background subtractions to account for non-B sources of real or fake electrons. The exclusive J/ψ decay modes give the cleanest signal, but suffer from low statistics, uncertainties in the $B \rightarrow J/\psi$ branching ratios, and in general, uncertainties in acceptance corrections associated with the J/ψ decay angular distributions. Figure 4 shows the CDF preliminary cross sections based on inclusive and exclusive semileptonic decays. The points give the measured b-quark cross sections above a p_T threshold, and the systematic errors are almost entirely common to all points, due to uncertainties in $b \rightarrow B$ fragmentation, non-B backgrounds, and efficiency corrections. The preliminary results from $B \rightarrow J/\psi\, K$ (not shown) are in fair agreement with the trend indicated by the electron data, namely that the observed b-quark rates are systematically higher than the next-to-leading order predictions by Nason, Ellis, and Dawson. This is good news from an engineering standpoint, and suggests that the Tevatron is indeed a B-factory.

The inclusive J/ψ sample could also be used to measure the b-quark cross section, in the same way as the prompt lepton sample. Unfortunately, this approach suffers from large uncertainties in the $B \rightarrow J/\psi$ branching ratios, the efficiency corrections for these modes, and the fraction of J/ψ's that come from B-decay. Theoretically, we expect comparable rates of J/ψ production from B decays and from decays of χ states; additional direct QCD production of J/ψ and ψ' is expected to be inhibited by the decoupling of J/ψ from two-gluon configurations. Two indirect methods have been employed to address what

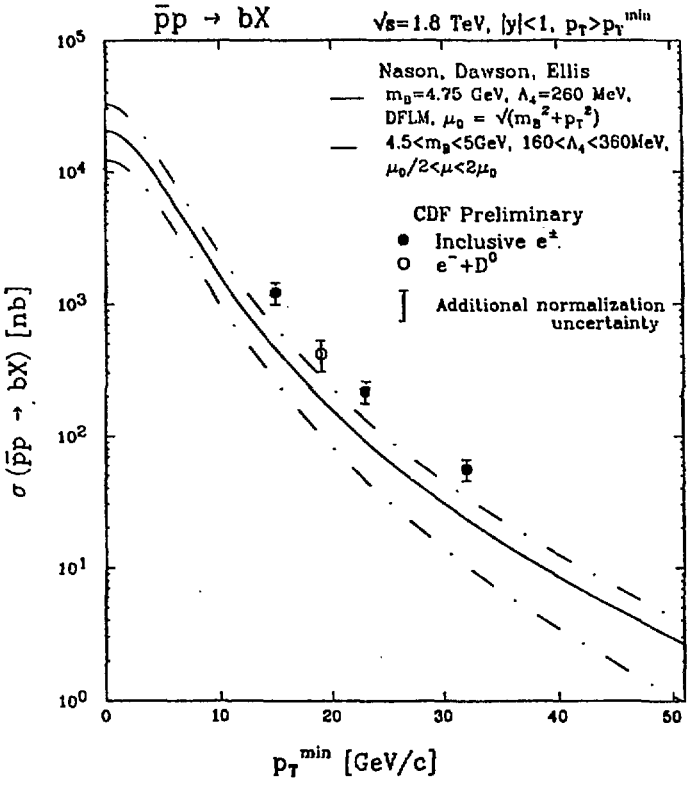

Fig. 4. Inclusive single-b production cross section, expressed as a function of p_T cutoff, compared with next to leading order theoretical predictions.

fraction of J/ψ come from B decays. The first method involves direct search for χ-states; the second involves analysis of the ψ' production rates, and relies on the fact that ψ''s do NOT come from χ-state decays.

Figure 5 shows a mass plot of inclusive J/ψ's with nearby single photon candidates in the central calorimeter. The photon production angle is measured precisely by the strip chambers at shower maximum, and the photon energy by the electromagnetic calorimeter. The mass difference, M(ψ-γ) - M(ψ),peaks at the value expected for the average of the three χ states, namely 430 MeV. This analysis indicates that a substantial number of J/ψ's are indeed produced by χ-state decays.

The second method to determine the fraction of J/ψ's that come from B decay uses the ψ' cross section. The observed $\psi' \rightarrow \mu^+\mu^-$ rate, shown in Fig. 6, can be compared with the ratio, ψ'/ψ measured at CLEO. Assuming that

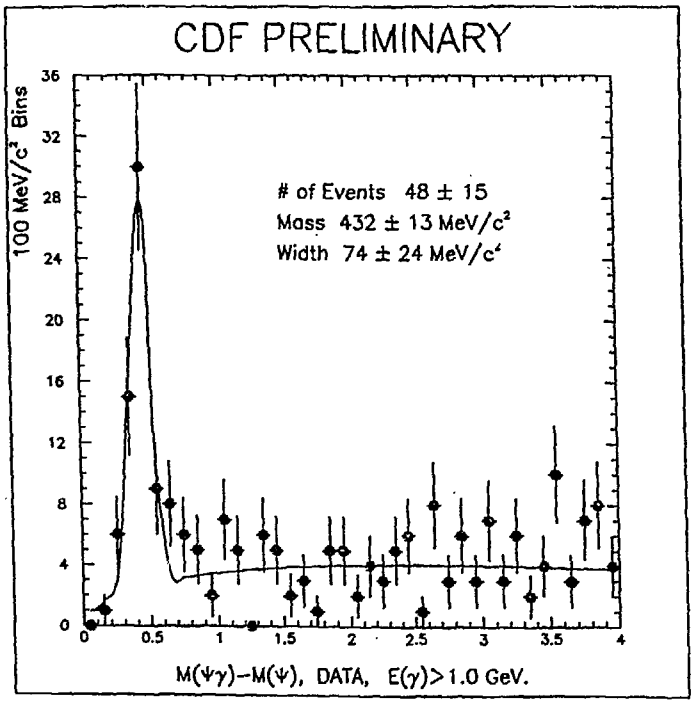

Fig. 5. Mass difference between $\psi\gamma$ and ψ for inclusive ψ plus single photon events.

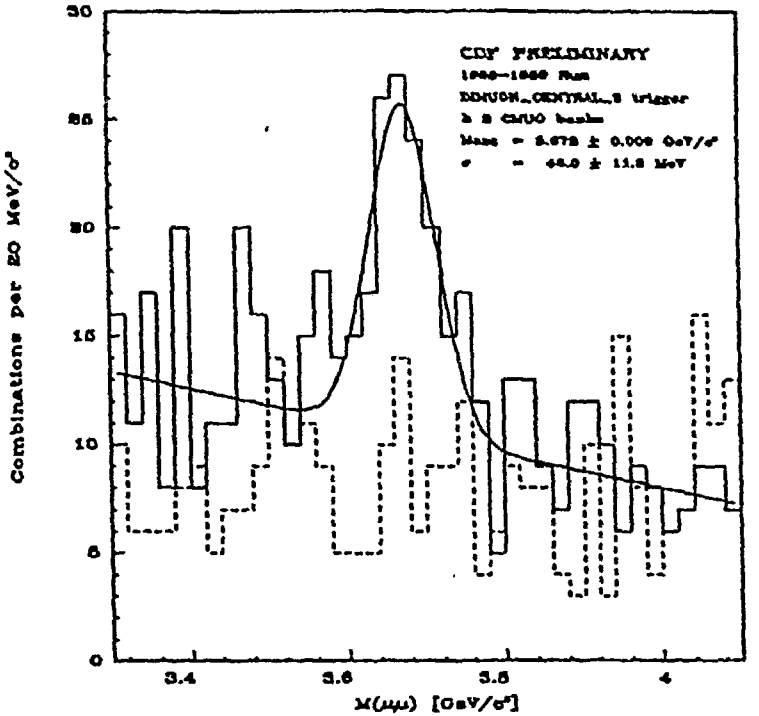

Fig. 6. Dimuon spectrum in the ψ' region (solid), together with like sign background (dashed).

nearly all ψ' come from B-decays, we obtain that 64% of J/ψ's come from B decays. The χ-state analysis indicates that roughly 36% come from χ decays.

As a byproduct of this analysis, CDF can set an upper limit (90% confidence) on the branching ratio for the rare FCNC decay,

$$BR\ (B^\circ \to \mu^+\mu^-) < 3.2\ 10^{-6},$$

significantly better than the present world average ($5\ 10^{-5}$). This limit is set by comparing the signal region at 5.28 GeV, with the ψ' signal, and correcting for the known $B^\circ \to \psi'\ X$ inclusive branching ratio. The dimuon spectrum in the signal region is shown in Fig. 7. There is no evidence for a B-peak; it can be seen that the upper limit determination bottoms out on dimuon background, which should be strongly suppressed in future, using secondary vertex information. The theoretical expectation for this BR is around 10^{-8}, similar to that for $K_L \to \mu^+\mu^-$.

With the installation of the silicon vertex detector, together with upgrades in the electron and muon detection systems, we anticipate a fruitful program of B-physics at CDF in the coming runs. (A. B. Wicklund)

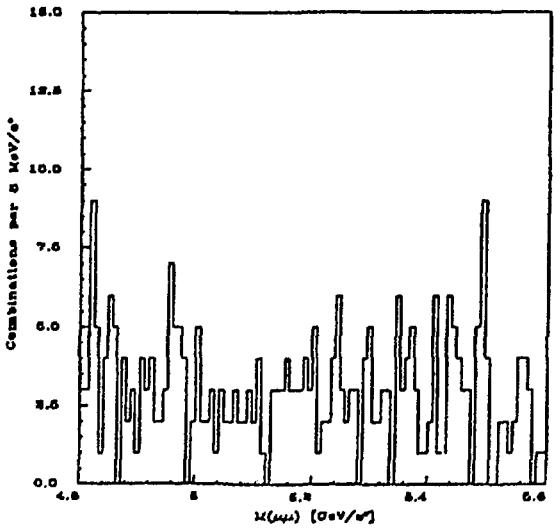

Fig. 7. Dimuon invariant mass in the B° region.

2. Soudan Data Analysis

Argonne physicists continued to work on the analysis of the large sample of high quality data recorded to date by Soudan 2. Substantial effort was focussed on the characterization of contained neutrino events and the search for magnetic monopoles, in addition to muon astronomy studies with Soudan 1 data.

The search for GUT magnetic monopole tracks in Soudan 2 suffered a serious setback when the Monte Carlo simulation revealed that cuts made to eliminate events with very large numbers of hits during track reconstruction resulted in very low efficiency for monopoles. The software can be easily changed; however, all of the data which have been examined to date will have to be reprocessed. A large effort to reprocess all past data with improved track-reconstruction and contained-event-recognition software was already scheduled for 1991.

An important part of the contained event analysis has been the determination of the particle identification capabilities of Soudan 2 from the large sample of ISIS test beam data. The electron and muon data have been extensively analyzed to develop an algorithm for separating electron showers from muon tracks. The efficiency of selecting electrons is shown in Fig. 8.

The muon efficiency is essentially constant with momentum and equal to the electron efficiency of 95% at 400 MeV/c, but at low energies the electron efficiency drops rapidly. This is because such low energy tracks do not develop large showers and are dominated by the track-like portion of the electron in the first few radiation lengths. This clearly affects the classification of low energy neutrino interactions into events produced by ν-e or ν-ν, as described below.

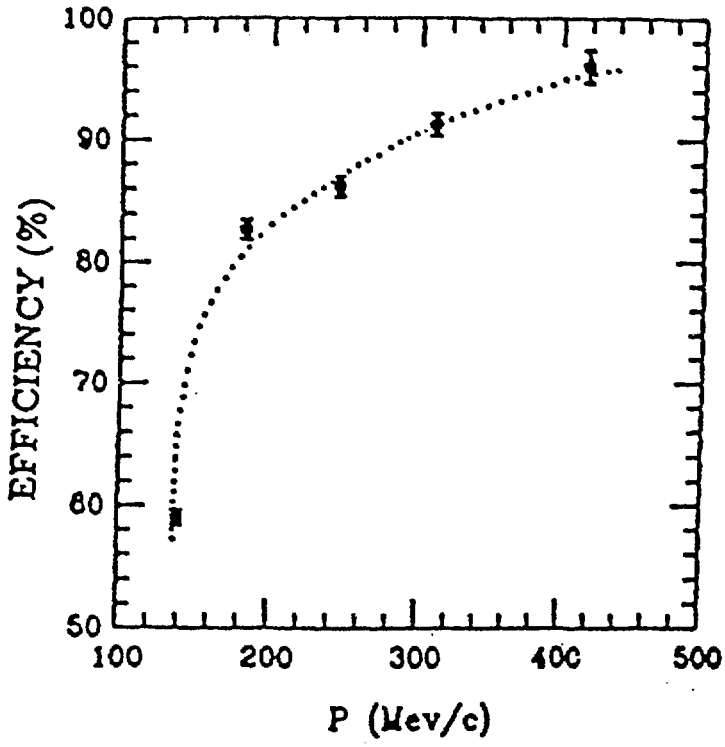

Fig. 8. The efficiency of Soudan 2 for selecting low energy electron tracks while rejecting muon tracks, from ISIS test beam data. The algorithm used distinguishes between electrons and muons using drift residuals of points from a continuous trajectory, the number of hit tubes not on a continuous trajectory, the number of missed tubes, and the largest contiguous set of missed tubes on a trajectory.

The ISIS test beam data have also been used to study the ability of Soudan 2 to distinguish between low energy muon and proton tracks. As described below, this capability is important for identifying neutron interaction events. Low energy (100-200 MeV) neutrons produced by cosmic ray muon interactions in the rock around the detector are detected as short recoil proton tracks. These tracks have dE/dx ionization which is about twice that of low energy muons. Figure 9 shows the result of comparing test beam data from muon and proton tracks. In order to optimize the dE/dx resolution of the modules in Soudan 2, the new half-tube database software is used to calibrate the detector response around the times and locations of neutron candidate events.

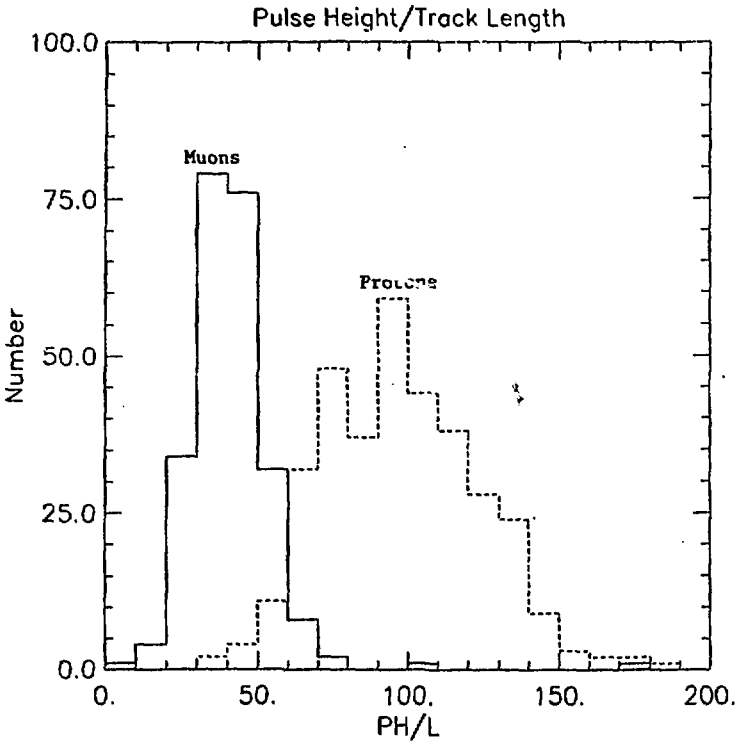

Fig. 9. The pulse height per unit track length for muons (full line) and protons (dashed line) recorded in a Soudan 2 module in the ISIS test beam. The ability to distinguish low energy muon and proton tracks is important for the identification of neutron interactions which produce recoil proton tracks in Soudan 2.

To date 43 contained events have been found within the fiducial volume of the detector. Of these, 23 events have hits in the active shield around the event time. Many of these are short heavily ionizing tracks which appear to be proton recoils from neutron interactions. The rate is consistent with calculations, performed at Argonne and Oxford, of the number of events expected from this effect. These calculations also indicate that nearly all such events will be accompanied by hits in the shield. The ionization of most of the neutron candidate events examined so far is consistent with expectations for recoil protons, as observed in data from the ISIS test beam shown in Fig. 9.

The remaining 20 events are interpreted as neutrino interactions. A Monte Carlo simulation of the interactions of atmospherically produced cosmic-ray neutrinos interacting in the detector has been performed. This calculation, including the Soudan 2 detector properties and event recognition efficiencies, predicts 21 detected neutrino events during the exposure analyzed to date. The 20 neutrino event candidates have been tentatively classified into the following final states:

$\nu N \rightarrow N'\mu$	quasi-elastic	6 events
$\nu N \rightarrow N'e$	quasi-elastic	11 events
$\nu N \rightarrow N'eX$	inelastic charged current	1 event
$\nu N \rightarrow N'\nu X$	inelastic neutral current	1 event
$\nu N \rightarrow N'\mu X$, $N'\nu X$	ambiguous	1 event

No candidates have been found for two body proton decays. The electron identification efficiency determined from the ISIS test beam calibration (Fig. 8) implies that a correction involving the transfer of one event from muon to electron should be made in the above table.

Figure 10 shows the momentum spectrum of electrons from the neutrino interaction candidates with the expected spectrum from the Monte Carlo calculation.

In addition to writing a number of internal PDK notes during the last half of 1990, Argonne physicists also coauthored several external documents submitted by the Soudan 2 collaboration. Most notable among these were the search for muons from Cygnus X-3 using the Soudan 2 active shield (published in Physical Review D), the paper on coincidence data between Soudan 1 and its surface array (submitted to Physical Review D), and the Fermilab Letter of Intent to perform a long baseline neutrino oscillation experiment with Soudan 2 (P-822). Conference papers describing initial data from Soudan 2 were submitted to the 25th I.C.H.E.P. in Singapore, Neutrino '90 at CERN, the Europhysics Conference in Bratislava, the 1990 Snowmass Summer Study, the Gamma Ray Astronomy Conference in Ann Arbor, and the Fermilab Calorimetry Conference. Two Ph.D. theses were submitted by graduate students in the Soudan

collaboration, one on the analysis of ISIS test beam data, by Carmen Garcia-Garcia (University of Valencia), and the other on a search for muons associated with Cygnus X-3 during the 1989 radio burst period, by Lucy Kirby-Gallagher Tupper (University of Oxford). (D. Ayres)

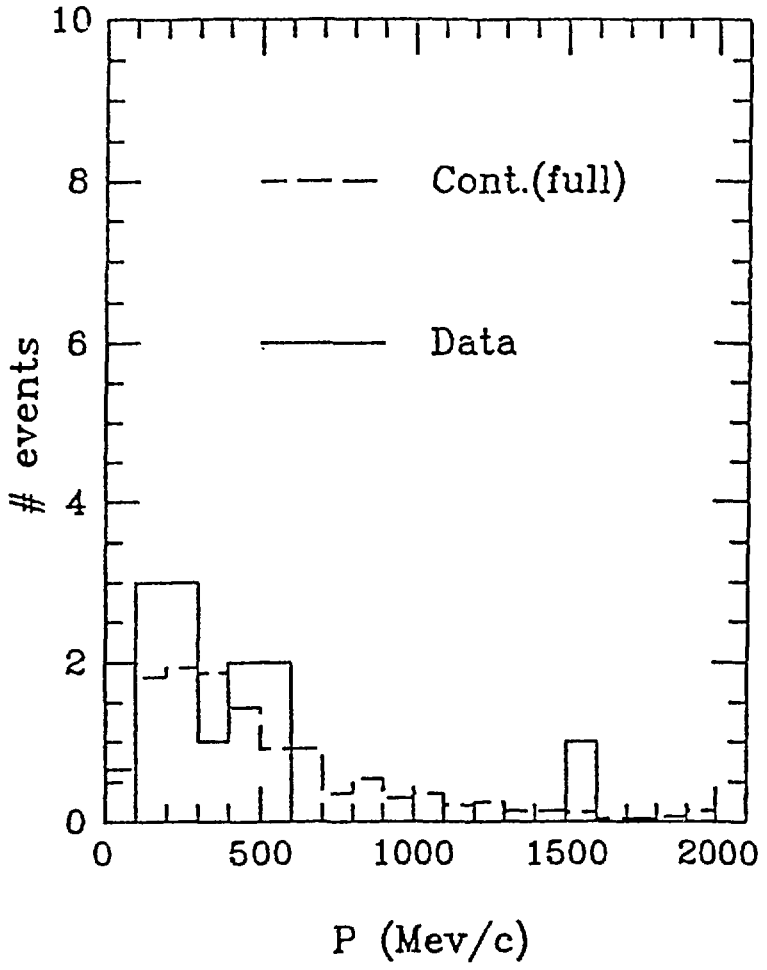

Fig. 10. Comparison of the momentum spectrum of electrons from neutrino interaction candidate events in Soudan 2 with that predicted by a Monte Carlo simulation. The two distributions are normalized to the same exposure and the Monte Carlo events are processed through an analysis path similar to that used for real events. The Monte Carlo events were generated in the full detector while the actual events occurred in the first half of Soudan 2.

3. High Resolution Spectrometer

A study of inclusive Λ hyperon production in e^+e^- annihilations at $\sqrt{s}$ = 29 GeV was completed in this period using the full 300 pb^{-1} HRS data sample. The Λ multiplicity was measured to be 0.192 ± 0.021 per hadronic event. The unlike (like) strangeness Λ pair production rate is 0.046 ± 0.020 (0.009 ± 0.028) per event. Figure 11 shows our inclusive cross section as a function of the energy variable z compared to other measurements in this energy range. When comparing these results to the Lund Monte Carlo model an important parameter is the strange to nonstrange diquark pair production δ specifically δ = (us/ud)/(s/d). A χ^2 fit performed to the cross section data gives a best value of δ = 0.59 ± 0.10 as shown in Fig. 12. This result when compared to the Lund default value of 0.32 implies that a larger fraction of the Λ's came from strange diquark pairs than was originally estimated.

(M. Derrick)

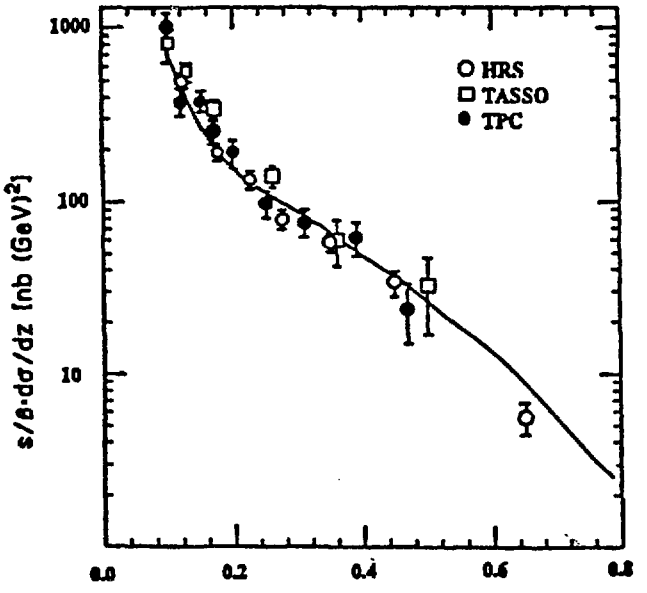

Fig. 11. Lambda inclusive cross section at 29 GeV.

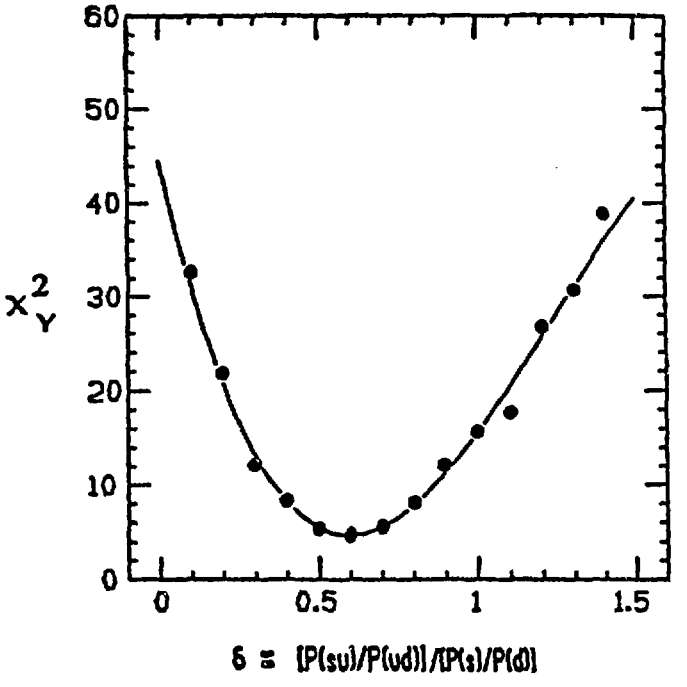

Fig. 12. Chi-square of fit to cross section vs delta.

4. Energy Flow in Hard Proton-Nucleus Collisions at 400 GeV/c. E609 Collaboration (Argonne, Fermilab, Lehigh, Michigan, Pennsylvania, Rice, and Wisconsin)

During this period, our final results on the azimuthal dependence of transverse energy flow for pA hard collisions (dijet events) observed in Fermilab experiment E609 were submitted for publication in Physics Letters B. Our two principal findings are as follows:

1) The azimuthal distribution of transverse energy for dijet events and mean $p_T > 4$ GeV/c, shown in Fig. 13, clearly indicates that the azimuthal angular width of jets from a Pb nucleus is only slightly larger than that of jets from pp collisions. The jet which is defined to be at $\phi = 0$ in Fig. 13 is an (unbiased) away side jet (i.e. did not participate in the trigger).

2) The distribution of azimuthal angle between the jet axes, shown in Fig. 14, is much broader for Pb dijets than for pp. The observed

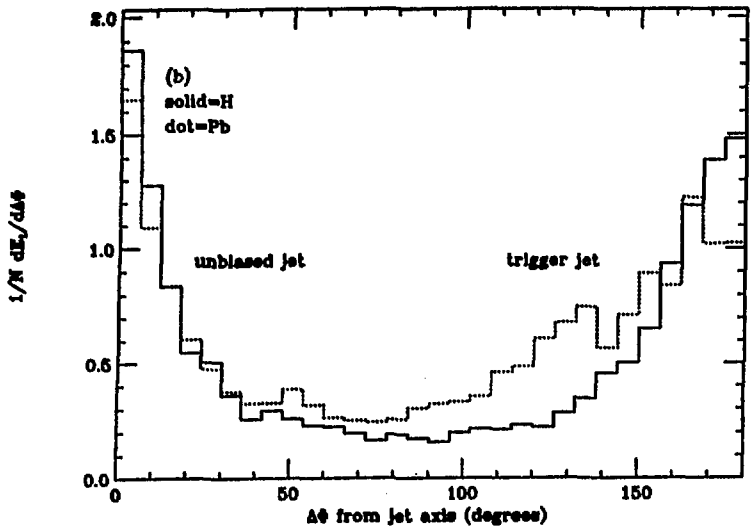

Fig. 13. Azimuthal distribution of transverse energy for dijet events with p_t > 4 GeV/c. Solid: dijets from H, with ϕ = 0 defined by the direction of the unbiased jet. Dotted histogram: same as solid, except using p-Pb events.

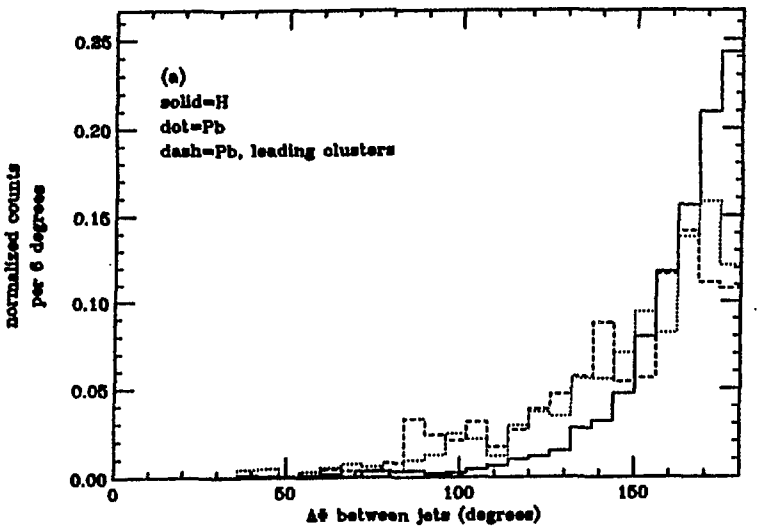

Fig. 14. Distribution of $\Delta\phi$, the azimuthal angle between the jet axes. The energy flow is plotted using calorimeter clusters. Solid: H events; dotted: Pb events; dashed: Pb events, using the azimuthal angles of the leading clusters.

distributions can be described in terms of additional transverse momenta $k_{T\phi}$ = 2.0 ± 0.2 GeV/c for p-Pb and 0.9 ± 0.2 GeV/c for pp.

This large value for $k_{T\phi}$ (Pb) offers a sharp contrast to the very small amount of nuclear scattering (for the incident quark) observed for Drell-Yan dilepton production in a heavy nucleus. For the Drell-Yan process, the nuclear contribution to k_T has been measured to be $\lesssim$ 0.4 GeV/c. This contrast may indicate that the incident quark in the Drell-Yan process is shielded by virtue of being bound in a hadron, whereas the scattered partons in our experiment are propagating through the nucleus as "free" colored partons and may therefore experience strong rescattering. A closely related physics issue is the fact that our large value for $k_{T\phi}$ (Pb) appears to be a strong contradiction to the QCD factorization theorem--the expectation that the cross section for a hard process within a nucleus should be A times that for a nucleon.

We plan to continue our study of the E609 pA → dijet data in order to further explore nuclear effects such as energy flow patterns as a function of polar angle, the detailed A^{α} dependence of the cross sections, and whether the observed large value for k_T(Pb) can quantitatively explain the $\alpha > 1$ nuclear enhancement (Cronin effect). (T. Fields)

5. Fermilab Polarized Beam

Activities associated with the Fermilab polarized beam were: i) E-704 data taking which started in early February 1990, ii) data analyses, and iii) documentation of experiments and experimental results. The experiments were carried out by an international collaboration from Europe, USSR, Japan, and the U.S. From Argonne's High Energy Physics Division, the following physicists participated in these experiments: D. P. Grosnick, D. A. Hill, D. Lopiano, Y. Ohashi, H. Spinka, D. G. Underwood, and A. Yokosawa. Important technical assistance was provided by H. Blair, T. Kasprzyk and J. Sheppard.

There were several experiments involved in E-704 consisting of single- and double-spin asymmetry measurements in π° production at high p_T, Λ (Σ°), $\pi^{\pm}$, π° production at large x_F, and $\Delta\sigma_L$(pp, $\bar{p}$p) measurements. We utilized the

allocated beam time efficiently and were able to meet our goals. For the $\Delta\sigma_L$ measurements, we were able to operate the polarized proton target successfully during this period.

We have initial results on asymmetry measurements in π° production while data for $\Lambda(\Sigma^\circ)$, $\pi^\pm$ production as well as $\Delta\sigma_L$ measurements are being analyzed.

Single-spin asymmetry in $p^\uparrow p \to \pi^\circ X$ and $\bar{p}^\uparrow p \to \pi^\circ X$ at high p_T

This experiment was carried out at incident proton momentum of 200 GeV/c. Preliminary data of the $p^\uparrow p$ reaction show that the asymmetry values (A_N) at $x_F \approx 0$ are approximately zero (or small and negative) up to $p_T = 3.5$ GeV/c and then begin to rise to $\sim +40\%$ in the region of $p_T = 4$ to 5 GeV/c as shown in Fig. 15. At lower energies as seen in the BNL ($p^\uparrow p \to \pi^+ X$), CERN ($pp^\uparrow \to \pi^\circ X$), Serpukhov ($\pi^- p^\uparrow \to \pi^\circ X$) data, this rapid rise from zero to large positive values, was also observed, as shown in Fig. 16, although none of the data exceeded $p_T = 3$ GeV/c. A new finding is that all the A_N data of π° or π^+ production at $x_F \approx 0$ show that the large positive asymmetries begin at $x_T = 0.4$ in the region $\sqrt{s} = 5$ to 20 GeV as shown in Fig. 17. This is an indication that we may be observing asymmetries caused by hard scattering. Theoretically single-spin asymmetries are discussed within the context of the QCD hard-scattering model. Based on the quark content of $\pi^+ = u\bar{d}$ and $\pi^\circ = (u\bar{u} - d\bar{d})/\sqrt{2}$, one may hypothesize that the polarized u quark in the polarized proton beam carries the spin information.

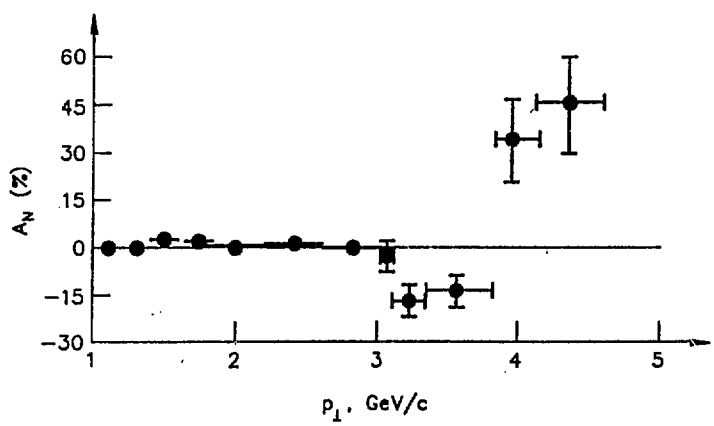

Fig. 15. p_T dependence of A_N at $x_F \approx 0$.

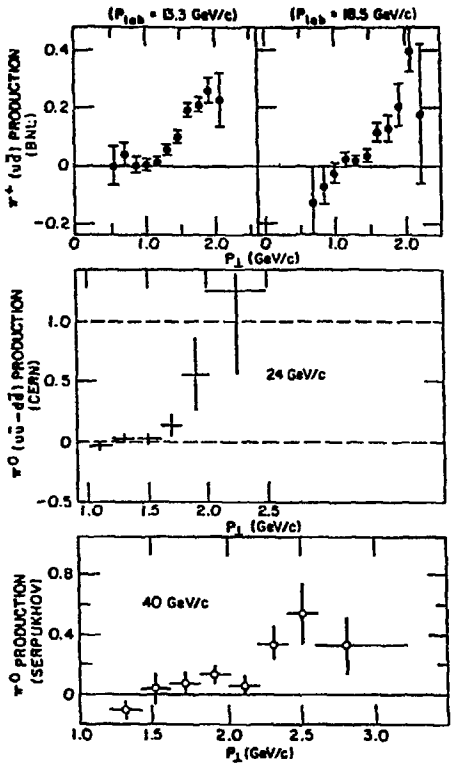

Fig. 16. Asymmetry $A_N(\%)$ vs. p_T at p_{lab} = 1.33 to 40 GeV/c.

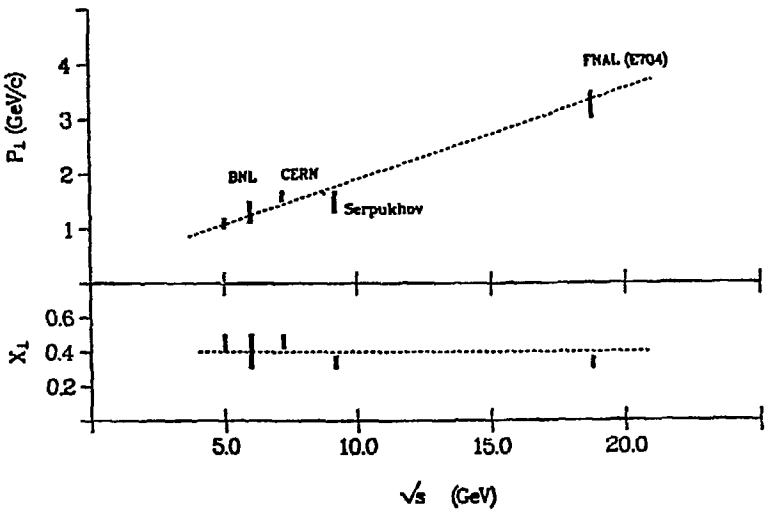

Fig. 17. Onset of structure in A_N vs. $\sqrt{s}$. Single-spin asymmetry in $\bar{p}^\uparrow p \to \pi^0 X$ shows a similar p_T dependendce as the $p^\uparrow p$ case. However, data are limited only up to p_T = 3.5 GeV/c.

x_F dependence of single-spin asymmetry in $p^\uparrow p \to \pi^\circ X$ and $\bar{p}^\uparrow p \to \pi^\circ X$

Measurements on the x_F dependence at 200 GeV/c for p_T up to 2 GeV/c were recently completed. Asymmetry values in the $p^\uparrow p$ reaction are consistent with zero up to x_F = 0.3 to 0.4, and then increase linearly to + 20% near x_F = 1.0 as shown in Fig. 18. The data suggest an influence of polarized u quarks at large x_F. They are consistent with earlier data taken at $\langle x_F \rangle$ = 0.52. This is the first x_F dependence data ever obtained in π production. It is interesting to notice that our data resemble the x_F dependence for Λ polarization in $pp \to \Lambda^\uparrow X$ where polarized s quarks are considered to be responsible for high polarization. Single-spin asymmetry in $\bar{p}^\uparrow p \to \pi^\circ X$ shows a similar x_F dependence as the $p^\uparrow p$ case.

A short summary of x_T and x_F dependences

There are two common phenomena observed in the x_T and x_F dependences of the one-spin asymmetries. The asymmetry values are zero or small for both x_T and x_F < 0.3 to 0.4. Then there is a rise from zero to large positive values for x_T and x_F > 0.3 to 0.4. It will be interesting to find out if these two phenomena are related. One hint is that polarized u quarks seem responsible for the rise in A_N at high $x_\perp$ and high x_T. It is interesting to investigate if these phenomena may be related to the origin of proton spin. High-p_T and high -x_F scattering phenomena may be interpreted as an indication for the existence of rotating color charges in polarized protons.

(A. Yokosawa)

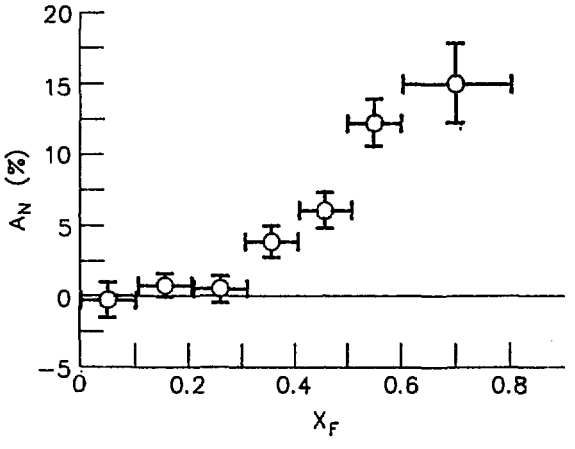

Fig. 18. x_F dependence of A_N at $p_\perp$ = 0.5 to 2.0 GeV/c (preliminary data).

6. Spin Physics at LAMPF

Over the past 8 years, the goal of the ANL-HEP medium energy physics program has been the measurement of the isospin-0 nucleon-nucleon elastic scattering amplitudes at beam kinetic energies of ~ 500-800 MeV. Many experiments have been performed to attain this goal by the ANL group and others. Significant progress was made on four neutron-proton scattering experiments that impact this goal during the past six months. Note that pp elastic scattering spin observables depend only on isospin-1 amplitudes, while np scattering depends on both isospin-0 and -1 amplitudes.

A short paper on experiment E-960, a measurement of the total cross section difference between antiparallel and parallel longitudinal spins for a polarized neutron beam on a polarized proton target ($\Delta\sigma_L$(np)), was written and accepted for publication in Physics Letters B. The results exhibit energy-dependent structure when combined with data at higher and lower energies collected at other accelerators. The bump seen in $\Delta\sigma_L$ (I = 0) could be interpreted as an isospin-0 dibaryon resonance. Using information from existing inelastic and total cross section data, it appears that the structure originates in one of the spin-singlet partial waves ($^1P_1$, $^1F_3$, ...) or a coupled-triplet partial wave ($^3S_1$, $^3D_1$, ...). The best fit of a Breit-Wigner resonance shape to the combined data set described above gives a mass of ~ 2210 MeV and a width of ~ 74 MeV. A long paper describing details of the experiment, and an instrumentation article about the neutron counter array used for the $\Delta\sigma_L$(np) measurements are both being written. These papers will complete the work on E-960.

There has been significant data analysis performed for experiment E-665/770, a measurement of the np elastic scattering spin observables C_{SS}, C_{SL}, and C_{LL} with polarized beam and target. Final results were obtained for C_{SL} and C_{LL} at 484 MeV and $\theta_{c.m.}$ = 80-130 degrees and at 788 MeV and $\theta_{c.m.}$ = 75-160 degrees. A major paper describing this experiment has begun, and it is hoped to complete this paper within the next six months. In addition, data on C_{SS} and C_{SL} for $\theta_{c.m.}$ ~ 30-80 degrees at 484, 634, 720, and 788 MeV are being analyzed and the results will be described in a separate article. Finally, spin parameters for the np → dπ^0 reaction over part of the angular range are

being analyzed by collaborators and a ANL summer visitor, and a draft of the paper describing these results has been written. When all the work on E-565/770 is completed, the results will have a major impact on the knowledge of the isospin-0 amplitudes.

Results from a third experiment, E-589, were published in Physical Review C. This experiment measured the small angle np elastic scattering polarization parameter at 790 MeV with much of the same apparatus as in E-665/770. These results were analyzed by Texas A&M physicists and are shown in Fig 19. Using the new data and results from other experiments, values of the polarization times the differential cross section for isospin-0 and for the interference of isospin-0 and -1 can be obtained. These are given in Fig. 20. (H. Spinka)

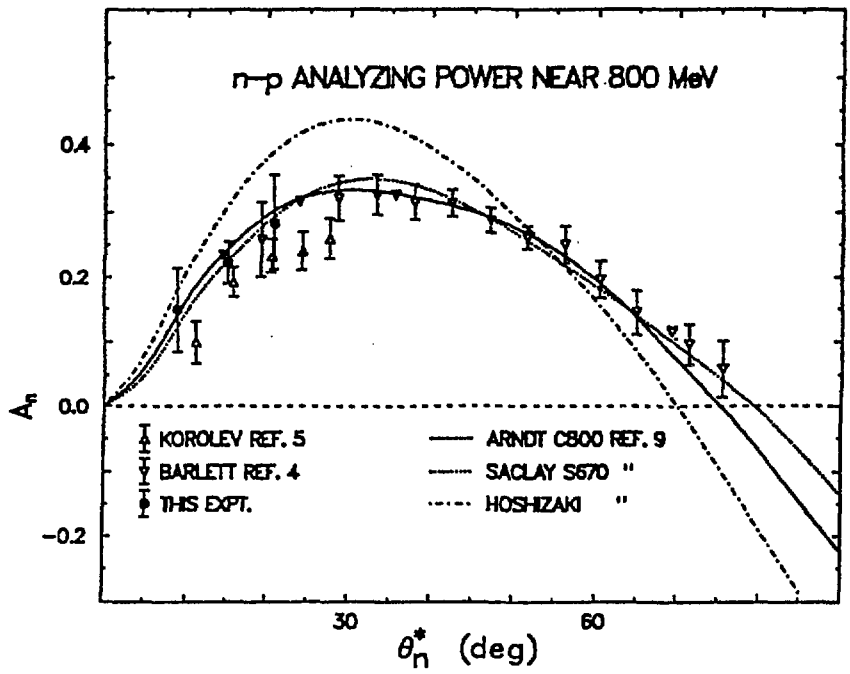

Fig. 19. Measured values of the np polarization parameter, A_n, near 790 MeV as a function of c.m. angle. The solid circles correspond to the E-589 results, and the triangles to previous elastic and quasielastic polarization measurements. The curves correspond to various phase shift predictions.

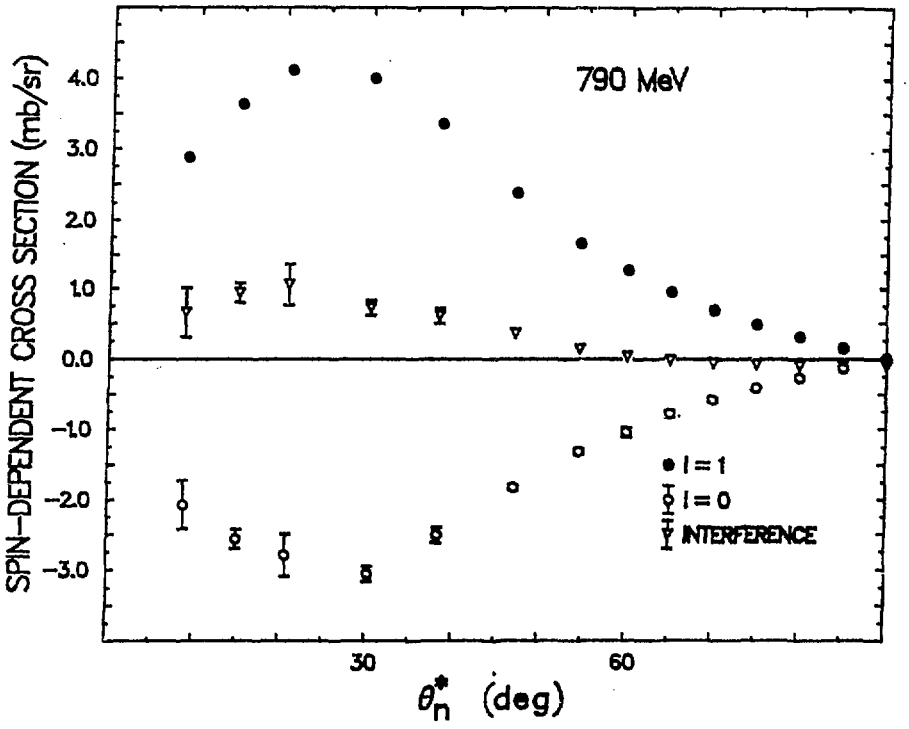

Fig. 20. Derived values of the nucleon-nucleon polarization parameter times the differential cross section for pure isospin-0 and isospin-1 and for the interference of isospin-0 and -1 as a function of c.m. angle at 790 MeV. Data from E-589 were used to obtain the values at the smallest angles.

7. Computational Physics

The computational physics effort continued to be devoted to lattice gauge theory simulations. These efforts were divided between lattice QCD whose goals are to predict the properties and interactions of hadrons and nuclear matter, and lattice QED whose aims are to understand the newly discovered strong coupling phase of QED. The hybrid microcanonical/Langevin simulation method with "noisey" fermions continued to be the simulation method of choice, allowing the use of staggered fermions with numbers of flavors which are not multiples of 4.

As a part of a large, multi-institutional collaboration, the HEMCGC "Grand Challenge" collaboration (currently 17 people), we have been using a "Grand Challenge" grant of computer time at the DOE's facility at Florida State University (SCRI) to measure hadronic mass spectra and other hadronic

matrix elements using lattice techniques. The papers reporting the high statistics results on baryon and meson masses from our ETA-10 runs on 12^4, 12^3 x 24 and 16^4 lattices mentioned in the last report have now been published. A paper reporting results on the glueball mass spectrum, string tension, and topological charge, from these ETA-10 runs, an area in which the Argonne contingent has been most active, has now been submitted for publication. These results were reported by D. Sinclair at the LATTICE'90 meeting in Tallahassee in October. In Fig. 21 a comparison is given of these glueball masses and the string tension with the hadron masses for our lowest quark mass runs on the 12^4 lattice where we have the highest statistics. Production runs are now underway on a 16^3 x 32 lattice on the Connection Machine (CM-2) at SCRI, both using the staggered fermion method of latticizing quarks and also using the alternate Wilson method, to compare the results obtained by the two methods. Our CM-2 codes have been enhanced by recoding the kernels in CMIS, a low level microcode assembler. We are now coding new glueball/topology measurement codes for the CM-2.

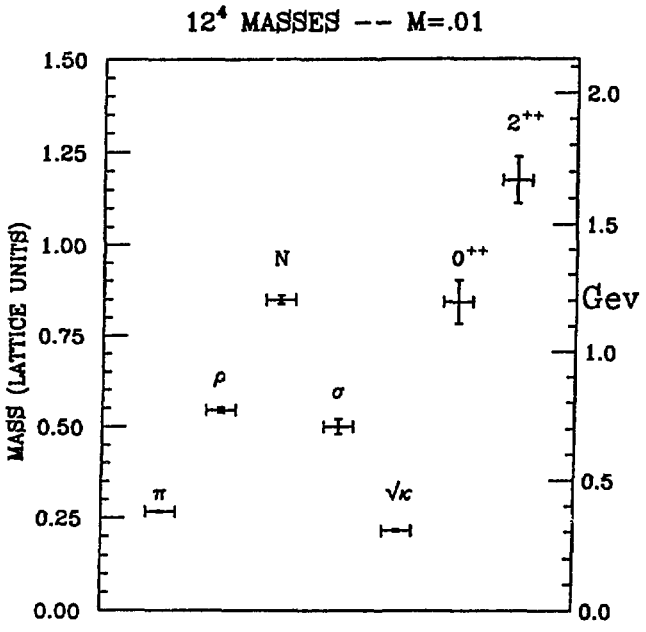

Fig. 21. Comparison of hadron masses, glueball masses and $\sqrt{\kappa}$ where κ is the string tension, on a 12^4 lattice with quark mass =. 01.

A subset of the HEMCGC collaboration is currently exploring the thermodynamics of 2 flavor QCD using the CM-2 recently installed at the Pittsburgh Supercomputing Center. With this we are studying the finite temperature transition from hadronic matter to a quark-gluon plasma on a $16^3 \times 8$ lattice with small quark masses (.0125 and .00625 in lattice units). Preliminary results from the simulations at m = .0125 indicate that the transition occurs for $6/g^2$ close to 5.5, and shows no hint of the first order nature reported on smaller lattices ($8^3 \times 4$).

In a related study, in collaboration with J. B. Kogut of the University of Illinois, we have been studying QCD with 2 light flavors and 1 heavy flavor on a $12^3 \times 6$ lattice. Again the first order transition observed on an $8^3 \times 4$ lattice was not seen. This result had been expected from our earlier $12^3 \times 4$ simulations where it was clear that the transition was weaker than that on the $8^3 \times 4$ lattice. We are here trying to determine whether or not this transition is accompanied by an increase in strangeness.

In collaboration with J. B. Kogut and R. Renken of the University of Illinois, S. Hands of the University of Glasgow, and A. Kocic of the University of Arizona, we have been extending the pioneering work of Kogut & Dagotto on lattice QED. We are performing simulations aimed at understanding the nature of the transition from strong to weak coupling for theories with 2 and 4 "flavors" of electron. The simulations on 10^4, 12^4 and 14^4 lattices have been performed on CRAYS, while those on 16^4 lattices are being carried out on the HEP division's ST-100 array processor and on CM-2's at the National Center for Supercomputing Applications and Northeast Parallel Architecture Center. During this period we have seen indications that the source of confusion in prior simulations by various groups has been due to the fact that the transition observed in these simulations is not the continuum transition, but a transition driven by magnetic monopole loops, a lattice artifact. We are thus performing further simulations to elucidate this observation. The preliminary results of these simulations were reported by K. C. Wang at LATTICE'90 in Tallahassee.

During this period we have commenced producing a code for performing quenched QCD simulations using a combination of Metropolis monte carlo and

overrelaxion methods. This code is being written in a manner such as to simplify porting it to the massively parallel Argonne/Caltech Intel Touchstone computer, where it will be used to generate quenched configurations on a 32^3 x 64 lattice. These will be used to calculate a quenched hadron spectrum.

Finally we have been part of a consortium of institutions who have prepared and submitted a preliminary proposal to the DOE seeking funds to obtain a computing system with performance capabilities in the Teraflop range for lattice QCD. We are planning to submit a final version of this proposal prior to the end of this fiscal year. The proposed timeframe for the acquisition of such a machine is 3 years. (D. Sinclair)

B. Experiments Taking Data

1. Soudan 2

The second half of 1990 was an exceptionally busy and productive time for the Soudan 2 experiment. Following the completion of the first half (550 tons) of the detector, two halfwalls (69 tons) of the second half of Soudan 2 were brought into full operation. The experiment operated for 125 days of livetime, giving a total exposure to date of 43% of a fiducial kiloton year. The installation of new online software reduced the event readout deadtime by a factor of four. The use of new diagnostic software and the installation of anode high voltage splitter hardware improved detector uniformity and efficiency. Time variation of the detector wireplane gas gain was eliminated by new software which automatically adjusts the anode high voltage to compensate for changes in atmospheric pressure. The Soudan 2 collaboration submitted a Letter of Intent to Fermilab for an experiment to search for neutrino oscillations in a beam aimed at Soudan 2, 800 km away.

Detector Operation

The Soudan 2 experiment recorded data for 125 days of livetime, giving a duty cycle of 69% during the second half of 1990. This brings the total exposure to 550 days, or 43% of a fiducial kiloton year for contained events.

The detector is operated for physics data primarily during night and weekend periods when installation work is not in progress and the underground laboratory is unoccupied (about 65% of the time). The improved duty cycle during the past six months is partly the result of new software which detects and corrects problems with the data acquisition process automatically.

The quality of the data from Soudan 2 has also improved significantly. The time variation of the wireplane gas gain has been almost completely eliminated by new software which automatically changes the anode high voltage to compensate for changes in atmospheric pressure. Commissioning of the new half-tube database software during the Summer allowed the responses of individual anode wires and cathode strips to be studied for the first time. It revealed that the gas gains of the edge anode wires in each wireplane were higher than those of the central wires. Increasing the edge wire offset voltage from 50 V to 75 V fixed this problem. In addition, a number of previously unsuspected electronics problems in individual channels, upstream of the point where calibration pulses are injected, were found and repaired. Finally, a major effort was mounted to repair a number of faulty channels in the active shield, increasing its efficiency and effective coverage.

The ISIS charged-particle test-beam calibration of a Soudan 2 module at the Rutherford Laboratory was completed during this period. The final data run used a special magnet to bend the beam up through the the bottom of the 5-ton module, perpendicular to the corrugated steel plates. The test beam data set now includes incident protons at 700 and 830 MeV/c, and pions, muons, and electrons at momenta between 140 and 400 MeV/c, for a variety of angles of incidence. (D. Ayres)

2. Spin Physics at LAMPF

Experiment (E-876) measured np elastic scattering of a polarized neutron beam from a liquid hydrogen target at 790 MeV. The momentum of the outgoing proton was measured in a magnetic spectrometer, and the proton spin determined in a carbon polarimeter. The outgoing neutron was detected in coincidence in the same neutron counter array used for E-960. ANL-HEP physicists

participated in the setup of the neutron counter array and some of the data collection. Preliminary values of the measured quantities K_{SS}, K_{SL}, K_{LS}, and K_{LL} are shown in Fig. 22. Additional running is planned on this experiment for late spring and summer of 1991, and perhaps 1992. The same parameters, and in addition K_{NN}, will be measured at 634 and 720 MeV in the future runs. A follow-on experiment to determine the neutron beam polarization more accurately has been proposed using the same apparatus (E-1234). This proposal will be presented to the LAMPF Program Advisory Committee in January 1991.

Finally, a new Department of Energy funding proposal was completed and submitted during the past six months. If approved, there will be new nucleon-nucleon measurements performed at the SATURNE accelerator in the Saclay Laboratory in France. The goals will include a determination of the isospin-0 nucleon-nucleon amplitudes up to ~ 2 GeV and measurements to understand structure seen in a number of pp elastic and total cross section spin observables as a function of energy near 2100-2200 MeV. This program is a logical extension of the LAMPF experiments that have been performed by the ANL group over the past 11 years. (H. Spinka)

C. Experiments in Preparation Phase

1. Collider Detector at Fermilab

The assembly of preradiator chambers for the CDF central calorimeter got up to speed and the first of the four calorimeter arches was instrumented. An in situ cosmic ray test has been developed as illustrated in Fig. 23. Although the fiscal year boundary caused a complete turnover in the technical manpower provided by Fermilab for assembling chambers, by the end of the year 33 of the minimum needed 96 were complete, and the rate had come back toward three per week.

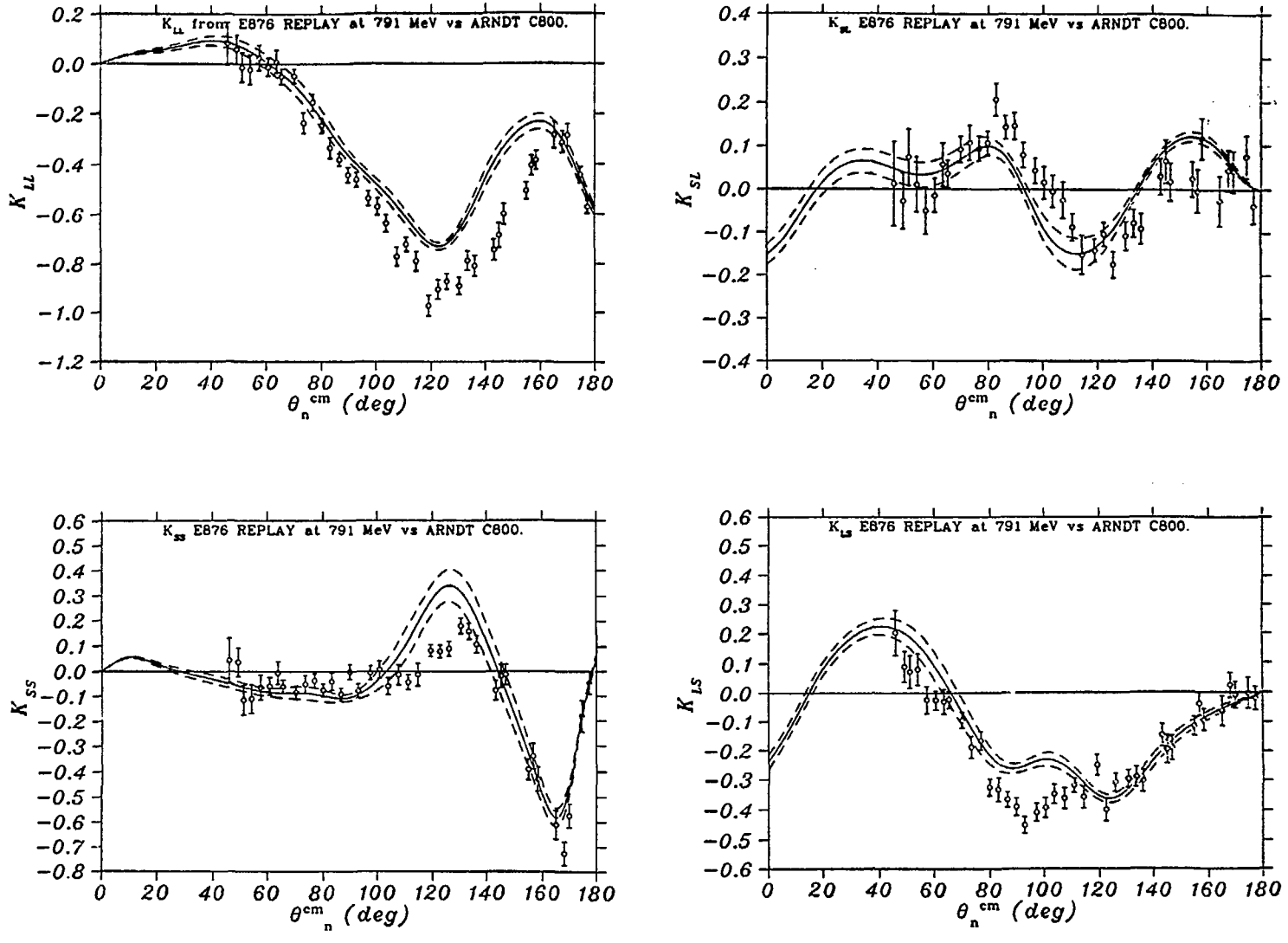

Fig. 22. Preliminary results from E-876 as a function of c.m. angle at a beam kinetic energy of 790 MeV. The curves are from a phase shift prediction of R. Arndt without the E-876 data included.

The current Fermilab long term schedule calls for nine months of running starting in late fall 1991 followed by five months for the linac upgrade installation then another nine months of collisions. Luminosity expectations are about 10^{31} for the first running period and 2 x 10^{31} for the second. After a year of fixed target running, the first multibunch run is expected in 94-95. If those luminosity projections prove realistic or conservative the CDF upgrade activity may need redirection as the central tracker viability in 94-95 would become a serious issue.

The CDF upgrade proposal is currently in the PAC process with questions and answers exchanged. A working group within CDF has been formed to consider the possible evolution of CDF for the study of b physics with CP violation in mind.

The Argonne group, along with Chicago and Michigan, is looking into improving the central electron trigger by including strip chambers and preradiator information at Level 2. This modification could be installed during the linac upgrade shutdown and would lead naturally to involvement in front end electronics for the multibunch era. (L. Nodulman)

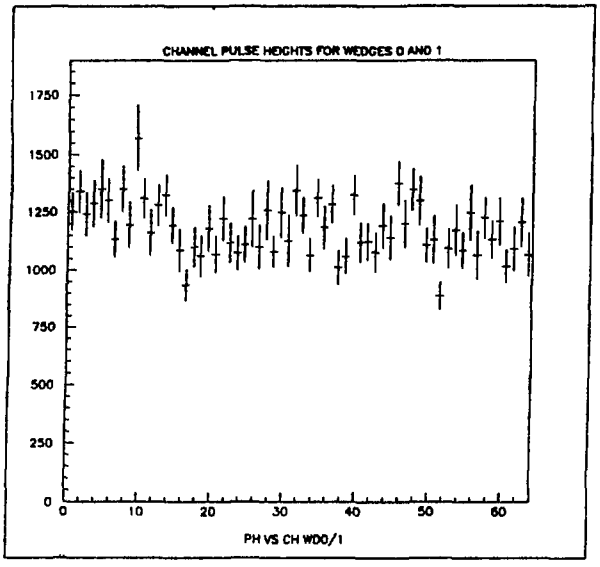

Fig. 23. Preradiator chamber post installation cosmic ray test results. The average pulse height (femtoCoulombs) for cosmics in each channel is plotted for four of the chambers installed on two 15° wedge calorimeter modules. The testing demonstrates that both the chambers and the installation are viable.

2. Soudan Detector Installation

The Soudan 2 experiment installation continued at a steady pace throughout the second half of 1990. Two additional halfwalls were installed and brought into operation, giving an operating mass of 619 tons. (A halfwall is a subassembly of eight 5-ton modules, stacked four across and two high.) The two new halfwalls were the first ones in the North half of the detector, and made use of new high-voltage, gas-purification, and calibration systems which had not operated previously. Twenty four 5-ton calorimeter modules were delivered to the Soudan mine site from the Argonne and Rutherford module factories during the period, bringing the total number of modules underground to 158 (679 tons).

A major upgrade of the Southeast quadrant took place during September, one month earlier than planned, in order to replace a 5-ton module with a broken anode wire (only the second broken wire in 18 months). The upgrade included installing anode high voltage splitters on 22 pairs of 5-ton module readout planes, which became accessible for the first time in over two years. The splitters allow individual readout planes to be operated at their optimum high voltages; previously, pairs of planes were constrained to operate at the same voltage.

The expansion of the fire protection system around the detector was nearly completed in December. Twenty new smoke detectors, which can shut off all electrical power in the event of an alarm, were installed and activated. In addition, special overcurrent detection circuits are being constructed at Argonne to turn off power to individual electronics racks when malfunctions occur. A prototype of this "smart fuse" electronics was installed and operated during the Fall.

New 8086 microprocessor online software was installed to reduce the readout deadtime. Data acquisition by the front end electronics may now proceed simultaneously with the CAMAC readout of the previous event. This reduces the the deadtime fraction from 8% to 2% at the current trigger rate of 0.4 Hz. This improvement will allow the entire 1000 ton detector to operate with an acceptable deadtime fraction. The increased data rate from the

growing detector also requires more computing power to allow the reconstruction processing and filtering of the raw data to keep up with data acquisition. To this end, three more VAXstations, additional disks, and memory upgrades to existing VAXstations were installed.

Installation of the new cosmic-ray air-shower surface array, which will operate in coincidence with Soudan 2, continued during the second half of 1990. The gas and high voltages systems were brought into operation, the turnon of the front-end electronics was completed, and much progress was made on the data acquisition system. Triggers from the underground Soudan 2 detector will cause the surface array data to be transferred to the underground computer. The surface array will measure the energies of the highest energy primary cosmic-ray showers which produce underground muon tracks in Soudan 2, and is expected to help determine the nuclear composition of the cosmic ray primary flux.

Soudan Activities at Argonne

The Argonne module factory completed the assembly of thirteen 5-ton module stacks (through Module #117) and fourteen pairs of readout planes (through Module #117). During the second half of 1990, sixteen U.S. modules were shipped to the Soudan mine site and one module was returned to Argonne to repair a stack problem which was not discovered until the module arrived at Soudan.

The Argonne electronics group completed construction of 47 sets of anode high voltage splitter units, which allow top and bottom modules in a halfwall to be operated at different anode high voltages. As originally designed, each anode wire of a top module is connected directly to the anode wire of the module below it in the halfwall. Both sets of wires run at the same high voltage and use the same preamplifiers. Because of small differences in readout plane gas gains, the optimum high voltage setting is sometimes different for top and bottom modules. The new hardware allows top and bottom modules to be run at different voltages while still using the same preamplifiers. This first production run was completed in time for the new

splitters to be installed during the upgrade of the Southeast quadrant, as described above.

The Argonne electronics group completed the fabrication of preamplifiers for the third quarter of the detector, which had been in progress for the past year. Production fabrication was started on a number "smart fuse" units, which monitor dc power supply currents in each electronics rack and can turn off the electrical power to the rack in the event of an overcurrent. The system allows current trip levels to be set much closer to actual operating currents than is possible with fuses, and provides improved protection against fires caused by short circuits in the electronics. Such fire protection measures are important because Soudan 2 operates unattended about 65% of the time.

Argonne physicists continued to play a major role in the installation, turnon, and data acquisition activities at the Soudan mine site. Important activities included installation and turnon of the new electronics and high voltage systems for the North half of the detector, and the upgrade of the high voltage control software to automatically adjust anode high voltage in response to atmospheric pressure changes.

In August the Soudan 2 collaboration submitted a Letter of Intent (P-822) to the Fermi National Accelerator Laboratory for a long baseline experiment to search for neutrino oscillations. A 30 GeV neutrino beam from the new main injector would be aimed at Soudan 2, 800 km away. The experiment would search for the appearance of tau neutrinos in the muon neutrino beam by measuring the neutral current to charged current ratio. Most tau neutrino events will appear to be neutral current events in Soudan 2. Argonne physicists took a lead role in the design study of this experiment, with particular emphasis on calculations of the neutrino beam flux and the expected sensitivity to oscillations. (D. Ayres)

3. ZEUS Detector at HERA

Excellent progress was maintained in HERA construction in the latter half of 1990, culminating in the cooldown of the proton ring in December. The projection was that detectors would be able to move in by June of 1991 for first operation. The BCAL installation was tentatively scheduled for April 1991.

Module Production. The delivery of uranium plates from Manufacturing Sciences Corporation was completed in November. It is expected that cladding operations at ANL will be concluded in January 1991, consistent with the schedule prepared in March 1989. This will constitute a remarkable achievement on the part of the system manager, R. Noland, and his crew. The stacking of both electromagnetic (EMC) and hadronic (HAC) sections proceeded very smoothly and by year end only three EMC and five HAC sections remained to be stacked. The actual completion of EMC stacking is expected to occur in February; the HAC stacking at ANL and KFA-Juelich will probably be completed in March.

In October, following assembly area enlargement at KFA-Juelich and extensive preparation by ANL, Ohio State and Louisiana State Universities, the scope of work at Juelich was enlarged to include mating EMC and HAC sections and final assembly for ten BCAL modules. This was started with the help of ANL technicians and will continue through March 1991 under the supervision of either an ANL or Ohio State physicist. By the end of year, some supply problems were emerging and action is required to ensure the production rate is not slowed. The floor layout at KFA-Juelich is shown in Fig. 24, there one may see five completed HAC sections in storage. Testing of completed modules is scheduled to begin in January. The status and disposition of all 32 BCAL modules as of December is summarized in Table I.

Module Calibration. The turnaround time on the cosmic ray stand settled down to two weeks per module by later in 1990. This included the laser light calibration, ^{60}Co source scan and cosmic ray data taking. The substantial problems encountered during the year in producing an encapsulated ^{60}Co source which would move freely down the source tubes installed in BCAL modules were finally overcome by December and source scanning promises to be routine.

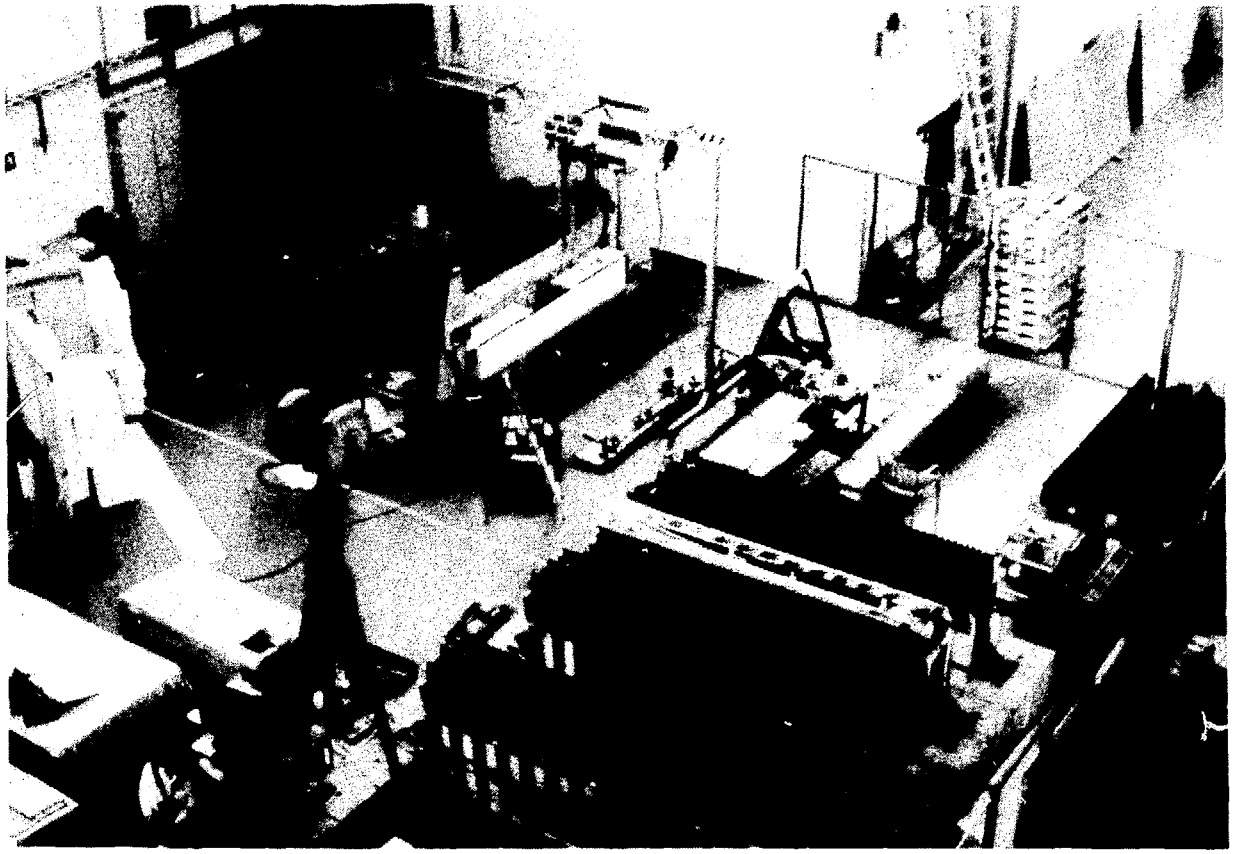

Fig. 24. The ZEUS BCAL module assembly area at the KFA-Juelich Laboratory.

Table I. Summary of ZEUS BCAL Module General Status.

MODULE NUMBER	STACKING STATUS	ASSEMBLY STATUS	PRESENT LOCATION	FINAL SIDE-COVERS	COSMIC RAY SCANNED	SOURCE SCANNED	TEST BEAM SCANNED	FINAL ELECTRONICS	REPAIRS/MODS NEEDED
#1	BUILT	COMPLETE	FNAL	YES	YES	YES		YES	
#2	BUILT	COMPLETE	DESY		YES	YES		YES	CONT. S. TUBE
#3	BUILT	COMPLETE	FNAL	YES	YES			YES	
#4	BUILT	COMPLETE	DESY		YES				
#5	BUILT	COMPLETE	ANL		YES	YES			YES
#6	BUILT	COMPLETE	DESY		YES				
#7	BUILT	COMPLETE	DESY		YES	YES			
#8	BUILT	COMPLETE	DESY		YES			YES	
#9	BUILT	COMPLETE	JUELICH	YES					
#10	BUILT	COMPLETE	DESY		YES				
#11	BUILT	COMPLETE	JUELICH						
#12	BUILT	COMPLETE	FNAL	YES	YES	YES		YES	
#13	BUILT	COMPLETE	JUELICH						
#14	BUILT	COMPLETE	DESY		YES	YES			
#15	BUILT		JUELICH						
#16	BUILT	COMPLETE	DESY		YES	YES			
#17	BUILT		JUELICH						
#18	BUILT	COMPLETE	DESY		YES	YES			
#19	BUILT		JUELICH						
#20	BUILT	COMPLETE	ANL		YES	YES			
#21	BUILT	COMPLETE	ANL	YES	YES	YES			
#22	BUILT	COMPLETE	ANL	YES	YES	YES			LASER SYST.
#23	BUILT		JUELICH						
#24	BUILT	COMPLETE	ANL	YES					
#25	BUILT		ANL						
#26	EMC ONLY		ANL						
#27	EMC ONLY		ANL						
#28	EMC ONLY		ANL						
#29	EMC ONLY		ANL						
#30	NICHTS								
#31	NICHTS								
#32	NICHTS								

The test beam in Lab E at FNAL, which was modified for ZEUS BCAL calibration, was finally commissioned in June - August. Some data were taken for three BCAL modules installed on the 'θ-ϕ' stand. However, because of the many problems encountered with the beam, these data were of limited use in understanding calorimeter performance in detail. It was possible, however, to check the optimal thickness of lead absorber required between modules in order to smooth out the inter-module gap perturbation of the calorimeter response; with this decided, the contract for the final module side covers was placed. Final side covers were installed on three modules by the end of the year.

It is hoped that extensive calibration of at least four BCAL modules can be carried out in the period January through March of 1991.

Module Shipping. Shipping of modules to DESY from ANL began in July and is summarized in Table I. No major problems were encountered although it is now decided to install nonreuseable, maximum g-force accelerometers on all modules to further monitor the process.

The procedures for checking modules received at DESY were established in this period, and the DAQ facility plus source scan manipulator to accomplish this were checked out at ANL before sending them to DESY in December. This checkout system will be used starting in January and is being set up by ANL and OSU personnel. Most of the modules presently at DESY will need to be retrofitted with the final module side covers, which include 0.75 mm of lead sheet. The final checkout will include laser light calibration and ^{60}Co source scan before installation in ZEUS.

Calorimeter Trigger. In December, an important step was taken in integrating the first level calorimeter trigger with the global first level trigger. This was done at DESY, and it involved both ANL and University of Wisconsin personnel. It is discussed in detail under Experimental Facilities. (B. Musgrave)

II. THEORETICAL PROGRAM

Theorists in the High Energy Physics Division have pursued a diverse range of topics covering both the formal and phenomenological aspects of particle theory.

Transverse Momentum Distributions for W and Z Bosons

work in this area by P. Arnold and R. Kauffman described in the previous semiannual report has now been published as Nucl. Phys. B349, 381 (1991).

Bottom-Antibottom Quark Correlations at the Fermilab Collider

E. Berger and R. Meng are studying bottom-antibottom quark correlations to next-to-leading order in α_s in QCD for the full range of the transverse momentum p_T of the quark pair. In the range $p_T << M$ they include the leading double log contributions to all orders in α_s. Their calculations should shed some light on questions relevant to a possible b-factory at the Fermilab collider. They could also provide a good test of QCD when experimental data become available. This research is continuing.

Calculations of Prompt Photon Production in QCD

Cross sections for prompt photon production at collider energies are not strictly inclusive because an isolation requirement is imposed whereby the photon is detected only if accompanied by a restricted amount of hadronic energy. In a recent paper ANL-HEP-PR-90-104 submitted to Physical Review, E. Berger and J.-W. Qiu provide a consistent treatment of the isolated prompt photon cross section in QCD perturbation theory. The isolation requirement reduces sensitivity of the cross section to poorly known long-distance fragmentation contributions. However, the normal cancellation of infra-red singularities is upset by the isolation cutoffs, rendering the short-distance perturbative calculation highly nontrivial. In their solution, Berger and Qiu address both the short- and the long-distance issues in detail, showing that well behaved predictions can be drived for a wide range of isolation

parameters. Scale dependence of the cross section is also examined.

Sextet Quarks and Collider Diffractive Physics

A. White and K. Kang (Brown University) have continued their work on the idea that a new threshold is implied by current measurements of the real part of the forward elastic scattering amplitude at CERN and the total cross-section at Fermilab. They have argued that this threshold could be related to exotic diffractive phenomena seen for some time in cosmic ray experiments and could have a fundamental explanation as due to a new color-sextet quark sector of QCD. They have made a number of presentations at recent conferences including the Fourth Asia Pacific Conference, the XXth International Symposium on Multiparticle Dynamics, and Beyond the Standard Model II. The emphasis of the talks has been on a particular outcome of their analysis that a short-lived axion-like sextet "eta" with a mass around 30 GeV with two photons as a major decay mode, should be produced diffractively in hadron colliders. (A recent paper by Hatsuda and Umezawa shows that this state could also be observed as a rare radiative Z decay at LEP). Written versions of the conference talks are available as both Argonne and Brown preprints.

Transverse Momentum Distribution of Higgs Bosons

R. Kauffman has calculated the transverse-momentum distribution for Higgs bosons at the SSC. For intermediate-mass Higgs bosons (50 GeV $< M_H <$ 200 GeV) the dominant production mechanism is gluon-fusion which proceeds through a top-quark loop. At large transverse momentum ($p_T \approx M_H$) the distribution is well-approximated by the leading-order processes: $gg \to Hg$, $gg \to Hq$, and $q\bar{q} \to Hg$. However, at small transverse momentum ($p_T << M_H$) the perturbative result for $d\sigma/dp_T^2$ diverges as $1/p_T^2$. Furthermore, the perturbation expansion contains large logarithms of the form $\log (M_H/p_T)$. These large coefficients signify the breakdown of the perturbation expansion. In order to cure this breakdown it is necessary to sum processes involving emission of multiple gluons. Such a resummation has previously been done by Hinchliffe and Novaes in the limit that the heaviest quark in the loop (presumably the top quark) is much heavier than the Higgs boson. However, with the top quark mass bounded

below 200 GeV, this is not a realistic scenario. Kauffman has found that the kinematic structure of the heavy quark mass limit is reproduced at any m_t in the limit $p_T << M_H$. Using this information, he has performed the resummation of soft gluons at small p_T and found that the shape of the distribution at small p_T is independent of the heavy quark mass.

In order to obtain a distribution valid at intermediate p_T it is necessary to add in the non-divergent terms, i.e., those that are not resummed. Kauffman has calculated these terms by taking the difference between the perturbative expansion of the resummed result and the perturbative result itself. The resulting distribution matches the soft-gluon resummation with the high-p_T perturbative result and is more accurate than either. A paper is being prepared for publication.

Higgs Boson Effects on Top Quark Polarization

D. Sivers is studying the polarization of top quarks produced in e^+e^- and hadron-hadron collisions. For the top quark, the Yukawa coupling to the Higgs sector is comparable in magnitude to the QCD coupling. Unitarity provides a relation between the polarization and the forces in the $t\bar{t}$ channel so the t-quark polarization is a measure of the Higgs sector. In ANL-HEP-PR-90-93 he calculated the polarization associated with Higgs exchange in $e^+e^- \rightarrow t\bar{t}$ and found it to be significant. The process $GG \rightarrow t\bar{t}$ is being studied in collaboration with G. Goldstein of Tufts.

Top-Quark Decay Distributions

The latest limit from CDF places the top quark mass above 89 GeV so that it invariably decays into a bottom quark plus a real W boson. With this decay channel open, the top quark decays quickly such that a measurement of its lifetime would be very difficult. R. Kauffman has studied the polarization of W's produced in top quark decay: a quantity which is both measurable and probes the top quark couplings and the dynamics of top quark decay. The relative widths for the three polarizations of the W are reflected in its angular decay distribution.

The cleanest measure of the W polarization is from semi-leptonic decays. However, the missing momentum of the neutrino disallows full reconstruction of the W. With knowledge of the top quark mass the angular distribution can be reconstructed from the dot product of the electron and b quark momenta. Information on the top quark mass can be gained from two sources. First, if the wrong top quark mass is used in extracting the angular distribution then the distribution will exceed its physical endpoints. Kauffman has shown how this "overflow" contrains the top quark mass. Secondly, the shape of the angular distribution varies as m_t^2, so the shape gives information on m_t as well. Kauffman has also calculated the angular distribution in the presence of right-handed couplings of $t \to bW$. (ANL-HEP-CP-90-98).

Anomalous Baryon Violation

P. Arnold and M. Mattis (Los Alamos National Lab) have continued to focus on the controversy of whether the weak interactions necessarily become strong at energies around 10 to 100 Tev. The speculation arose from a low-energy calculation done by Ringwald and Espinosa using instantons. Arnold and Mattis have shown how the high-energy corrections to the instanton result can be organized by finding an appropriate distortion of the low-energy instanton. They are currently working on extending this procedure to a full high-energy calculation. They have also just computed the next-to-leading order corrections in the energy $E \to E \to 0$. This is an important diagnostic for checking the suggestions of various authors for computing the rate at arbitrary energy.

Baryon Number Violation in High Energy Collisions

't Hooft showed many years ago that the electroweak instanton induces a low-energy effective Lagrangean which gives rise to processes such as $uu \to \bar{d}e^+\bar{c}ss\nu_\mu\bar{t}t\bar{b}\tau^+$, but with an unobservably small amplitude: $\exp(-8\pi^2/g_2^2) \sim 10^{-80}$ Recently, Ringwald and others have attempted to calculate the electroweak-instanton-induced amplitudes for scattering to final states in which the fermions are accompanied by large numbers of gauge and Higgs bosons, using the

naive instanton approximation. Their results suggested that the total cross section for B+L-violation might become large enough to be observed at SSC energies.

In Phys. Rev. Lett. 65 (3377) 1990, R. Meng (in collaboration with G. Farrar, Rutgers University) studied the phenomenology of baryon number violation induced by the electroweak instantons. Farrar and Meng find that if the naive-instanton amplitudes were valid for arbitrarily high energies, the event rate at the SSC could be a few per hour. A typical event would consist of 3 "primary" antileptons and 7 "primary" antiquark jets, accompanied by ~ 85 electroweak gauge bosons, having a sharp threshold in the total subenergy at about 17 TeV. However, the instanton approximation is not valid at such high energy (above the sphaleron energy), so that the question of the experimental observability of baryon number violation in high energy collisions cannot be convincingly addressed theoretically until a reliable computational scheme for energies higher than the sphaleron is developed.

Quantum Algebras

In the aftermath of the Argonne Workshop on Quantum Groups, (April 16-May 11), C. Zachos and D. Fairlie (Univ. of Durham, U.K.) turned their attention to Multiparameter Quantum Heisenberg Algebras Phys. Lett. 256B (1991) 43. Quantum algebras appear in nature when symmetric structures are perturbed by anisotropies, minute violations of a principle, or quantum corrections. There have been several works in the literature lately which attempt to systematize experimental limits on the absolute validity of Pauli's exclusion principle in atomic physics--so far negative ones. These works rely on a one-parameter family of q-oscillators to build the appropriate Hilbert space in which the potential violations of the exclusion principle would manifest themselves. Zachos, however, noted that these efforts were actually nonassociative, thus greatly circumscribing their physical import. With Fairlie, he undertook a systematic search for associative q-oscillators, i.e., oscillators whose deformed algebra depends on a number of parameters. These parameters may be roughly thought of as a road to interpolate between Fermi and Bose statistics, thereby describing "anyons", also of some use in modelling high T_c

superconductivity. The general solution they found was new and promising, involving the largest number of parameters encountered in this context so far. It led to the construction of new deformations of GL(N) that bear some (perhaps remote) hope for understanding features of the standard model; it also solved a number of technical problems.

Invited to summarize the subject at the "Symmetries in Science V" conference in Schloss Rofen (Austria), Zachos wrote an introductory overview of quantum algebras, which is proving helpful to physicists interested in accessing the field and is being expanded and updated to a longer review than the one appearing in the proceedings of that conference [ANL-HEP-CP-90-61].

Oscillators may also be interpreted as coordinates and derivatives, so that q-oscillators define new noncommutative manifolds, actively explored by, e.g., Manin, and Wess and Zumino. S. Vokos investigated the differential geometric structure of the above mentioned new class of quantum algebraic solutions, as well as the already known solutions of Pusz &Woronowicz and Wess & Zumino. Vokos constructed the corresponding general multiparametric algebra of quantum-GL(N): this extraordinary structure is based on the realization of the quantum version of the general linear group of NxN matrices in a basis of the above q-oscillators. He thus provided the most general formulation of this algebra, complete with its comultiplication, i.e., the rule of combining representations ("addition of angular momenta"). He then discovered that these results reduce to the special case of quantum-GL(2) that Schirrmacher, Wess and Zumino constructed out of the covariance group of a quantum plane. Such a connection had not been universally anticipated. He is pursuing applications of this discovery. [ANL-HEP-PR-91-07].

Analytic Multi-Regge Theory and the Pomeron in QCD

A. White is preparing Part II of a long article on the Pomeron in QCD. Part I (which will shortly be published in the International Journal of Modern Physics A) is a development of the general formalism of analytic multi-Regge theory based on the analyticity properties of many-particle amplitudes. The review aspect of Part II covers known results on the Regge behavior of vector

bosons and fermions in spontaneously-broken gauge theories and the organization and extrapolation of these results into a full reggeon diagram description of the high-energy behavior of such theories. The aim of the original development of Part II is to extract the high-energy behavior of QCD (that is the Pomeron) via an infra-red analysis of the reggeon diagrams describing the corresponding spontaneously-broken theory-as the symmetry-breaking is systematically restored. A key part of the analysis is the role played by massless fermions in producing a reggeon-condensate at the stage when the full SU(3) gauge symmetry is partially restored to SU(2). This condensate is identified with the Pomeron condensate of the super critical theory described in Part I. As a result, contact is made between the critical and super critical Pomeron theories described in Part I and the Pomeron in QCD.

Large N_c Hadrodynamics

A chasm of ignorance separates quantum chromodynamics (the theory of quarks and gluons) from quantum hadrodynamics (the theory of baryons and mesons). One bridge across that chasm is supplied by the large N_c limit, N_c being the number of colors. P. Arnold and M. Mattis (Los Alamos National Lab) have shown that, to leading order in $1/N_c$, an infinite class of arbitrarily complicated exchange-diagram contributions to meson-baryon scattering and to the baryon-baryon potential can be summed in closed form. The result is a set of coupled nonlinear differential equations strongly reminiscent of vector-meson-augmented Skyrme models. This work has been published in Phys. Rev. Lett. 65, 831 (1990).

Semi-Inclusive Deeply Inelastic Scattering at HERA

In anticipation of experiments at the HERA Electronen-Proton Collider, R. Meng (in collaboration with F. Olness and D. Soper from the University of Oregon) has proposed a measurement of angular distributions of hadronic energy with respect to the scattered electron direction at HERA. Meng and collaborators have shown that this measurement is another good test of quantum chromodynamics. The measurement has the merits of having small systematic

errors and allowing parity violating contributions to be separated from parity conserving contributions in the same experiment. Meng et al. also found an effective kinematic cut to increase the gluonic contributions in semi-inclusive deeply inelastic scattering which is significant for measuring gluon distributions in the proton.

Spin Observables in $\gamma D \to pn$ at Large Angles

The process $\gamma D \to pn$ has been found experimentally to obey a scaling law,

$$\frac{d\sigma}{dt} \approx \frac{f(\theta)}{s^{11}} \quad (1)$$

at fixed angles. This suggests that the photodisintegration of the deuteron can be used to test ideas in the application of perturbative QCD to exclusive processes. In work presented at the Argonne Workshop on Nuclear and Particle Physics, D. Sivers proposed a model for the independent helicity amplitudes for $\gamma D \to pn$ that is based on perturbative QCD and the effective amplitude approximation. These amplitudes can be used to predict a number of spin observables which are accessible experimentally. Proposals to do experiments with polarized photons on deuteron targets are in the planning stage and the work is being continued with an eye to future publication.

Gluonic Contribution to the Proton's Spin-Dependent Structure Functions

Several years ago, the proton's spin-dependent structure function g_1 was measured by the EMC collaboration. The value of the first moment of g_1 deduced from that measurement is consistent, in the naive parton model, with the statement that none of the proton's spin is carried by the spins of the quarks. It has been suggested that this surprising conclusion might be avoided by invoking the presence of a hard gluonic contribution to the first moment of g_1.

Some time ago G. Bodwin (ANL) and J.-W. Qiu (SUNY Stony Brook) pointed out that the presence or absence of such a hard gluonic contribution is entirely a matter of the factorization convention chosen in defining the spin-

dependent quark distributions. Bodwin and Qiu showed that, if the ultraviolet regulator used in defining the quark distributions respects parton-level analyticity and gauge invariance of Green's functions, then the hard gluonic contribution to the first moment of g_1 vanished. They also showed that one can obtain a non-vanishing hard gluonic contribution by defining the quark distributions through the use of a k_T-cutoff regulator.

More recently, Bodwin and Qiu have found that such a k_T-cutoff procedure corresponds, in operator-product-expansion language, to a mixing between matrix elements of the axial-vector current and a gluonic operator. The gluonic operator's expectation value in the proton state corresponds to the spin-dependent gluon distribution. The operator matrix elements can be written in a form that is local, but gauge variant, or in a form that is manifestly gauge invariant, but nonlocal. There is no gauge-invariant, local form--which is why such an operator does not appear in conventional operator-product analyses. This work was presented at the Polarized Collider Workshop at Pennsylvania State University, and the contribution to the proceedings of that workshop is available as ANL-HEP-CP-90-125. A publication describing further details of the work is in preparation.

Direct Photon Production in Polarized pp Collisions

In a paper to be published in the proceedings of the Polarized Collider workshop held at Pennsylvania State University, E. Berger and J.-W. Qiu argue that inclusive direct photon production at large transverse momentum in proton-proton interactions with longitudinally polarized beam and target is an incisive probe of the polarized gluon distribution in a proton. They provide predictions of cross sections for a range of reasonable choices of the polarized gluon distribution. At current fixed target energies, the cross sections are small but measurable. At collider energies, such as the SSC energy, isolated direct photon production should be considered in order to minimize the nonperturbative contribution due to fragmentation.

Spin Amplitudes for NN → NN

Work in this area was described in the previous semiannual report. During the period reported on here an early version was reported.

The Standard Model on the Lattice

Recently, G. Bodwin (ANL) and E. Kovac (Fermilab) proposed a new method for implementing gauge theories involving chiral fermions on the lattice.

Linearized QED on the Lattice

There has been a good deal discussion in the literature in recent years regarding a conjecture that the short distance, strong-coupling limit of QED, as a stand-alone theory without electroweak unification, is well-defined and non-trivial. This conjecture, if true, would open the possibility that theories that are not asymptotically free might, nevertheless, be meaningful. Such a conclusion would have important implications for our understanding of field theory in general and for specific attempts at model building.

Lattice simulations are one tool for exploring the strong-coupling limit of QED. A difficult problem in such lattice simulations is to distinguish universal strong-coupling physics from lattice artifacts. In order to test the independence of lattice results from the specific lattice formulation, Hands, Kogut, and Sloan have proposed an alternative lattice formulation of QED, which is known as linearized QED.

Recently, G. Bodwin (ANL), E. Kovacs (Fermilab), and J. Sloan (Ohio State) have pointed out that linearized QED is not an adequate lattice transcription of continuum QED in perturbation theory. Although, linearized QED possesses a formal gauge invariance, Bodwin, Kovacs, and Sloan have shown that, because of the presence of massless modes associated with the gauge denominator of the transverse photon, one cannot use Ward identities to draw the usual conclusions about renormalization counterterms. In particular, the transverse photon develops a quadratically divergent mass, light-by-light scattering is logarithmically divergent, and, even in the absence of dynamical

fermions, the coupling constant undergoes a finite renormalization ($Z_1 \neq Z_2$). These findings cast serious doubt on the utility of linearized QED. A publication describing this work is in preparation.

III. EXPERIMENTAL FACILITIES RESEARCH

A. Mechanical Support

ZEUS

Construction. During the period July 1, 1990 to December 30, 1990 Argonne completed 6 BCAL modules, and a similar number were completed at KFA Julich. The plan for complete assembly of modules at KFA was implemented and work commenced at KFA during this same period. This plan was devised in order to relieve the need for shipping partially completed modules from KFA to Argonne for final fitting and instrumenting. The modules completed at KFA will go directly to DESY Hamburg.

Shipping. The shipping containers and their internal support and damping systems that were designed and built at Argonne were used for the first time to ship ZEUS module # 5 from Julich to Argonne. The system performed as expected with only minor problems.

Also during the six month period ending in December, module # 7 was shipped from KFA to Argonne and 10 completed modules were shipped to DESY Hamburg.

Installation. Work was started on writing procedures for final installation of the modules into the BCAL, and the design of the necessary fixtures for alignment was started. These tasks will be completed early in 1991 to meet installation schedules.

Proton Decay (PDK)

Steel. An order was placed for corrugated steel plates to complete 15 modules. This steel will provide enough for approximately half of the 1991 module assembly schedule.

Module Construction. During the six month period July to December 1990, 14 PDK modules were completed along with their associated wire planes and high voltage distribution boxes. Modifications were completed on the stacking press to provide more flexibility during the compression phase of module construction. Modules were shipped to the mine at Tower, Minnesota to keep pace with the installation.

Collider Detector at Fermilab (CDF)

Preradiator Chambers. After two Fermilab temporary technicians were trained to assist in the assembly of the preradiators, the rate of construction was up to approximately 10 chambers per month. These technicians were laid off in October and a new group of Fermilab techs were brought on board. The rate of construction slowed, but 24 chambers were built between July and December. Twenty four chambers were mounted on one arch at Fermilab in September and tested.

Solenoidal Detector Collaboration (SDC)

A design study for a depleted uranium/scintillator calorimeter was started prior to July, but most of the work was done during the six month period July - December 1990. This study was conducted in collaboration with our industrial partners, Westinghouse Science and Technology Center, Pittsburgh. A decision to use a lead-scintillator design was made, primarily driven by the cost of depleted uranium and the preliminary structural analysis which indicated good stability using lead as the absorber instead of uranium.

Further work was done on lead alloys and reinforcement by Westinghouse under the guidance of Argonne physicists and engineers.

With the addition of a new mechanical engineer to the Mechanical Support staff, work on the SDC electromagnetic calorimeter was begun in earnest. The EM test section that will be used in the Fermilab test beam in early 1991 was designed and the finite element analysis for this section was completed. Fabrication of the test section will commence in January for completion in March of 1991.

Wakefield

Some design effort was commenced late in this period for the wake field program; this effort was primarily on the Phase 0 of the preaccelerator section of the wakefield accelerator project.

Tiger Team Inspection

The Mechanical Support Group personnel contributed a major portion of the effort that went into the Division's self assessment in preparation for the Tiger Team inspection and carried out many of the corrective actions necessary following the formal inspection in September. The group has also continued to work on procedures and corrective measures since the inspection. (N. Hill)

B. Electronics Support

Construction and repair support for the Soudan Nucleon Decay experiment continued. The following is a summary of this work:

a) Smart Fuse Protection System	Designed and produced prototype
b) Fan Units	Produced 4
c) Drift High Voltage Modules	Produced 3
d) Anode High Voltage Modules	Produced 3
e) Top/Bottom Splitter Cards	Produced 100
f) High Voltage Feeder Cards	Produced 26
g) Gas Over-Pressure Protection Control	Produced 1
h) Anode Front Preamp Card	Produced 26
i) Anode Back Preamp Card	Produced 28
j) Long Cathode Front Preamp Card	Produced 48
k) Long Cathode Back Preamp Card	Produced 48
l) Short Cathode Front Preamp Card	Produced 16
m) Short Cathode Back Preamp Card	Produced 16
n) Calibration Pulse Driver Card	Produced 48
o) Battery Effect Filter -	Produced 24
p) Tuft's Voltage Sensing Cards	Produced 12
q) Repaired existing electronics as required	

A major area of effort during the period was on the ZEUS Calorimeter First Level Trigger Processor (CFLTP). The sixteen different algorithm cards were designed and the designs captured in ORCAD, the CAD software we use. A prototype of the communication card was built and taken to DESY for the first integration tests with the Global First Level Trigger being built by our collaborators from Tokyo University. These tests were run in December and all objectives were achieved. The tests involved exercising the handshake protocols, generating first level accepts from dummy calorimeter data in the CFLTP, and exercising the crossing number synchronization logic. An extensive integration test is planned for May 1991. The DC Test Stand which we had built was run for several months collecting stability data on calorimeter modules. The DC Test Stand will be shipped to Julich in January 1991 and will be the only test facility there for the ZEUS Calorimeter modules which will be stack at Julich. An agreement was made with the group doing MHD Propulsion research to handle the data acquisition system for the tests which will begin in March/April 1991. A conditioning amplifier was designed, production was begun, and all parts required were ordered. This data acquisition system is very similar to the ZEUS DC Test Stand, and therefore requires very little engineering effort. A major effort was made to have our facilities ready for the Tiger Team Inspection. This included putting in place our new quality control and inventory control procedures as well as cleaning up the lab and eliminating safety violations. (J. Dawson)

C. Polarized Target

The two-spin portion of FNAL E-704 ended in July and the polarized target operation was shut down. The target material was extracted and weighed. This was necessary, since E-704 included some total cross section measurements. A short report was prepared concerning the measured target constant and the estimated helium background.

The cause of the observed air leakage into the mixer insulating vacuum space was investigated and found to originate in a pinhole burned in the

microwave vacuum window. It is not yet known why this happened. Some work was done on the Dilution Refrigerator thermometry board in order to reduce sensitivity to room humidity.

A summary of the technical aspects of the target operation for the period of April through July was prepared and distributed to the collaboration. An analysis of the target calibration data remains to be done.

Some effort was devoted to prospective planning and the development of budgetary estimates for the modifications to the target that would be needed for the next scattering experiment. As a part of this, a market search was performed for high frequency microwave sources. The conclusion was that the highest frequency at which adequate power is currently obtainable is 140 GHz.

Considerable time was spent on DIN-list activities. The major task was general housecleaning of the target labs, offices, and the material test area in building 366A. The inventory of polarized target chemicals was substantially reduced, and material safety information was collected for the remaining inventory. (D. Hill)

IV. ACCELERATOR RESEARCH AND DEVELOPMENT

A. Advanced Accelerator Test Facility (AATF) Program

The principal activity at the AATF during this period involved the measurement of wakes in a prototype 11 GHz (X-Band) accelerating structure in collaboration with physicists from SLAC. The eventual goal of this work is the study of schemes to suppress multibunch instabilities in the Next Linear Collider (NLC) by damping or detuning parasitic deflecting wakefields in the accelerating cavities. This initial experiment was performed using a simple iris-loaded structure to demonstrate that wakes could be measured with sufficient sensitivity in this class of device. Of particular concern was whether drive and witness beams could be tuned through the 7 mm aperture of the structure. This proved not to be difficult, and the wake measurements were easily carried out. Figure 25 shows the longitudinal and transverse wakes for this device. A detuned cavity (in which the individual cells are designed to have identical TM01 frequencies but a spread in HEM1 frequencies) is presently under construction at SLAC, and it is expected to be ready for experiments early in 1991.

B. Progress on the Argonne Wakefield Accelerator (AWA)

The AWA is a new facility for the study of high gradient wakefield acceleration, having as its goal a 1 GeV demonstration wakefield-based linac. Phase-I of the AWA has been approved and will consist of a high current photoinjector, 20 MeV preaccelerator, and a new wakefield facility providing significantly better measurement capabilities than the AATF. Work on the mechanical design of AWA Phase-I neared completion during this period, and various issues of component placement and fabrication were resolved. The focussing solenoid design was finished, as was the optics design of the new wakefield beamlines. It is currently planned to reuse as many magnets from the AATF as possible. The layout for Phase-I of the AWA is shown in Fig. 26. Note that in keeping with our heightened awareness of laboratory safety the shielding has been modified to allow for a second egress at the downstream end of the facility. Work on the preliminary safety analysis report (PSAR) for

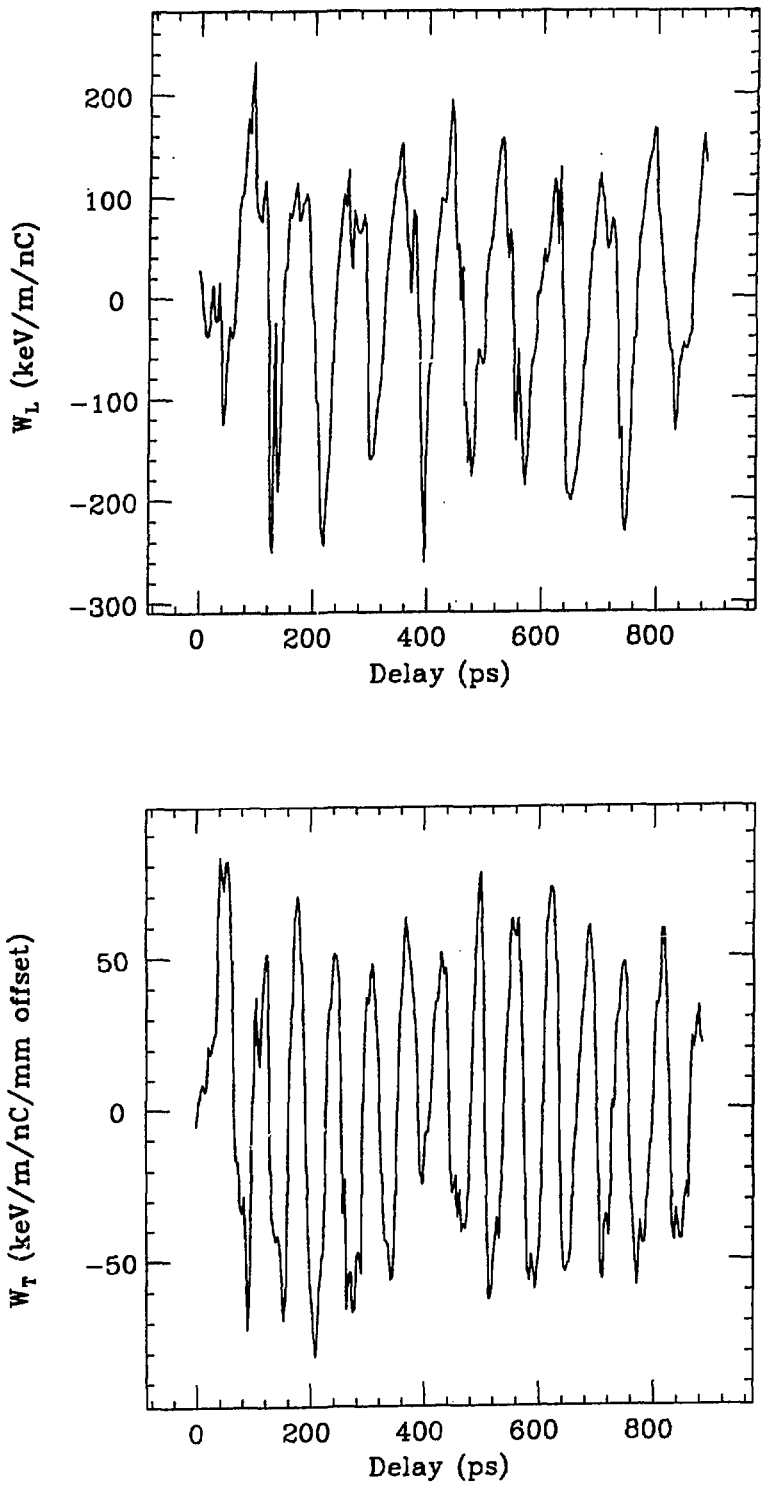

Fig. 25. AATF measurements of the longitudinal and transverse wakes in a prototype SLAC X-Band structure.

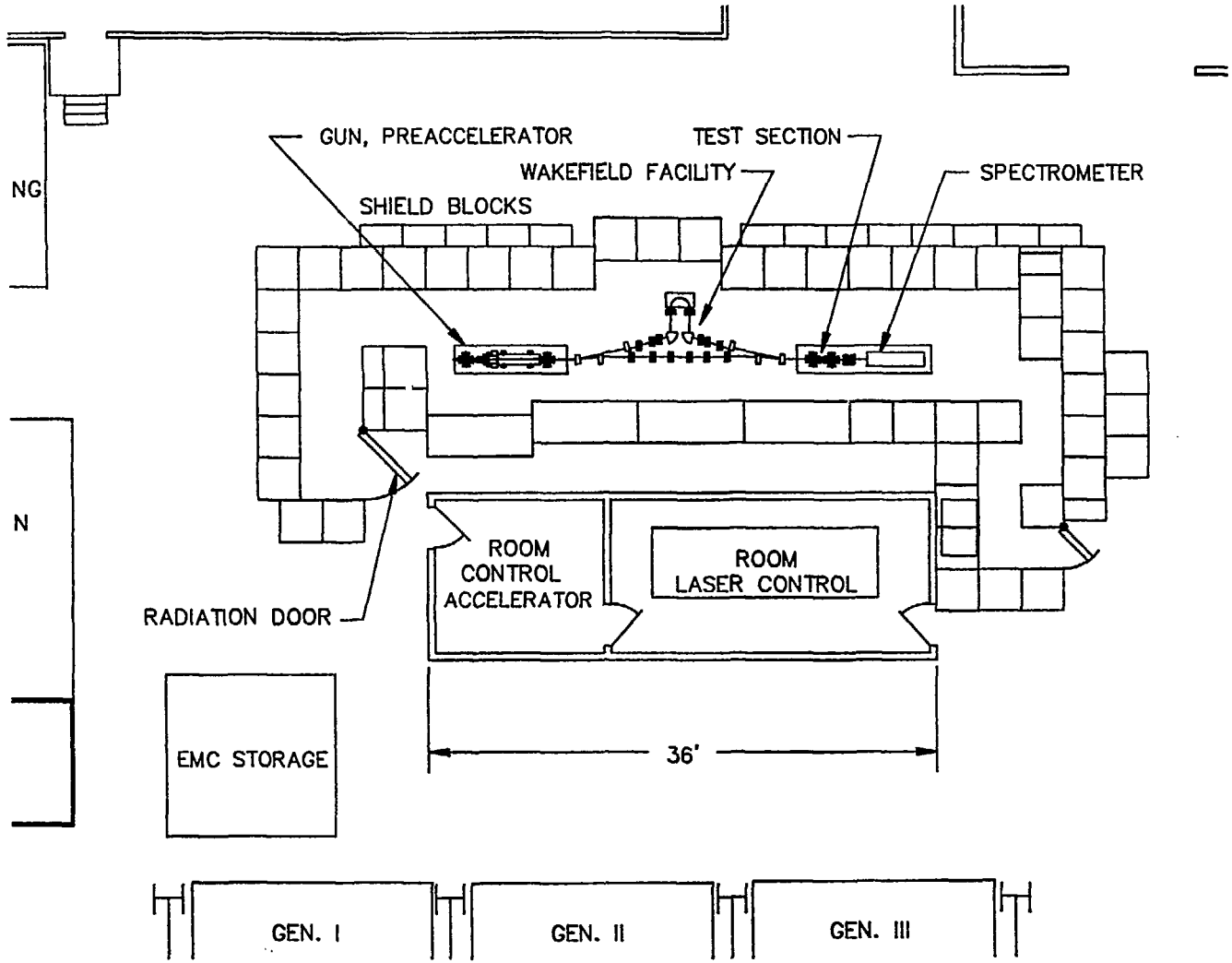

Fig. 26. Layout of the Argonne Wakefield Accelerator, Phase-I.

the AWA has been initiated. The specifications for the rf system were completed and a formal request for quotes was issued. All bids are expected to be submitted for technical evaluation by the end of January 1991. The RFQ for the laser system should also be ready by this time. An amplitude stabilization system ("noise eater") for the laser is under development. A fraction of the laser pulse will be split off to a fast photodiode which controls a Pockels cell. This in turn provides a feed-forward amplitude adjustment on the main laser pulse. It should be possible to hold the pulse to pulse jitter at the 1% level using this scheme. The assembly of this system is now complete, and tests will begin shortly using a laser in the ANL Chemistry division. A vacuum test stand was constructed in building 366. This will provide experience in the high vacuum techniques required for the AWA as well as an opportunity to test the various pumps and controllers. A program to control the vacuum system from a PC has also been developed.

C. Accelerator Physics

A serious concern relating to high gradient wakefield acceleration is the deflection of the tail of the drive bunch by the transverse wakes of the head, the so-called beam breakup instability. A particle simulation code (BBU) to model beam breakup effects in dielectric wakefield devices was developed. BBU uses the analytic wake potentials to compute the forces on a drive bunch with a specified initial offset from the device axis. External focussing fields may also be imposed. Initial results are in accord with previous calculations based on a single mode approximation, which show that the use of external focussing can control this instability in a useful high gradient device. The possible use of coupled wake tube devices to accelerate ion beams was investigated. In this geometry the luminal wake produced by an electron drive bunch is fed to a dielectric structure with the same frequency but a phase velocity equal to the injection velocity of the ion beam to be accelerated. While high gradients may in principle be attained in this fashion, the concomitant low group velocity in the accelerating tube results in significant energy loss by the wakefield rf pulse, leading to an unacceptably low efficiency. (P. Schoessow)

V. SSC DETECTOR RESEARCH AND DEVELOPMENT

A. Overview of ANL SSC Related R&D Programs

SDC Detector

The SDC Detector collaboration passed several milestones during the second half of 1990, including approval by the Laboratory to receive funding for the next stage of engineering. This next stage will culminate with the submission of the proposal in April 1992.

The SDC technical organization came into full activity during this period. Many of the working groups and technical steering committees took advantage of the Snowmass Workshop, which brought much of the collaboration together for an extended period, to meet at length and map out plans of work. Included were working groups on calorimetry, computing and physics, which are cochaired by Argonne physicists. Technical developments led or participated in by Argonne physicists included the following:

1. Study of calorimeter options and selection of technologies for engineering support during FY 1991. Starting with a calorimeter review at Snowmass in June and continuing through the November, 1990, collaboration meeting at LBL, the calorimeter steering committee and working group studied the four styles of calorimetry still being actively pursued: scintillator tiles, scintillator fiber, liquid argon, and warm liquid. In November, the steering committee recommended support of engineering for scintillator plate and liquid argon systems, with continued R&D on warm liquid. The latter technology is principally of interest as an option for the forward ($|\eta| > 3$) calorimetry. Argonne and Fermilab are leading the collaboration's effort on scintillator plate calorimetry (see discussion of major subsystem R&D below).

2. Physics calculations for the Letter of Intent (LOI). The Physics working group put most of its efforts into answering the questions posed by the PAC (a) after the Expression of Interest, due at the end of the Snowmass meeting; and (b) for the LOI, due November 30.

3. Magnet style selection. A task force chaired by an Argonne physicist, worked from July to September to recommend which style of magnet to use in SDC. Options considered were "Long" (extending through the calorimeter), "Short" (extending to the endcap calorimeter) and "Iron" (the geometry of short with an iron-loaded endcap calorimeter to give a more uniform field). The task force recommendation was for one of the latter two options, which have the same geometry and can be used with the same calorimeter and muon system layout.

4. Air core toroid task force. The SDC EOI described an option for enhancing the muon system in the intermediate angle region with a superconducting air-core toroid (ATC) system. The task force reported at the September and November collaboration meetings, recommending dropping of the ATC option. Although the cost of the ATC was not well understood, the task force concluded that it would probably cost more than the iron alternative and that the additional cost was not justified by the improvement in muon momentum measurement. An Argonne physicist had been coordinating engineering studies of the ATC option.

5. Initial costing of the detector for the LOI. Results from the major subsystem project on scintillator calorimetry were used for the calorimeter costing.

Argonne physicists participated strongly in the writing and editing of the LOI. Although limited to 50 pages, the LOI referred to detailed technical documents for backup. Argonne physicists wrote substantial parts of the calorimetry and physics sections of the LOI.

SDC collaborations meetings were held in July at Snowmass, August at FNAL, September at SSCL, and November at LBL.

Physics and Detector Simulation

As noted above, the physics calculations efforts of the SDC collaboration were devoted to producing documents for the PAC. For the initial round of questions worked on at Snowmass, Argonne physicists were involved in calculations of $t \to H^+b$, H → gamma gamma, and $H \to ZZ \to llqq$. Argonne

physicists also worked on the writing and editing of the document. For the physics section of the LOI, Argonne worked with FNAL to answer the question about hadronic decays of Z's and Z''s. In addition, we continued the calculations on $t \rightarrow H^+b$ and provided coordination and editing of the physics section.

Question 3 from the PAC for the LOI asked for the resolution of reconstructing Z's or Z''s (mass 1 TeV) decaying hadronically. It was regarded as a way of comparing physics capabilities of the calorimeters envisioned by each collaboration. To answer the question for SDC, we had to deal with the nonspecificity of the question and the problem that the resolution depends on the process involved (which was not specified) through the associated kinematics, number of particles in the underlying event, etc. Accordingly, we simulated a large number of conditions, in order to demonstrate what variables most influence the resolution. We found that resolution was affected strongly by kinematics (p_T, mass of the parent particle, etc.) but only weakly by parameters of the calorimeter (segmentation, resolution, etc.). The one exception was the increase in mass resolution caused by a strongly noncompensating calorimeter (e/h = 1.3). A typical mass spectrum, fitted to a gaussian and a fourth-order polynomial, is shown in Fig. 27. Mass resolutions (σ from the gaussian part of the fit is quoted) are given for many conditions in Table II. The study was done using Argonne's GEANT-based simulation program, ANLSIM.

Results from the study of $t \rightarrow H^+b$ are shown in Fig. 28. We found that it will be possible for SDC to measure this branching fraction down to a value of 1%. Both of these calculations are documented in SDC notes. Argonne physicists have contributed to the development of a combined simulation program, based on programs developed by ANL, LBL, Indiana, KEK, and other institutions in SDC. This effort started with the collaboration meeting at FNAL in August. It is expected to deliver an initial working program in February.

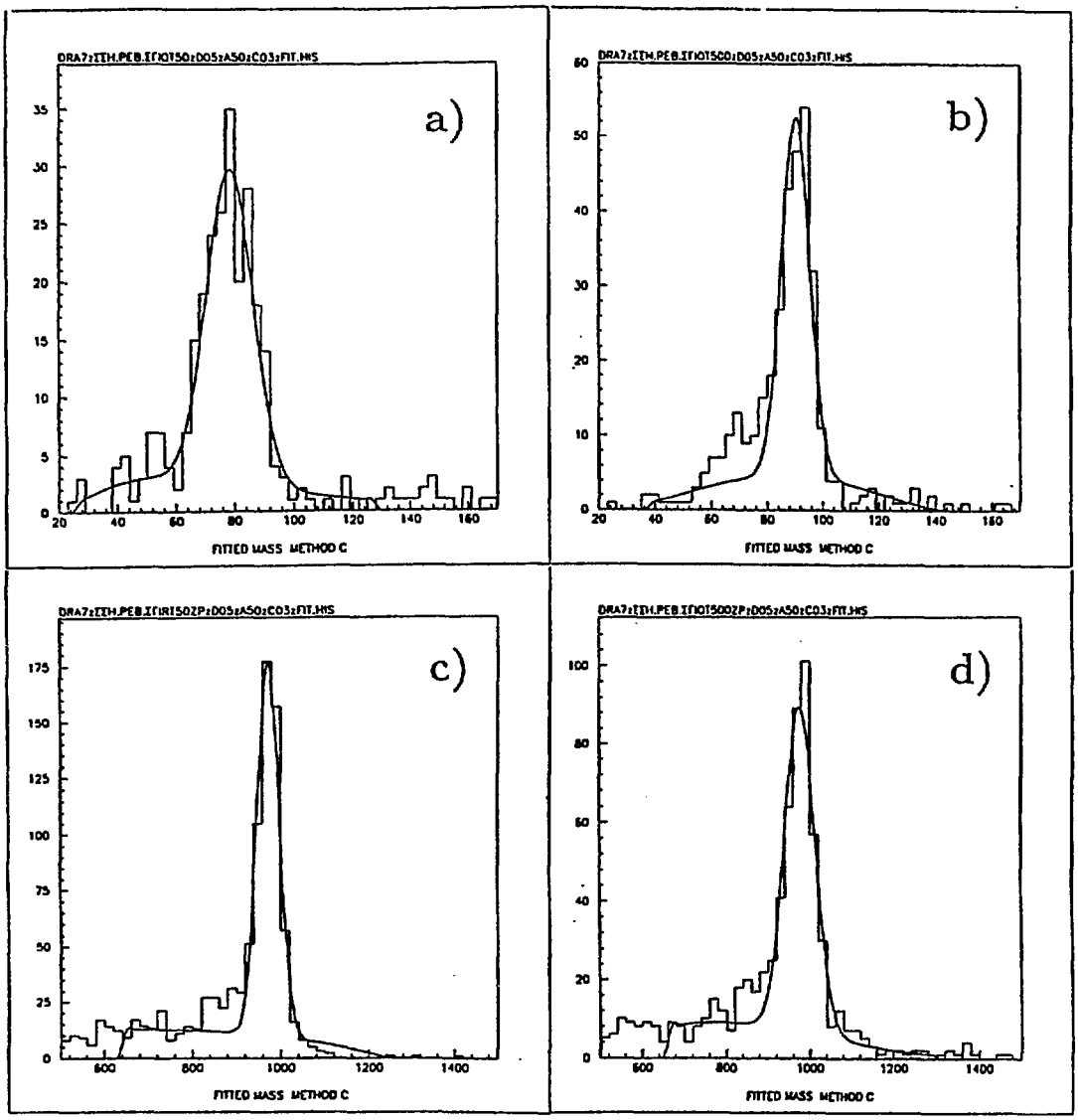

Fig. 27. Reconstructed mass plots for dijets from Z and Z' → jet jet decays. For each particle, simulations were made for p_T = 50 and 500 GeV/c. a) Low p_T Z; b) High p_T Z; c) Low p_T Z'; d) High p_TZ'.

Table II. Summary of fitted resolutions. The columns give the particle type (P), either Z or Z', the transverse momentum (p_T), the calorimeter segmentation (s), the hadron calorimeter stochastic coefficient (h_s), and constant term (h_c), the electromagnetic stochastic coefficient (e_s), the clustering radius R, the clustering algorithm C, e/h, fitted peak mass M, and fractional width with fitting error (σ_M/M). The value of C is 'Pythia' for use of particles generated by Pythia for clustering with no calorimeter simulation; 'Quarks' for use of the Pythia quark directions as seeds for clusters of simulated calorimeter towers; or 'Seed' for use of simulated calorimeter towers themselves as seeds for clusters.)

P	p_T (GeV/c)	s	h_s	h_c	e_s	R	C	e/h	M (GeV)	σ_M/M
Z	50	No Cal. Simulation				0.7	Pythia		89.6	0.0289 ± 0.0032
Z	50	.05	0.00	.00	.00	0.7	Quarks	1.0	78.4	0.0830 ± 0.0090
Z	50	.05	0.30	.02	.15	0.7	Seed	1.0	78.6	0.0957 ± 0.0098
Z	50	.05	0.50	.03	.15	0.7	Seed	1.0	78.2	0.1000 ± 0.0073
Z	50	.05	0.70	.04	.15	0.7	Seed	1.0	81.2	0.0970 ± 0.0085
Z	50	.05	1.00	.05	.15	0.7	Seed	1.0	83.6	0.1204 ± 0.0122
Z	50	.05	0.50	.03	.25	0.7	Seed	1.0	78.3	0.0910 ± 0.0073
Z	50	.05	0.50	.03	.15	0.7	Seed	1.3	70.0	0.1034 ± 0.0080
Z	50	.10	0.50	.03	.15	0.7	Seed	1.0	79.3	0.0982 ± 0.0078
Z	50	.15	0.50	.03	.15	0.7	Seed	1.0	80.5	0.0929 ± 0.0073
Z	500	No Cal. Simulation				0.7	Pythia		91.1	0.0192 ± 0.0017
Z	500	.05	0.00	.00	.00	0.7	Quarks	1.0	90.4	0.0515 ± 0.0055
Z	500	.05	0.00	.00	.00	0.7	Seed	1.0	88.9	0.0509 ± 0.0053
Z	500	.05	0.30	.02	.15	0.7	Seed	1.0	89.4	0.0493 ± 0.0055
Z	500	.05	0.50	.03	.15	0.7	Seed	1.0	90.1	0.0558 ± 0.0044
Z	500	.05	0.70	.04	.15	0.7	Seed	1.0	90.8	0.0596 ± 0.0044
Z	500	.05	1.00	.05	.15	0.7	Seed	1.0	92.3	0.0635 ± 0.0050
Z	500	.05	0.50	.03	.25	0.7	Seed	1.0	89.7	0.0662 ± 0.0047
Z	500	.05	0.50	.03	.15	0.7	Seed	1.3	82.1	0.0653 ± 0.0053
Z	500	.10	0.50	.03	.15	0.7	Seed	1.0	91.9	0.0745 ± 0.0082
Z	500	.05	0.50	.03	.15	0.4	Seed	1.0	86.4	0.0514 ± 0.0095
Z	500	.05	0.50	.03	.15	1.0	Seed	1.0	91.7	0.0663 ± 0.0062
Z'	50	No Cal. Simulation				0.7	Pythia		1001	0.0136 ± 0.0007
Z'	50	.05	0.00	.00	.00	0.7	Quarks	1.0	975.0	0.0236 ± 0.0016
Z'	50	.05	0.00	.00	.00	0.7	Seed	1.0	969.7	0.0200 ± 0.0011
Z'	50	.05	0.30	.02	.15	0.7	Seed	1.0	970.9	0.0234 ± 0.0014
Z'	50	.05	0.50	.03	.15	0.7	Seed	1.0	972.6	0.0251 ± 0.0012
Z'	50	.05	0.70	.04	.15	0.7	Seed	1.0	975.9	0.0272 ± 0.0014
Z'	50	.05	1.00	.05	.15	0.7	Seed	1.0	985.4	0.0323 ± 0.0027
Z'	50	.05	0.50	.03	.25	0.7	Seed	1.0	973.0	0.0254 ± 0.0012
Z'	50	.05	0.50	.03	.15	0.7	Seed	1.3	889.8	0.0358 ± 0.0021
Z'	50	.10	0.50	.03	.15	0.7	Seed	1.0	973.2	0.0243 ± 0.0012
Z'	50	.15	0.50	.03	.15	0.7	Seed	1.0	974.6	0.0261 ± 0.0014
Z'	50	.05	0.50	.03	.15	0.4	Seed	1.0	966.6	0.0235 ± 0.0019
Z'	500	No Cal. Simulation				0.7	Pythia		1008	0.0114 ± 0.0007
Z'	500	.05	0.00	.00	.00	0.7	Quarks	1.0	972.9	0.0375 ± 0.0027
Z'	500	.05	0.00	.00	.00	0.7	Seed	1.0	969.4	0.0395 ± 0.0033
Z'	500	.05	0.30	.02	.15	0.7	Seed	1.0	970.5	0.0399 ± 0.0026
Z'	500	.05	0.50	.03	.15	0.7	Seed	1.0	975.6	0.0370 ± 0.0023
Z'	500	.05	0.70	.04	.15	0.7	Seed	1.0	978.5	0.0382 ± 0.0027
Z'	500	.05	0.50	.03	.25	0.7	Seed	1.0	975.7	0.0358 ± 0.0022
Z'	500	.05	0.50	.03	.15	0.7	Seed	1.3	890.3	0.0506 ± 0.0033
Z'	500	.10	0.50	.03	.15	0.7	Seed	1.0	977.7	0.0369 ± 0.0024
Z'	500	.15	0.50	.03	.15	0.7	Seed	1.0	978.9	0.0356 ± 0.0029
Z'	500	.05	0.50	.03	.15	0.4	Seed	1.0	975.4	0.0365 ± 0.0043
Magnetic field off:										
Z	500	.05	0.00	.00	.00	0.7	Seed	1.0	88.3	0.0606 ± 0.0036
Z	500	.05	0.50	.03	.15	0.7	Seed	1.0	88.9	0.0613 ± 0.0042
Z	500	.05	0.70	.04	.15	0.7	Seed	1.0	89.7	0.0666 ± 0.0045
Z	500	.05	1.00	.05	.15	0.7	Seed	1.0	91.1	0.0678 ± 0.0047
Z	500	.05	0.50	.03	.25	0.7	Seed	1.0	89.2	0.0616 ± 0.0039
Z	500	.05	0.50	.03	.15	0.7	Seed	1.3	80.4	0.0641 ± 0.0049
Z'	50	.05	0.30	.02	.15	.7	Seed	1.0	962.9	0.0263 ± 0.0043
Z'	50	.05	0.50	.03	.15	.7	Seed	1.0	972.2	0.0286 ± 0.0027
$1.0 < \lvert\eta\rvert < 2.5$:										
Z	500	.05	0.50	.03	.15	0.7	Seed	1.0	94.6	0.0641 ± 0.0052

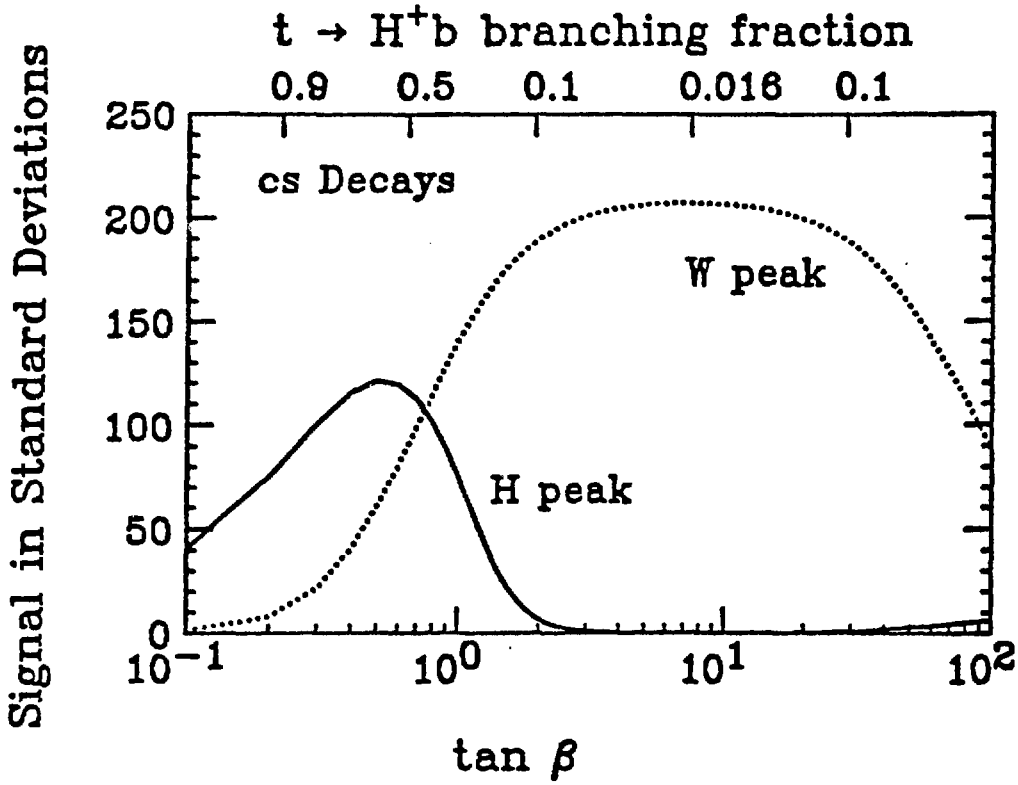

Fig. 28. The statistical significance (number of standard deviations) of the charged Higgs (solid) and W boson (dotted) peaks in the two-non-b-jet invariant mass distribution as a function of tan β. We assume one SSC year of running and have taken m_t = 250 GeV/c^2 and $m_{H^\pm}$ = 150 GeV/c^2.

The ability to do computation for SDC physics and detector evaluation was enhanced substantially with the installation of a system of five Silicon Graphics computers in December. Three of the computers are configured as workstations and will be located on physicists' desks. The remaining two are configured as servers, with large disk stores attached to them. During the coming year, we plan to add up to four more workstations to the system to increase computing power, and give all active computer users in the group access through a workstation. SSCL also chose Silicon Graphics for the compute-engine portion of their facility. Thus we are in a good position to

move computing between our facility and that at SSCL depending on where cycles are available.

Substantial detector simulation effort was directed to evaluating calorimeter configurations within the major subsystem R&D project. This work, which involved full simulation calculations to evaluate unit cell compositions, and ANLSIM parameterized calculations to evaluate larger-scale geometric choices, is described below with the major subsystem work.

(L. Price)

B. Compensating Scintillator Plate Calorimeter Subsystem for the SSC

Program Overview

The FY90 R&D program was directed towards developing calorimeter designs for: lead absorber with scintillator tile and wavelength shifting fiber readout; and depleted uranium absorber with scintillator plate and wavelength shifting plate readout. The choice between these two approaches was to be based on: finite element analysis of candidate structures; simulation data on physics performance; acceptance losses due to the dead spaces required for readout elements and mechanical support structures; and cost. In the early part of the above period, the decision point was reached, the data presented for review at a collaboration meeting held at Argonne in August and the subsequent R&D program for FY91 developed.

Acceptable mechanical designs with respect to stress and deflection were obtained for both options with the caveats that for the lead option, the lead be an alloy having high tensile strength and be cast into a supporting shell capable of supporting the gravitational load (Fig. 29). The uranium absorber, was identified as having the disadvantage of exhibiting delayed energy release from neutron capture reactions. This contributes some 3-10% of the total signal over a time period of 200-500 nsec from the initial collision. The effect of this energy release on potentially higher luminosity running is an important reason to prefer lead over uranium. However, the overwhelming reason to prefer lead over uranium is fabrication and raw material cost. This has been estimated to be $45M more for the uranium option. Dead space for mechanical support were comparable for both options (although slightly

SDC TILE/FIBER CALORIMETER

Single Module (Half Length)

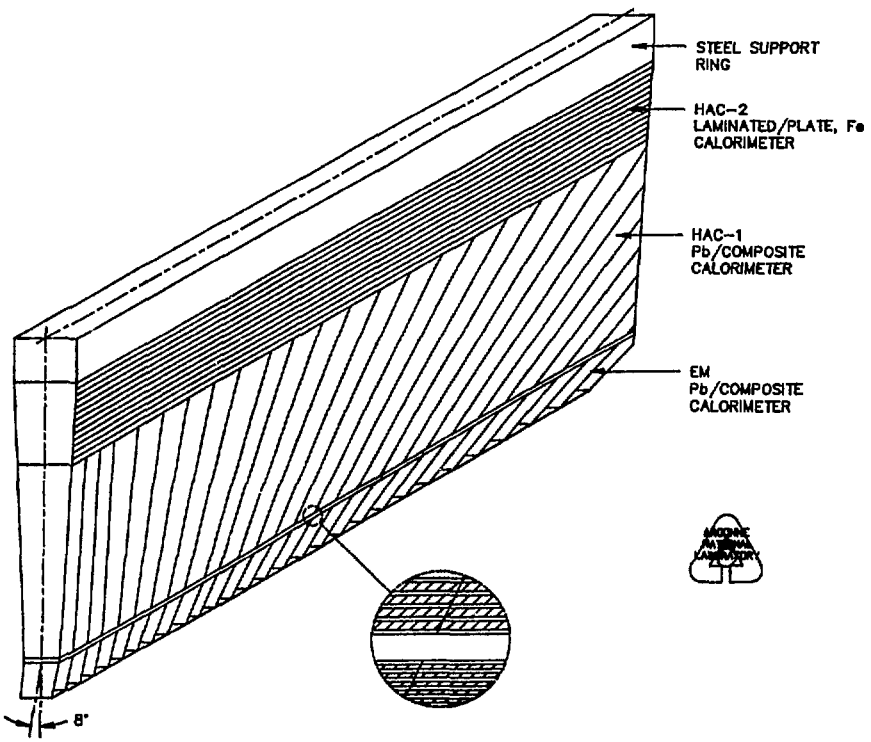

Fig. 29. Schematic of calorimeter assembly, indicating support shell within which the lead plates and scintillator slots are cast.

favoring a cast lead technology). No relative deficiencies were identified in the lead option, and it was the consensus of the collaboration that we proceed with a fabrication approach based on casting lead modules for both electromagnetic and hadronic compartments of the calorimeter.

The choice of optical readout was also straightforward. Wavelength shifting plates introduce a loss of good fiducial volume of at least 6% more than fiber. In addition, they do not easily allow transfer of azimuthal load, as was found to be necessary for all mechanical designs. Data on light yield and uniformity of the tile/fiber optical system, presented by proponents of a separate subsystem collaboration showed that anticipated problems with uniformity could be overcome. Hence the consensus of the collaboration was to pursue only the tile/fiber option. As a result the subsystem itself amalgamated with the parallel collaboration developing an iron/tile/fiber

calorimeter and submitted a combined proposal for FY91 to the SSC Laboratory in September 1990.

Several papers on work carried out by this collaboration were presented at the Fort Worth Conference on Detector R&D in October 1990.

Mechanical Design

All of the engineering effort in this period has been devoted to the development of an electromagnetic calorimeter module using a lead casting fabrication process.

Westinghouse Electric Corporation, under subcontract, carried out lead casting experiments to study issues such as pour and mold temperatures, solidification control, surface finish, mold release agents and materials for reuseable plate inserts. These tests culminated in a series of five castings of an 18 slot test mold, which were used to study the fabrication process, achievable dimensional tolerances and surface finish. These castings were carried out in December. Though not as successful as had been anticipated due to a problem with the mold, the results were very promising. Use of poured lead at 800°F into a mold at 625°F gave excellent dimensional tolerance and surface finish. No significant longitudinal shrinkage was measured. The plate dimensional uniformity at the bottom edge as a function of position in cell is shown in Fig. 30. This distribution has a mean value of 5.04 mm (c.f. 5.00 mm design) with a spread of 0.9%, and corresponds to a uniformity of about five times better than required for the electromagnetic calorimeter. Work is now in progress to design the mold for a 2 × 5 mm test section prototype.

Argonne has developed a fully engineered design for a 2 × 5 mm test section prototype (Fig. 31) and has performed finite element analysis on a full barrel electromagnetic module. The major issue under study was the degree of bulkhead stiffening required to support the gravitational loads at the extreme angle in the module (Table III). The conclusion of this analysis is to use two stiffeners of 1.5 mm thickness to minimize deflections and stress with an acceptable safety margin. These calculations are now being repeated using ANSYS and a finer analysis mesh prior to proceeding with mechanical modeling.

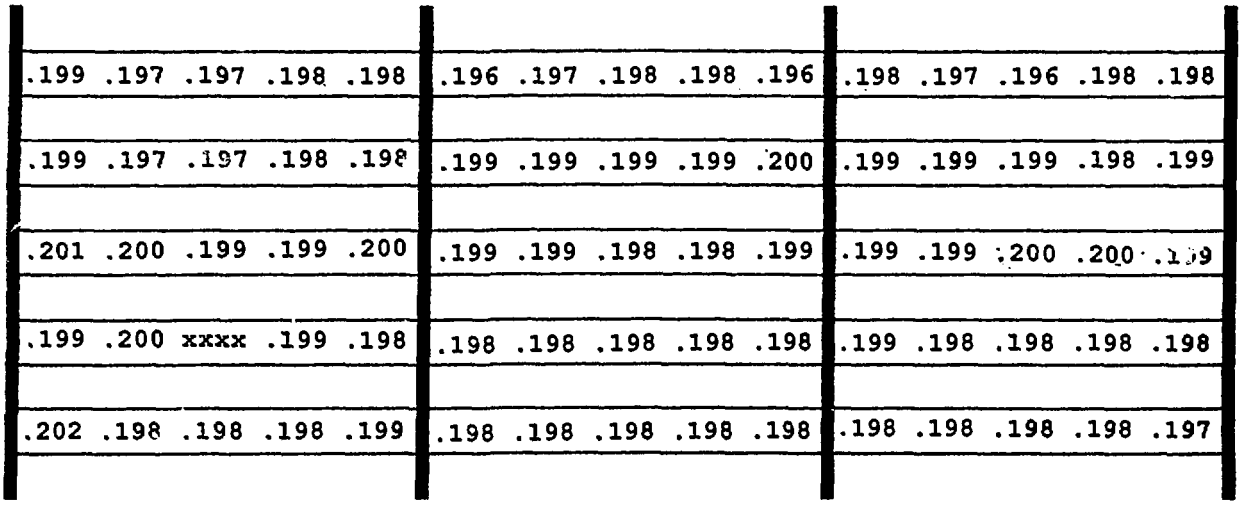

Fig. 30. Plate thickness (inches) as a function of location on plate with respect to layer and bulkhead in 18 slot test casting.

Table III

Loading at 12 and 6 O'Clock Positions

Case	Bulkhead Thickness (mm)	Maximum Radial Stress psi	Maximum Displacement (in)
No Stiffeners	1.5	2001	0.0023
	1.0	2973	0.0036
3 Flat Stiffeners	1.5	725	0.0004
	1.0	1460	0.0007
2 Stepped Stiffeners	1.5	765	0.0001
	1.0	1131	0.0002

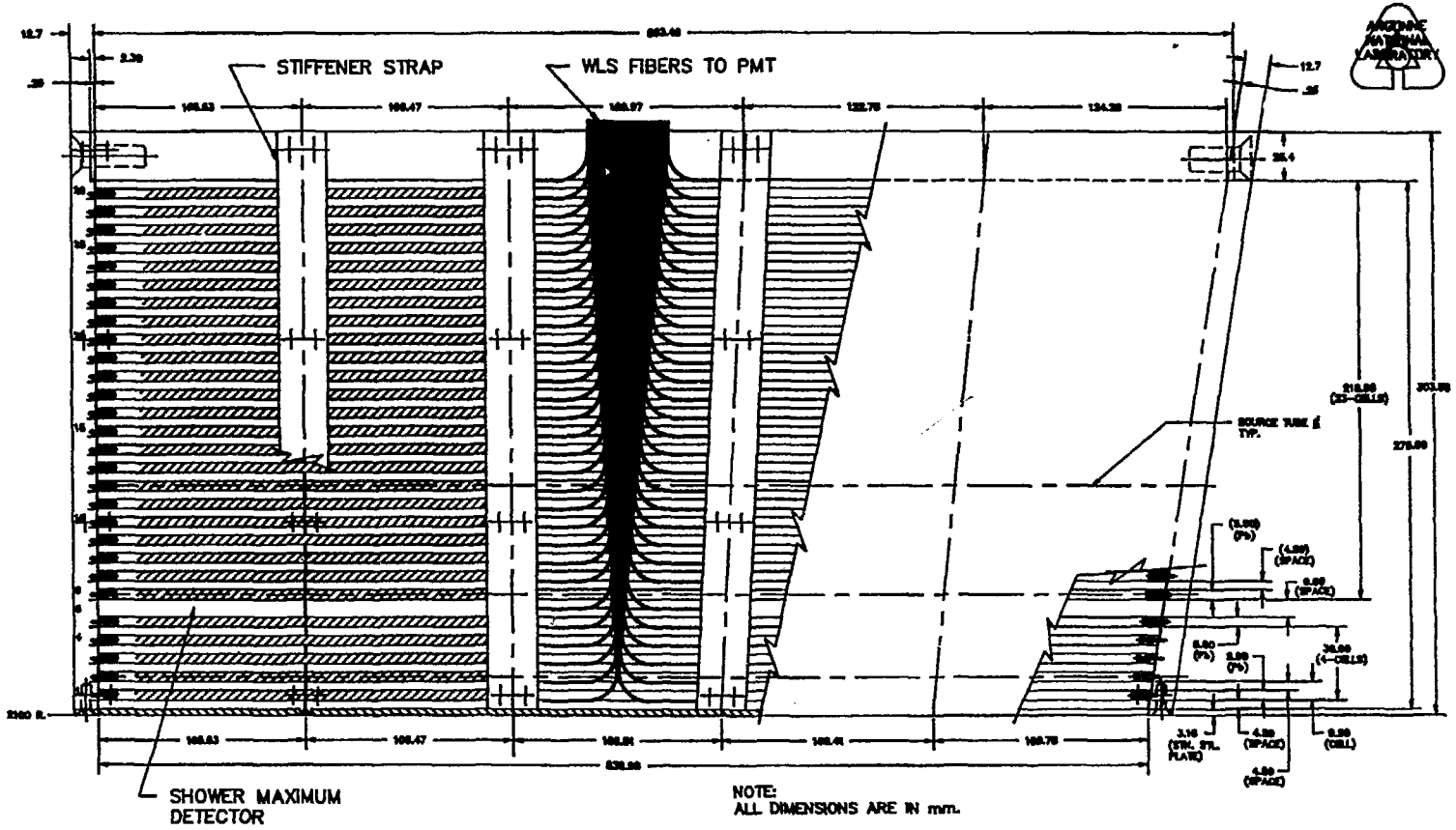

Fig. 31. SDC tile/fiber calorimeter. Truncated EMC module for testbeam.

Simulation Studies

In the early part of the above period, work on simulation concentrated on those issues most relevant to the choice of calorimeter absorber option: lead or uranium (with regard to work being carried out under this subsystem) and iron (with regard to work being carried out by the tile/fiber collaboration). In addition to absorber composition, the sampling frequency and time dependence of signal response was investigated using the CALOR code system. The relative response of electrons to pions (e/h) as a function of absorber thickness and composition is shown in Fig. 32. Whereas both lead and uranium absorbers allow e/h = 1 (compensation), a pure iron absorber does not. This, in conjunction with the time dependence of energy release in the uranium system, were the principal performance reasons for our decision to pursue lead as the passive absorber in our FY91 program.

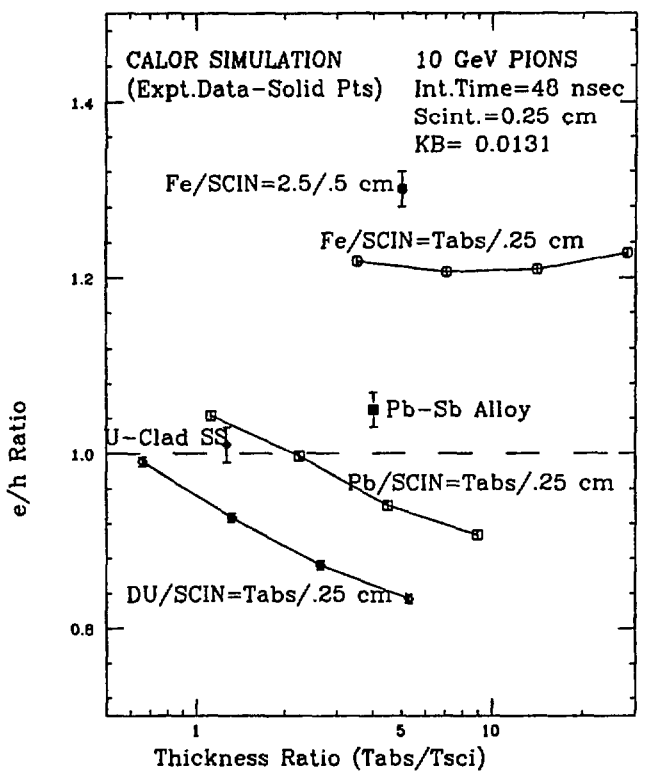

Fig. 32. Relative response of electrons to pions at 10 GeV as a function of absorber to scintillator plate thickness. The solid points indicate experimental data. The dashed line shows the compensating value of e/h = 1.

In the same period, a study of the impact of mechanical support structures was also carried out. In particular, the transition region between the barrel and calorimeters was simulated using the GEANT code. Our conclusion was that for an endplug design, the angle between the barrel and plug should project at a point at least 50 cm offset in z from the interaction point to minimize energy loss and fluctuations. However, for the endcap design now being followed, the appropriate choice is on a vertical cut. This analysis is described in more detail in a technical report.

Following the adoption of lead as the absorber medium, our simulation studies have expanded to survey more subtle mechanical effects which will affect the response, linearity and uniformity (e.g. alloy materials). Firstly, we were concerned that the introduction of standard alloy materials required for strengthening, cadmium and antimony, with strong neutron absorption cross sections might significantly affect the response of the calorimeter to hadron showers. This has been shown not to be the case for concentrations up to 20% by volume. Our interpretation is that the thermal neutrons which are absorbed by cadmium are capable of producing little light by the (n,p) reaction in the scintillator. These and other systematic studies (such as the collision model itself) are continuing.

Optical System

The subsystem collaboration is investigating several possibilities and optimization methods for the optical system for the scintillator based calorimeter. Along with Argonne, LSU, Fermilab and others are also involved. At Argonne we are concentrating on the EM part, because it will require better resolution and longer light paths, which imply the need for more light collection and better uniformity. Investigations underway for this reporting period included the effects on light collection of direct pressure on the scintillator tiles, setup of a mapping system to optimize fiber placement, initial radiation damage tests using a beam dump, and continued development of radiation hard scintillator. Each of these projects is described below.

Pressure Tests

We are interested in the effects of mechanical pressure on scintillator because one design for the calorimeter would hold the scintillator/lead stack together with banding, similar to the ZEUS calorimeter. The CDF central electromagnetic calorimeter is held in this way with about 4 psi with no apparent ill effects. A proposed SDC full tower would need about 50 psi.

For the tests done so far, we used two stacks of scintillator and aluminum plates, 10 cm square, with about eight layers each (Fig. 33). The purpose of this was to use one as a reference while pressure was applied to the other. This was particularly important for longer term tests. Also, the laser output fluctuated by more than a factor of two and the effect of interest is of order 1%. One stack used SCSN38 scintillator, 5 mm thick, from CDF. The other was RH5 scintillator from Bicron, 2.5 mm thick.

To stimulate light output from the scintillator in a way that was similar to that from showers of particles, we used ultraviolet light from a nitrogen laser. It was injected some distance from the edges of the scintillator sheets by means of quartz optical fibers. Several sheets were excited simultaneously. The laser pulse was less than 12 ns long and the output from the scintillator, waveshifter, phototube chain was less than 25 ns.

The light collection was done with Y7 waveshifter plates on the sides of the stacks, and R580 tubes were used. There was one layer of typing paper in each scintillator to aluminum interface to prevent damage from local irregularities and to simulate materials which might be used as reflection masks for improving light collection uniformity. The data were read in with LeCroy 2249 ADC's in CAMAC. Typical data runs consisted of 100 events. We typically took two runs at each pressure.

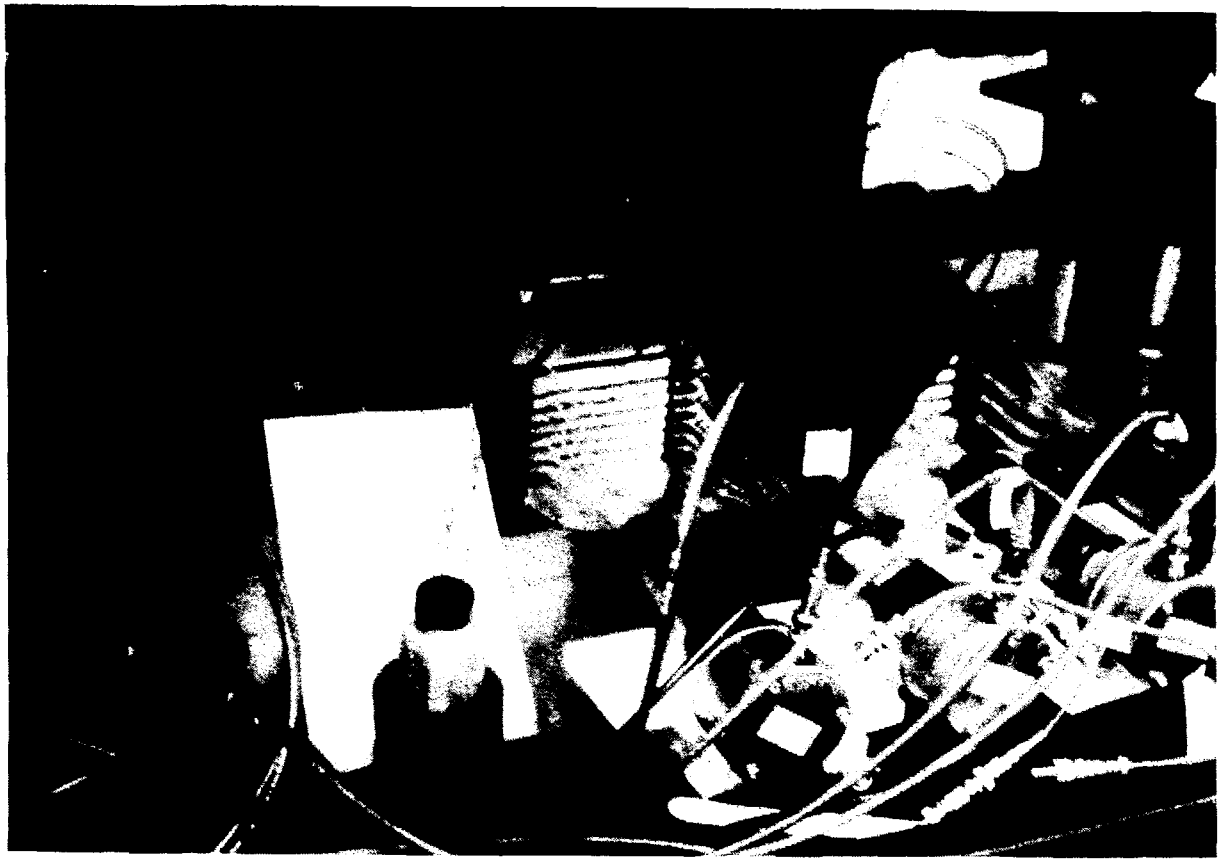

Fig. 33. Scintillator tile compression test setup.

Results:

The short term tests established that the loss of light went as the pressure squared. There was about 8% loss at just over 100 psi. This loss was reversible. It probably has to do with the optical contact "wetting" of the scintillator surface. It is not understood in that the contact area of a single wood fiber in paper would not go as pressure squared but more like the square root.

The long term tests (about 40 days so far) show the same ratio of pressure-on to pressure-off light output. The data on absolute output over time is still being analyzed.

Scintillator Mapping

We intend to do scintillator mapping to determine the optimum way to place the waveshifter fibers for both light output and uniformity. We also may have to develop corrective reflector masks to improve the uniformity. These would be designed and tested on the basis of response maps. Also, we want to study how the response map changes after radiation damage. There may be something to be learned by comparing response maps with high energy electrons only vs. a mixture of photons and electrons as found in real showers. We will compare maps with beam impinging on the side with waveshifter vs. the opposite side.

For the mapping, we are developing 1) a 3 MeV beam from a Ruthenium source and magnetic spectrometer (Fig. 34), 2) a motor driven x-z moving system in the vertical plane, suitable for either source or beam work, 3) a hodoscope of scintillating fibers for adjusting the system and for confirming electron trajectories though the scintillator tile, 4) a data acquisition system based on standard fast electronics in CAMAC, readout with an IBM AT style computer, and 5) data analysis computer programs for the PC and VAX.

Due to the timing of the funding, much of the motion system including motor drivers, controllers, motors and lead screws is being constructed at Argonne or assembled from existing parts left from past projects.

Remaining to be done are the construction of the vacuum chamber/source holder, the mounting of the spectrometer parts, the tuning of the permanent magnet spectrometer, the mounting of the x-z mapper parts, the writing of some parts of the software, the construction and testing of the hodoscope, and some improvements in the mounting of the scintillator to be mapped. We hope to do the first maps in late January and to do serious studies for optimizing the scintillator/waveshifter combination in late January and early February.

Radiation Damage Test

A feasibility test for doing radiation damage tests to lead-scintillator stacks was performed in a neutral beam dump at Fermilab in August. Significant damage to auxiliary materials (other than scintillator) which might be used in a calorimeter was observed. Also, variation of damage with depth in low Z materials in electromagnetic showers may have been observed. This will be studied in a further similar test in the spring of 91. The dose measured in the calorimeter by means of radiographic dye films agreed to better than 30% with the calculated dose from the collimated neutral beam from a production target. This work is described in an Argonne technical memo.

Radiation-Hard Scintillator Development

Development of radiation hard scintillator plate based on the RH program of Bicron (used for radiation hard scintillator fiber) has been carried out under a subcontract with Bicron. First measurements of RH1 plate were made at Florida State University in July and August. These showed that the RH1 plate was capable of absorbing $\geq$ 3 MRad with minimal loss of light yield and transmission (Fig. 35). These results are discussed in more detail in a paper presented at the Fort Worth Symposium. This material had however one major disadvantage in that its surface was prone to crazing which increased with age (due in fact to its production process beginning without the use of mold release agents). In the latter quarter of 1990, nine copolymer variations on

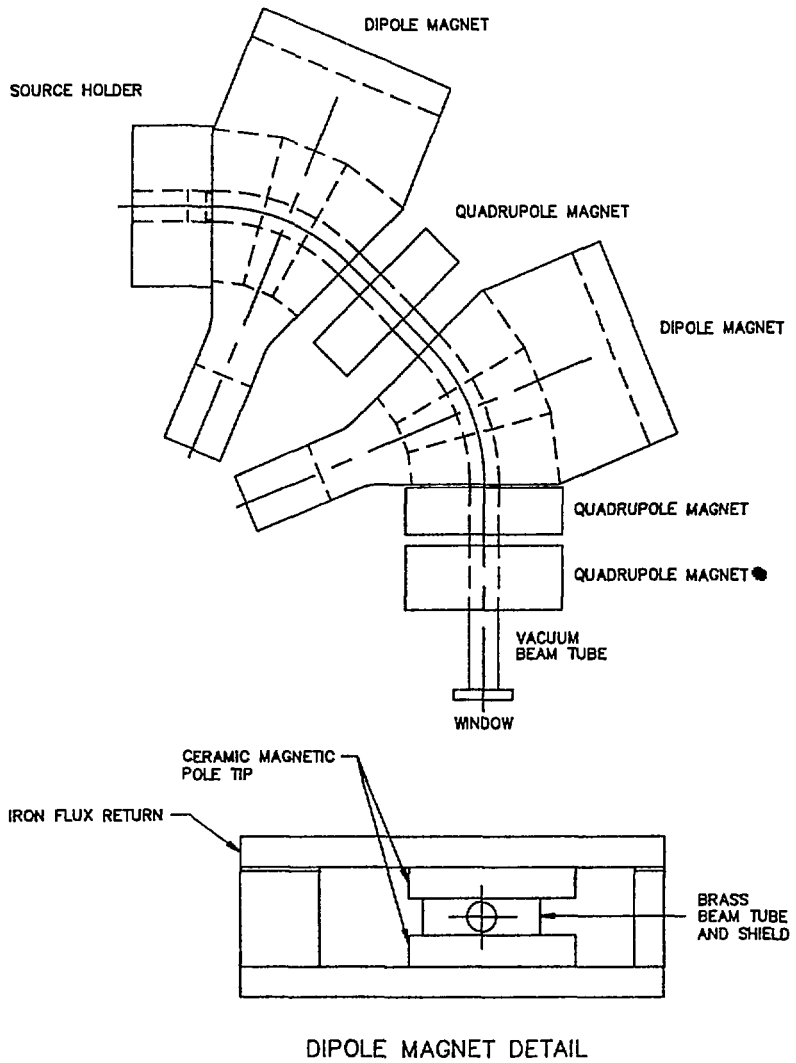

Fig. 34. Ru^{106} Source Beamline Layout.

this process were fabricated and subjected to radiation damage tests by our collaborating groups at Florida State University and Louisiana State University. One of these (RH4) showed promise both from its mechanical and radiation-hardness qualities and was selected for larger scale production and systematic tile and tile fiber studies to be carried out in the first quarter of 1991.

Test Beam Program

It is our intention to use a high energy beam at Fermilab to measure the performance of the design embodied in the electromagnetic test section module. We anticipate that this beam test will commence in March 1991. To this end, we initiated discussions with Fermilab in October 1990. At the present time the text of the MOU and details therein are the subject of ongoing discussions with the Fermilab management and we expect to conclude this MOU in January 1991. (J. Proudfoot, D. Underwood)

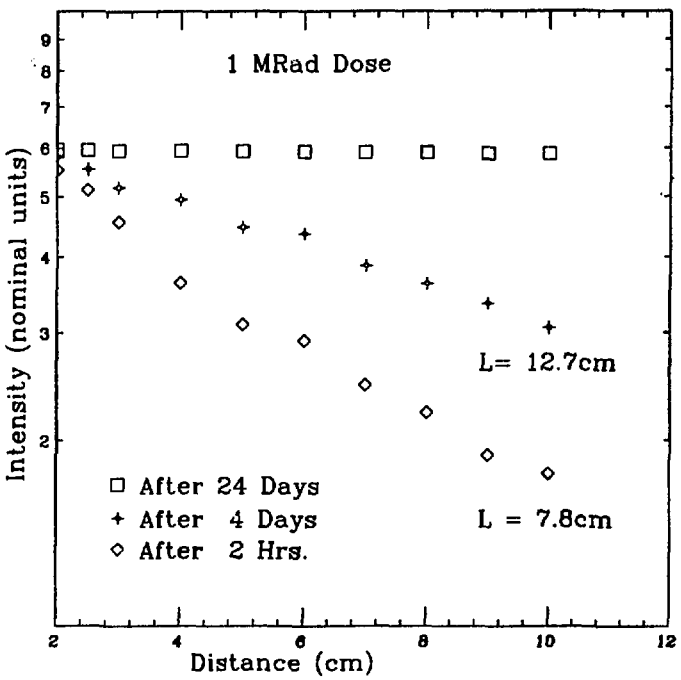

Fig. 35. Light yield of 10 x 2 x 0.5 cm^3 RH-1 plate scintillator. L is attenuation length. The first 2 cm was not irradiated for normalization purposes.

C. Superconducting Toroid Subsystem and Muon Subsystem Studies

SDC Air Core Toroid Design

Our earlier conceptual design for an SDC forward superconducting air core toroid (ACT) was developed in more engineering detail during this period. This work was carried out at Argonne and by Advanced Cryo Magnetics Inc. Among the crucial engineering issues which we analyzed were fabrication methods, conductor cooling options, magnetic field shape, and construction cost estimates. Our analyses indicated that excellent performance and low cost could be achieved with this design. Our design work is well documented in two SDC notes.

Many aspects of superconducting toroid design for SSC and LHC detectors were discussed during a special roundtable session which we organized at the Ft. Worth Symposium on Detectors for the SSC (October 1990). This session was attended by superconducting magnet designers from six countries, and superconducting magnet designs were described for each of the three proposed large SSC detectors. A wide variety of approaches to superconducting toroid design and cost estimating were presented and discussed during this roundtable session.

During this period the SDC collaboration made the decision to base its Letter of Intent (November 1990) on the use of a forward iron toroid rather than a superconducting air core toroid. This decision was cost-driven by the mandate from the SSC Laboratory to descope the SDC design in order to save 20% from the cost estimate given in the May 1990 Expression of Interest. An important aspect of the toroid cost issue is the uncertainty of the ACT cost estimate: our work at Argonne yielded a cost estimate of $10 M per toroid; other groups in the SDC collaboration quoted a cost estimate about 3 times larger.

The use of a forward iron toroid will lead to a loss of dimuon invariant mass precision, particularly for a very high luminosity situation (say $\mathcal{L} \geq 10^{34}$ $cm^{-2}sec^{-1}$) where the external muon detectors are likely to be operating in a "standalone" mode. This loss of precision can lead to

additional background under the $Z^0 \rightarrow \mu^+\mu^-$ mass peak. Another difference is that the mass of the air core toroids would be about 100 Tons each, whereas the iron toroids will be 20-30 times heavier. (T. Fields)

D. Superconducting Strip Detector R&D

Superconducting strip detector development research centered on attempts to detect minimum ionizing particles in submicron strips. The important experimental steps toward this goal during the latter half of 1990 were i) two more exposures of a granular aluminum strip to high energy pions at Fermilab, ii) continued study of granular aluminum films with electrons from a radioactive beta source, and iii) initial development of tungsten strips for particle detection.

The Fermilab experimental runs did not show any evidence of switching being produced by ionization energy deposited by minimum ionizing pions. This is in contrast to our initial run at Fermilab in which superconducting to normal transitions were observed to occur in coincidence with beam traversing the strip detector. The second run suffered from RF noise pickup in the detection electronics and no useful data could be collected. Following this the cryostat and cabling were revamped. RF shielding was added to the cryostat and all signals were carried on differential shielded pairs. The third run at Fermilab indicated that all noise problems had been solved, but no switching in coincidence with the pion beam was observed to occur.

The films used in the Fermilab tests along with similar granular aluminum films were exposed at Argonne to a ^{90}Sr beta source with a 2.2 MeV endpoint energy to further study the strips' sensitivity to ionization energy loss. At near critical currents particle detection efficiencies of ~ 70% were recorded. The efficiency of the strip gradually decreased as the bias current in the strip was reduced. This is in contrast to the response of the strip to 6 keV x-rays where a distinct plateau in detection efficiency is observed to occur over a wide range of bias current. Two mechanisms can possibly account for this behavior. First, at low currents the strip may be only sensitive to the larger than minimum ionizing electrons that make up about 25% of the beta

spectrum. The second possibility concerns the energy loss mechanism in very thin films. This spectrum is dominated by energy loss from plasmon creation. Plasmons typically have peak energies of tens of eV and lie below the minimum ionization energy loss peak. Moreover, calculations indicate that for our 0.4 μm thick granular aluminum strips the mean number of collisions producing a plasmon is 1.6. The hotspot created by these interactions is less than the strip width and will be detected only for bias currents large enough to drive the remaining cross section normal. This has prompted us to look for new materials that have both a low T_c and a larger probability for collision per unit length.

We have recently made a few tungsten test strips. The energy loss in tungsten is estimated to be approximately ten times that in aluminum. This would result in a hotspot with ~ 3 times the radius of that produced in aluminum. Studies of these strips with the beta source tentatively show promise of improved detection efficiency. We have, in fact, observed for the first time self-recovering hotspots produced in superconducting strips by beta decay electrons. Figure 36 shows the strip voltage versus time during a self-recovering superconducting to normal transition induced by a beta particle. The signal was passed through a x100 amplifier. The pulse duration was ~ 200 ns and corresponds to a normal region length in the strip of about 1 μm. Our current efforts are directed toward improving the quality and uniformity of the tungsten strips so as to achieve a detector suitable for further testing in the high energy pion test beam at Fermilab. (R. Wagner)

E. Radhard Electronics R&D for SSC

During the reporting period the effort in radiation hard electronics development for SSC detectors at Argonne has been concentrated in the area of testing and evaluating commercially available rad-hard processes from several vendors. In order to facilitate the testing we have developed good working relationships with neutron- and gamma ray-sources at ANL. Recently we have done our neutron irradiations at the Dynamitron Fast Neutron Generator. This

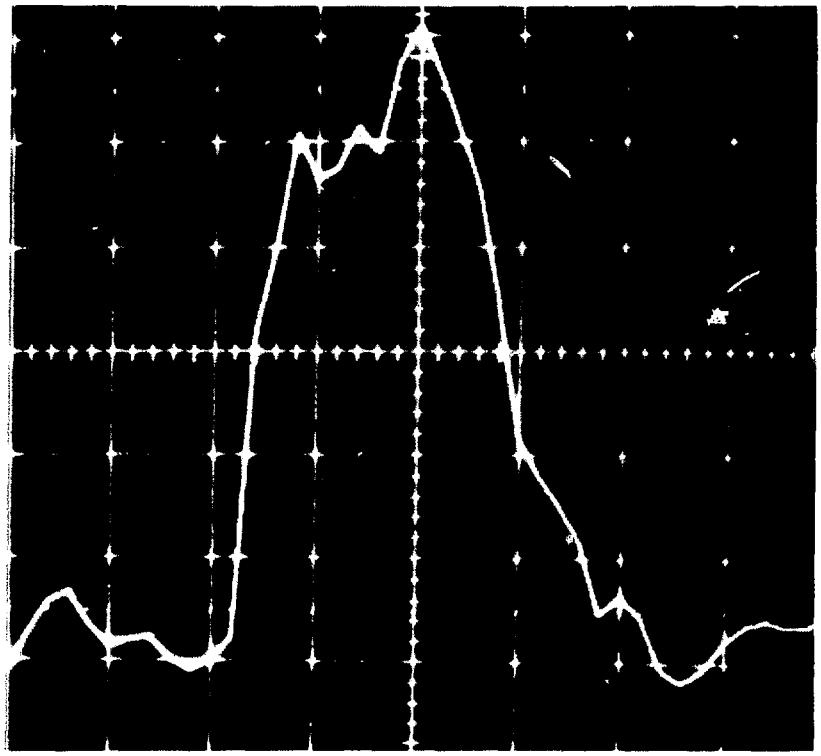

Fig. 36. Example of a self-recovering superconducting to normal transition produced by ionization energy loss in a tungsten strip. The oscilloscope trace shows the strip voltage versus time. The vertical axis is 10 mV/division; the horizontal axis is 50 ns/division. The pulse duration implies a normal region maximum length before collapse of ~ 1 μm.

is quite adequate for lower fluences and is much easier to use than the IPNS facility. The absence of thermal neutrons and the easily accessible port makes experiments easy to perform. Gamma-ray irradiation is conducted at Argonne Biological and Medical Research Division using a Cobolt-60 source which can provide a dose-rate of up to 2 MRad(Si)/hour. Commercially available rad-hard processes from UTMC and Hughes Aircraft have been tested. UTMC provided us with a 1.5 micron CMOS process that performed very well both after neutron irradiations of up to 10^{14} neutrons/square cm and doses of ionizing radiation of up to 10 MRad(Si). The threshold shifts were on the

order of 150 mV, and thermal noise increased by between a factor of 2 and a factor of 5. A BiCMOS process from Hughes Aircraft was irradiated with similar doses and showed significant degradation of the CMOS structures, while the bipolar devices performed very well after exposure. Threshold shifts were as severe as 700 mV for n-channel devices after 10 MRad(Si), but the degradation of forward beta of the bipolar transistors was only a factor of 2, and the worst case beta was still above 50. We are currently in the process of testing SOS (Silicon On Saphire) devices from Hughes Aircraft and expect to soon receive cryogenic CMOS devices. Several outside users have showed interest in using the ANL irradiation facilities, and neutron damage experiments have been performed on Ga-As devices from INFN, Italy, and bipolar circuits from University of Pennsylvania.

A Sun Sparcstation 1 running a subset of the Berkeley tools for circuit simulation and layout is the core of our integrated circuit design program. We have designed and fabricated a chip with test structures through the MOSIS prototyping service, and we are currently waiting for the first version of an analog pipeline/storage chip to come back from fabrication. Efforts are under way to integrate the OCTTOOL design environment in our CAD system in order to further automate the design and layout procedures. With those tools in place we will be able to automatically generate layouts from schematics and truth tables. Support for the CAD environment effort is given by our collaborators at ORNL. (J. Dawson)

VI. HIGH ENERGY PHYSICS RETREAT

In December, HEP Division physicists held an on-site 'retreat' to discuss the Division's experimental program for the remainder of the 1990's. Each of the Division's present projects was examined to determine its likely status in 1995, considering physics interest, possible upgrades, and use of Division resources. An important focus for the discussions was the question of whether the Division should initiate a new, non-SSC experimental project in the mid 1990's, given the Division's physics interests and technical expertise. SSC-related activities were not explicitly considered, except to assume that they would require about one-third of the Division's resources. The retreat consisted of a two-day meeting devoted to talks and discussion, followed a week later by a short session to consider conclusions. Many of the prepared talks were presented by the younger physicists in the Division. A program of the presentations is appended. Unlike the two earlier HEP Division retreats, held in 1980 and 1986, the 1990 retreat was not motivated by any specific proposal for the initiation of a new experimental project.

At the final retreat session, Division Director, T. Kirk, represented the conclusions of the retreat by a table showing the distribution of physicist effort among projects over the next ten years. The division of effort is based on the relative priorities of projects, as determined by a physics "splash" factor, current Division expertise and involvement, physics prospects for success, and future opportunities. The table includes two new initiatives: A B-factory experiment was chosen by the retreat participants as the most interesting possibility for a concrete new project. Very high energy collisions of polarized protons at RHIC was the other new project favored by the retreat participants, although involvement would probably require medium energy funds such as those which now support the Division's LAMPF program.

Even if the plans which emerged from the 1990 retreat are not be implemented in exactly the form now envisaged, the retreat itself was an extremely valuable exercise. Strong participation from the theory, accelerator, and computational physics groups, in addition to all the

experimental groups, yielded excellent talks and stimulating discussion. The retreat provided a unique opportunity for all Division physicists to consider physics and planning issues in a Division-wide context. Future retreats are contemplated to be held every few years.

VII. PUBLICATIONS

A. Journal Publications, Conference Proceedings, Books

B Factory via Conversion of 1 TeV Electron Beams into 1 TeV Photon Beams
S. Mtingwa (ANL/HEP), M. Strikman (Leningrad Nucleaar Physics Inst. USSR)
Phys. Rev. Lett. 64, 1522 (1990).

Summing Graphs in Large-N_c Quantum Hadrodynamics
P. Arnold (ANL/HEP), M. Mattis (LANL)
Phys. Rev. Lett. 65, 831 (1990).

Jet-Fragmentation Properties in $\bar{p}p$ Collisions at $\sqrt{s}$ = 1.8 TeV
L. Nodulman, R. Blair, R. Diebold, W. Li, J. Proudfoot, P. Schoessow, D. Underwood, R. G. Wagner, A. Wicklund (ANL/HEP) and the CDF Collaboration
Phys. Rev. Lett. 65, 968 (1990).

A Measurement of the W-Boson Mass
L. Nodulman, R. Blair, R. Diebold, W. Li, J. Proudfood, P. Schoessow, D. Underwood, R. G. Wagner, A. Wicklund (ANL/HEP) and the CDF Collaboration
Phys. Rev. Lett. 65, 2243 (1990).

Interference Effects in $K\eta$ and $K\eta'$ Decay Modes of Heavy Mesons Clues to Understanding Weak Transitions and CP Violation
Harry J. Lipkin
Phys. Lett. B254, 247 (1991).

Where is the Spin of the Proton?
H.J. Lipkin (ANL/HEP)
Phys. Lett. B237, 130 (1990).

Deforming Maps for Quantum Algebras
C. Zachos (ANL/HEP), T. Curtright (Univ. of Miami)
Phys. Lett. B243, 237 (1990).

Energy Flow in Hard Proton-Nucleus Collisions at 400 GeV/c
M. Arenton, W. Ditzler, T. Fields, G. Thomas (ANL/HEP); R. Moore et al. (Rice Univ.); M. Harrison (Fermilab), A. Kanofsky (LeHigh Univ.); R. Gustafson (Univ. of Michigan); L. Cormell et al (Univ. of Pennsylvania), H. Chen et al. (Univ. of Wisconsin)
Phys. Lett. B244, 347 (1990).

G_A/G_V, Magnetic Moments and the Spin of the Proton
H. A. Lipkin (ANL/HEP)
Phys. Lett. B251, 613 (1990).

Analyzing Power Measurment for Forward Angle n-p Scattering
G. Glass et al. (Texas A&M), K. Johnson, H. Spinka, R. Stanek (ANL/HEP), M. Rawool (New Mexico State Univ.), R. Jeppesen (Univ. of Montana), G. Tripard (Washington State Univ.), C. Newsom (Univ. of Iowa)
Phys. Rev. C41, 2732 (1990).

Modelling Parton Spin-Transfer Densities
D. Sivers, D. Richards, J. Qiu (ANL/HEP), G. Ramsey (Loyola Univ.)
Phys. Rev. D41, 83 (1990).

Measurement of the Branching Ratio for the Decay $\tau^- \to e^- \nu_e \nu_\tau$
A. Abachi, M. Derrick, P. Kooijman, B. Musgrave, L. Price, J. Repond, K. Sugano (ANL/HEP), D. Blockus et al. (Indiana Univ.), C. Akerlof et al. (Univ. of Michigan), P. Baringer et al. (Purdue Univ.)
Phys. Rev. D41, 1414 (1990).

Quark Hadronization Probed by K^0 Mesons
A. Abachi, M. Derrick, P. Kooijman, B. Musgrave, L. Price, J. Repond, K. Sugano (ANL/HEP), D. Blockus et al. (Indiana Univ.), C. Akerlof et al. (Univ. of Michigan), P. Baringer et al. (Purdue Univ.)
Phys. Rev. D41, 2045 (1990).

The Gluonic Contribution to G_1 and its Relationship to the Spin-dependent Parton Distributions
G. Bodwin (ANL/HEP)
Phys. Rev. D41, 2755 (1990).

Production of Top Quarks Via Vector-Boson Fusion in e^+e^- Collisions
R.P. Kauffman (ANL/HEP)
Phys. Rev. D41, 3343 (1990).

A Collider Diffractive Threshold, Hadronic Photons and Sextet Quarks
A. White, (ANL/HEP), K. Kang (Brown Univ.)
Phys. Rev. D42, 835 (1990).

Baryon Violation at the SSC? Recent Claims Re-examined
P. Arnold, HEP/ANL, M. Mattis, LANL
Phys. Rev. D42, 1738 (1990).

Longitudinal and Transverse Wake Field Effects in Dielectric Structures
M. Rosing, W. Gai (ANL/HEP)
Phys. Rev. D42, 1829 (1990).

Hard-Scattering Scaling Laws for Single-Spin Production Asymmetries
Dennis Sivers (ANL/HEP)
Phys. Rev. D43, 261 (1991).

Top Quark Backgrounds to Higgs $\to W^+W^-$
C. Yuan and R. Kauffman (ANL/HEP)
Phys. Rev. D42, 956 (1990).

Superconducting Detector for Minimum Ionizing Particles
A. Gabutti, R. Wagner, (ANL/HEP); K. Gray, R. Kampwirth, (ANL/MST), R. Ono, (Nat'l. Inst. of Stand. and Tech., Boulder, CO)
Nucl. Inst. and Methods A278, 425 (1989).

Granular-Aluminum Superconducting Detector for 6 KeV X-Rays and 2.2 MeV Beta Sources
A. Gabutti, R. Wagner (ANL/HEP); K. Gray, (ANL/MST); R. Ono, (Nat'l. Inst. Stand. and Tech., Boulder, CO)
Nucl. Inst. and Methods A289, 274 (1989).

Gravity and False Vacuum Decay Rates: O(3) Solutions
P. Arnold (ANL/HEP)
Nucl. Phys. B346, 160 (1990).

W and Z Production at Next-to-Leading Order: from large q_T to small
P. Arnold and R. Kauffman
Nucl. Phys. B349, 381 (1991).

Noether's Theorem for Local Gauge Transformations
D. Karatas, K. Kowalski (ANL/HEP)
Am. Jour. Phys. 58, Number 2 (1990).

Confinement and the Pomeron
A. White (ANL/HEP)
Proceedings of the Elastic and Diffractive Scattering Conference, Northwestern Univ.
Nucl. Phys. B12 (Proc. Suppl.) 190 (1990).

Hadron Collider Physics at Fermilab
L. Nodulman (ANL/HEP)
Proceedings of the International Europhysics Conference on High Energy Physics, Madrid, Spain, Nucl. Phys. B16 (Proc. Suppl.) 40 (1990).

Infinite Dimensional Algebras and A Trigonometric Basis for the Classical Lie Algebras
C. Zachos (ANL/HEP), D. Fairlie et al. (Univ. of Durham)
Jour. of Math. Phys. 31, 1088 (1990).

New Experimental Results for Intermediate- and High Energy Polarization Asymmetry
A. Yokosawa (ANL/HEP)
Int. Jour. of Mod. Phys. A, 5 (No. 16), 3089 (1990).

Multiparameter Associative Generalizations of Canonical Commutation Relations and Quantized Planes
D. B. Fairlie (Univ. of Durham) and C. K. Zachos (ANL/HEP)
Phys. Lett. 256B, 43 (1991).

Quantum Algebra Deforming Maps, Clebsch-Gordan Coefficients, Coproducts, U and R Matrices
C. Zachos (ANL/HEP), T.Curtright et al., (Univ. of Miami)
J. Math Phys. 32, 676 (1991).

Surface Underground Coincidences at the Soudan Mine
I. Ambats, D. Ayres, L. Balka, W. Barrett, J. Dawson, T. Fields, M. Goodman, N. Hill, D. Jankowski, F. Lopez, E. May, L. Price, J. Schlereth, J. Thron (ANL/HEP); U. Dasgupta et al. (Rutherford-Appleton Laboratory); D. Benjamin et al. (Tufts Univ.)
Proceedings of the 21st International Cosmic Ray Conference, (University of Adelaide, Australia, 1990), Vol. 9, p. 327.

Cosmic Ray Events in Soudan 2
I. Ambats, D. Ayres, L. Balka, W. Barrett, J. Dawson, T. Fields, M. Goodman, N. Hill, D. Jankowski, F. Lopez, E. May, L. Price, J. Schlereth, J. Thron (ANL/HEP); J. Kochocki et al, (Univ. of Minn.); W. Allison et al. (Rutherford-Appleton Laboratory); D. Benjamin et al. (Tufts Univ.)
Ibid, 9, 343 (1990).

Contained Events in Soudan 2
I. Ambats, D. Ayres, L. Balka, W. Barrett, J. Dawson, T. Fields, M. Goodman, N. Hill, D. Jankowski, F. Lopez, E. May, L. Price, J. Schlereth, J. Thron (ANL/HEP); P. Border et al. (Univ. of Minn.); W. Allison et al. (Univ. of Oxford); G. Alner et al. (Rutherford-Appleton Laboratory); D. Benjamin et al. (Tufts Univ.)
Ibid, 9, 378 (1990).

Underground Muon Observations in the Soudan 2 Detector
I. Ambats, D. Ayres, L. Balka, W. Barrett, J. Dawson, T. Fields, M. Goodman, N. Hill, D. Jankowski, F. Lopez, E. May, L. Price, J. Schlereth, J. Thron (ANL/HEP); P. Border et al. (Univ. of Minn.); W. Allison et al. (Univ. of Oxford); G. Alner et al. (Rutherford-Appleton Laboratory); D. Benjamin et al. (Tufts Univ.)
Ibid, 9, 406 (1990).

Studies of μ's Underground with the Soudan 2 Tracker
I. Ambats, D. Ayres, L. Balka, W. Barrett, J. Dawson, T. Fields, M. Goodman, N. Hill, D. Jankowski, F. Lopez, E. May, L. Price, J. Schlereth, J. Thron (ANL/HEP); J. Kochocki et al, (Univ. of Minn.); W. Allison et al. (Rutherford-Appleton Laboratory); D. Benjamin et al. (Tufts Univ.)
Ibid, 9, 409 (1990).

Underground Muons from the Direction of Cygnus X-3
D. Ayres, T. Fields, E. May and L. Price (ANL/HEP), K. Johns et al. (Univ. of Minn.)
Proceedings of the 24th International Conference on High Energy Physics, edited by R. Kothaus and J. Kuhn (Munich, West Germany, 1989), p. 24.

Experimental tests of Proton Spin Models
G. P. Ramsey (ANL/HEP/Loyola Univ.)
Proceedings of the IUCF Topical Conference on Physics with Polarized Beams on Polarized Targets, (World Scientific Publishing Company), edited by J. Sowinski and S. Vigdor (McCormick's Creek State Park, IN, 1989), p. 263.

Transverse Spin Observables in Chromodynamics
D. Sivers (ANL/HEP)
Ibid, 284 (1990).

Portable Parallel Programming in a Fortran Environment
E. May (ANL/HEP)
Proceedings of the 89' Conference on Computing in High Energy Physics, (North Holland Publishing Company), (New College, Oxford, UK, 1989), pp. 278-284.

The τ One-Prong Problem and Recent Measurements by the HRS Collaboration
J. Repond (ANL/HEP)
Proceedings of the 24th Recontre de Moriond on Electroweak Interactions and Unified Theories, (Centre National de la Recherche Scientifique and Commissariat a l'Energie Atomique, Les Arcs, France, 1989), p. 313.

Electron Identification in the CDF Central Calorimeter
J. Proudfoot (ANL/HEP) of the CDF Collaboration
Proceedings of the Workshop on Calorimetry for the Superconducting Supercollider, (University of Alabama, 1990), 1, p. 1.

New Infinite-Dimensional Algebras, Sine Brackets, and SU (∞)
C. Zachos (ANL/HEP), C. Fairlie (Univ. of Durham)
Proceedings of the String '89 Conference, (World Scientific Publishing Company), edited by R. Arnowitt et al. (College Station, TX, 1989).

Multi-Regge Theory and the Infra-Red Analysis of QCD
A. White (ANL/HEP)
Proceedings of the 32nd Semester of the Stefan Banach International Mathematical Center -- Gauge Theories of the Fundamental Interactions, (World Scientific Publishing Company), (Warsaw, Poland, 1990), p. 145.

The Soudan 2 Experiment
D. Ayres for the Soudan 2 Collaboration (ANL/HEP), University of Minnesota, Tufts University, Oxford University and Rutherford Laboratory
Proceedings of the 10th and Final Workshop on Grand Unification, (World Scientific Publishing Company), (University of North Carolina, Chapel Hill, North Carolina, 1989), p. 28.

Quantum Deformations
C. K. Zachos
Proceedings of Argonne Workshop on Quantum Algebras, (World Scientific Publishing Company), edited by T. Cartright et al., p. 62.

Quantum Maps for Deformed Algebras
C. Zachos (ANL/HEP)
Proceedings of the Rice Meeting of the APS, (World Scientific Publishing Company), edited by B. Bonner and H. Miettinen (Rice University, TX, 1990), p. 853.

New Physics Opportunities Possible with Polarized Beam in the Main Injector
D. G. Underwood (ANL/HEP)
Proceedings of Physics in the 1990's, (Breckenridge, Colorado, 1989), 1, p. 518.

Conceptual Design for a Superconducting Toroid
T. Fields
Proceedings of the International Workshop of SSC Solenoidal Detectors, (KEK Report 90-10, 1990), p. 435.

Wakefield Calculations on Parallel Computers
P. Schoessow (ANL/HEP)
Proceedings of the Workshop on Accelerator Computer Codes, (Los Alamos National Laboratory, Los Alamos, NM, 1990), p. 377.

Development of Radhard VLSI Electronics for SSC Calorimeters
J. Dawson, L. Nodulman (ANL/HEP)
Proceedings of the International Industrial Symposium on the Supercollider 1, (Hilton Riverside and Towers, New Orleans, LA, 1989), pp. 203-216.

B. Papers Submitted for Publication and ANL Reports

Measurements of $\Delta\sigma_T$(np) Between 500 and 800 MeV
M. Beddo, G. Burelson, J. Faucett, S. Gardiner, G. Kyle (New Mexico State); R. Garnett, D. Grosnick, D. Hill, K. Johnson, D. Lopiano, Y. Ohashi, et al. ANL-HEP-PR-90-116
Phys. Lett. B

Top Quark Backgrounds to Higgs $\rightarrow W^+W^-$
C. Yuan, R. Kauffman (ANL/HEP) ANL-HEP-PR-90-13
Phys. Rev. D.

Coulomb Interactions and Fermion Condensation
K. C. Wang ANL-HEP-PR-90-31
Phys. Rev. D

The W-Top Background to Heavy Higgs Production
G. A. Ladinsky and C. P. Yuan ANL-HEP-PR-90-60
Phys. Rev. D

Baryon Number Violation with New Improved Instantons
P. B. Arnold (ANL/HEP), M. P. Mattis (LANL) ANL-HEP-PR-90-78
Phys. Rev. Lett.

Analytic Multi-Regge Theory and the Pomeron in QCD--Part I
A. White (ANL/HEP) ANL-HEP-PR-90-28
Int. Jour. of Mod. Physics A

C. Papers or Abstracts Contributed to Conferences

Simulation Studies for Design Optimization of a Scintillator Plate Calorimeter
Presented by J. Proudfoot (ANL/HEP) (ANL-HEP-CP-90-88)
Symposium on Detector Research and Development for the Superconducting Supercollider, Ft. Worth, TX.

CALOR89 Calorimeter Simulation, Benchmarking and Design Calculations,
Presented by T. Handler, U. of Tennessee
Symposium on Detector Research and Development for the Superconducting Supercollider, Ft. Worth, TX.

Design of Readout Electronics for a Scintillating Plate Calorimeter
Presented by H. B. Crawley, Iowa State Univ.
Symposium on Detector Research and Development for the Superconducting Supercollider, Ft. Worth, TX.

First-Level Trigger Processor for the ZEUS Calorimeter
J. Dawson, R. Talaga, G. Burr, R. Laird (ANL/HEP), W. Smith et al. (Univ. of Wisconsin) ANL-HEP-CP-90-02
IEEE Trans. Nucl. Sci.

Choosing the Factorization/Renormalization Scale in Perturbative QCD Calculations
J. Collins ANL-HEP-CP-90-58
Proc. of Workshop on Hadron Structure Functions and Parton Dist., Batavia, IL 4/26-28/90.

Polarized Drell-Yan Experiments
J. Collins ANL-HEP-CP-90-52
Proc. of Workshop on Hadron Structure Functions and parton Dist., Batavia, IL 4/26-28/90.

Factorization at Small x
J. Collins ANL-HEP-CP-90-62
Proc. of DESY Topical Mtg. on Small x Behavior of Deep Inelastic Structure Functions in QCD, Hamburg W. Germany 5/14-16/90.

High Power, High Frequency Lasertron RF Sources
J. Norem, E. Chojnacki, and R. Konecny (ANL/HEP) ANL-HEP-CP-90-53
Proceedings of European Particle Accelerator Conference.

Believability of Signals from Cosmic Ray Souces
M. Goodman ANL-HEP-CP-90-118
Proceedings of the Michigan Gamma Ray Conference 1990.

Radhard Electronics Development Program for SSC Liquid-Argon Calorimeters
A.Stevens and J. Dawson (ANL/HEP), H. Kraner, V. Radeka, S. Rescia (BNL) ANL-HEP-CP-90-33
Supercollider 2, M. Mcasha, ed., Plenum, NY

Scientific Research in the Soviet Union
S. K. Mtingwa ANL-HEP-CP-90-51
National Society of Black Physicists 90' Conference Proceedings

QCD Thermodynamics with Light Quarks and Glueball Spectra with Dynamical Quarks
D. Sinclair ANL-HEP-CP-89-126
Proceedings of the Lattice `89 Conference, Capri, Italy, Sept. 18-21, 1989.

Is There a Hard Gluonic Contribution to the First Moment of g_1?
G. T. Bodwin and J. Qiu ANL-HEP-CP-90-125
Proceedings of the Polarized Collider Workshop, Penn State Univ., Nov. 15-17, 1990.

Progress in the Chemistry of Chromium (V) Doping Agents used in Polarized Target Materials
M. Krumpolc (Univ. of Ill. at Chicago); D. Hill (ANL); H. Stuhrmann (DESY-HASYLAB, Hamburg, Germany) ANL-HEP-CP-90-97
Proceedings (Springer-Verlag Series)

Hamiltonian Flows, SU(∞), SO(∞), USp(∞), and Strings
C. Zachos (ANL/HEP) ANL-HEP-CP-89-55
Proceedings of the XVIIIth International Conference on Physics and Geometry, Lake Tahoe, July 2-8, 1989. Edited by L. Chan and W. Nahm.

Jets, W's, and Z's at $\sqrt{s}$ = 1.8 TeV
S. Kuhlmann (ANL/HEP) and the CDF Collaboration ANL-HEP-CP-89-60
Proceedings of the XXIVth Rencontres de Moriond, Saclay Laboratory and Universite Paris, Sud, France, Les Arcs, Savoie, France, March 11-22, 1989.

Intermittency Study in e^+e^- Annihilations at 29 GeV
K. Sugano (ANL/HEP) ANL-HEP-CP-90-37
Proceedings of the Santa Fe Workshop on Intermittency in High Energy Collisions, Santa Fe, NM, March 18-22, 1990.

A New Approach to Chiral Fermions on the Lattice
G. Bodwin and E. Kovacs (Fermilab) ANL-HEP-CP-90-117
Proceedings of the Lattice '90 Symposium, Tallahassee, FL, Oct. 8-12, 1990.

Paradigms of Quantum Algebras
C. Zachos ANL-HEP-PR-90-61
Symmetries in Science V, B. Gruber (ed.), Plenum

Radiation Tolerance Implications for the Mechanical Design of A Scintillator Calorimeter for the SSC
J. Proudfoot ANL-HEP-CP-90-34
Proceedings of the Workshop on Radiation Hardness of Plastic Scintillator, Tallahassee, FL.

Scintillating Plate Calorimeter Mechanical Design
H. Spinka ANL-HEP-CP-90-92
Conference Proceedings

The Fermilab Polarized Beam Facility
D. P. Grosnick ANL-HEP-CP-90-103
Proceedings of the Workshop "Physics at UNK"

Recent Polarization Asymmetry Measurements at High and Medium Energies
A. Yokosawa ANL-HEP-CP-90-91
Proceedings of the 25th Int. Conf. on H.E.P., Singapore

Structures in the Nucleon-Nucleon System
A. Yokosawa ANL-HEP-CP-90-100
Proceedings of the 9th Int. Symp. on H.E. Spin Phys., Bonn

Experiments with Fermilab Polarized Proton and Antiproton Beams
A. Yokosawa ANL-HEP-CP-90-101
Proceedings of the 9th Int. Symp. on H.E. Spin Phys., Bonn

D. Technical Notes

AMZEUS-106	Test of BCAL Modules with Cosmic Rays J. Repond
ANL-HEP-TR-90-108	Report on Radiation Exposure of Lead-Scintillator Stack D. G. Underwood
CDF-1253	Measuring the Bottom Quark Cross Section Using the Inclusive Electrons J. Proudfoot, F. Ukegawa, A. B. Wicklund
CDF-1297	Photon Conversion Background in the Inclusive Electron Sample J. Proudfoot, F. Ukegawa, A. B. Wicklund
CDF-1299	Level-2 Central Electron Trigger Using CES/CPR F. Ukegawa, A. B. Wicklund
PDK-460	The Soudan 2 Honeycomb Calorimeter C. Garcia-Garcia
PDK-462	Soudan 2 Nucleon Decay Experiment Quarterly Activity Rept. (Oct./Dec 90) D. Ayres
PDK-463	Decisions of the U. K. Collaboration Meetings, January 24-30, 1991 D. Ayres, N. West
SDC-90-73	A First Simulation Study of the Barrel-Endcap Transition Region in a Calorimeter of the Scintillator Tile Design J. Proudfoot, H-J. Trost.
SDC-90-129	Matching Forward Toroids to a Central Solenoid T. Fields
SDC-90-139	Radiation Damage to Scintillator and Wavelength Shifter and the Resulting Effects on Calorimeter Performance, J. Proudfoot.
WF-158	Bremstrahlung Radiation Electrobeam Monitoring Systems (BREMS) J. Norem

VIII. COLLOQUIA AND CONFERENCE TALKS

D. Ayres

"Initial Data from the Soudan 2 Experiment"
25th I.C.H.E.P., Singapore (August 1990).

P. Arnold

"Baryon Number Violation in Standard Electroweak Theory"
1990 Annual UK Particle Physics Theory Meeting, Rutherford Laboratory, UK (December 1990).

E. Berger

"Spin Physics"
Summer Study on High Energy Physics, Snowmass, CO (July 1990).

"The Top Quark"
Virginia Polytechnic Institute and State University (November 1990).

"Particle Physics Opportunities and Facilities in the 1990's"
ANL High Energy Physics seminar (December 1990).

R. Blair

"Prompt Photon Production at CDF"
Singapore (August 1990).

G. Bodwin

"A New Approach to Chiral Fermions on the Lattice"
Cornell University, Laboratory of Nuclear Studies, Theory Group (September 1990).

"A New Approach to Chiral Fermions on the Lattice"
Lattice 90 Conference, Florida State University., Tallahassee, FL (October 1990).

"Is There a Hard Gluonic Contribution to the Proton's Spin-Dependent Structure Functions?"
Fermilab Theory Group (October 1990).

"Is There a Hard Gluonic Contribution to the First Moment of g_1?"
Polarized Collider Workshop, Penn State University, State College, PA (November 1990).

M. Derrick

"Comments on the Interaction between Theory and Experiment in High Energy Physics"
Oxford (July 1990).

T. Ekenberg

"Radiation Damage Testing of Transistors for SSC Front-End Electronics"
Symposium on Detector R&D for the SSC, Ft. Worth, TX (October 1990).
IEEE Nuclear Science Symposium, Arlington, VA (October 1990).

T. Fields

"Nuclear Rescattering of High Energy Partons"
ANL Physics Division Nuclear Physics Theory Institute (August 1990).

M. Goodman

"The Elusive Neutrino"
Ball State University (October 1990).

D. Grosnick

"The Fermilab Polarized Beam Facility"
Workshop "Physics at UNK", Protvino, USSR (September 1990).

R. Kauffman

"W and Z Production: From Large p_T to Small"
Argonne, High Energy Physics (October 1990)
University of Pennsylvania (November 1990)
SUNY @ Stony Brook (November 1990)
Brookhaven National Laboratory (November 1990)
University of Maryland (November 1990)
University of California, Berkeley (December 1990)
Stanford Linear Accelerator Center (December 1990)
University of Washington (December 1990).

E. May

"Parallel Computer System Benchmarking Methodology and Results"
SSC Laboratory (September 1990).

R. Meng

"Baryon Number Violation at High Energy Colliders"
Erice, Italy (September 1990).

"Monte Carlo Simulation at SSC"
Erice, Italy (September 1990).

S. Mtingwa

"Theory of the Dielectric and Anisotropic Ferrite Wakefield Acceleration of Charged Particles"
2nd Bouchet International Conference on Science and Technology (August 1990).

J. Norem

"The Argonne Wakefield Acceleration Program"
IHEP Beijing, China (November 1990).

"Wakefield Acceleration at Argonne"
KEK, Japan (November 1990).

L. Price

"Computing Requirements of SDC"
SSC Laboratory (September 1990).

"Recent Progress in Detector Simulation"
SSC R&D Symposium, Fort Worth (October 1990).

J. Repond

"Design, Construction and Test of the ZEUS Calorimeter"
Saclay, France (September 1990).

"Design and Construction of the ZEUS Barrel Calorimeter"
International Conference on Calorimetry in High Energy Physics, Fermilab (October 1990).

J. Simpson

"Wake Field Acceleration"
Linac Conference, Albuquerque, NM (September 1990).

D. Sivers

"Transverse Spin Observables in Hadron-Hadron and Hadron-Nucleus Collisions"
Polarized Collider Workshop, Penn State University (November 1990).

"Spin Observables for $\gamma D \rightarrow pn$ at Large Angles"
Nuclear and Particle Physics Workshop, Argonne (August 1990).

H. Spinka

"Conceptual Design for a Polarized Antiproton Beam"
TRIUMF, University of British Columbia, Vancouver, Canada (July 1990).

"Nucleon-Nucleon Scattering at Fermilab Energies"
TRIUMF, University of British columbia, Vancouver, Canada (July 1990).

"Scintillation Plate Calorimeter Mechanical Design"
Forth Worth, Texas, SSC Detector Symposium (October 1990).

"Mechanical Design for a Compensating Scintillator Plate Calorimeter Subsystem," Snowmass, CO (July 1990).

D. Underwood

"Partial Snakes of the First and Second Kinds and Numerical Searches for Snake Solutions"
Workshop on Siberian Snakes, Bonn, Germany (September 1990).

"Proposals for Experiments in Polarized Collisions"
Polarized Collider Workshop, Penn State University (November 1990).

A. White

"Hadronic Photons and Collider Diffractive Physics"
XXth International Symposium on Multiparticle Dynamics, Gut Holmecke, Germany (September 1990).

"A Collider Diffractive Threshold, Hadronic Photons and Sextet Quarks"
Diffraction Workshop, Fermilab (September 1990).

B. Wicklund

"B Physics at CDF"
Argonne (October 1990)
Cornell University (November 1990).

A. Yokosawa

"Experiments with Fermilab Polarized Proton and Antiproton Beams"
9th International Symposium on H.E. Spin Physics, Bonn, Germany (September 1990).

"Recent Results and Future Prospects for the Polarized Beam Program at Fermilab"
Polarized Collider Workshop, Penn State University (November 1990).

"High Energy Spin Physics"
ANL Physics Division Colloquium (November 1990).

C. Zachos

"Paradigms of Quantum Algebras"
Symmetries in Science V Symposium in Schloss Hofen, Vorarlberg, Austria (July 1990).

IX. HIGH ENERGY PHYSICS COMMUNITY ACTIVITIES

E. Berger

Chairman, Executive Committee, Division of Particles and Fields, American Physical Society, 1990.

Fellowship Committee Chairman, Division of Particles and Fields, American Physical Society, 1990, 1991.

Chairman, Organizing Committee, 1990 Summer Study on High Energy Physics, "Research Directions for the Decade", Snowmass, CO, June 25 - July 13, 1990.

International Advisory Committee, 1991 General Meeting of the Division of Particles and Fields, University of British Columbia, Vancouver, Canada, August 1991.

Advisory Committee, Polarized Collider Workshop, Pennsylvania State University, November 15-17, 1990.

Scientific Program Committee, XXVI Recontre de Moriond, "High Energy Hadronic Interactions", Les Arcs, France, March 1991.

Parallel Session Coordinator, Fourth Conference on the Intersections between Particle and Nuclear Physics, Tucson, Arizona, May 1991.

Member, Texas National Research Laboratory Commission's Research and Development Review Subpanel, 1990-1991.

Member, Committee on Meetings, American Physical Society, 1990-1992.

Scientific Advisory Board, Hadron '91, University of Maryland, August 12-16, 1991.

International Advisory Committee, DPF Meeting, Fermilab, October 1992.

M. Derrick

Member, Organizing Committee of International Conference on Calorimetry in High Energy Physics, October 1990.

T. Fields

Organized Symposium on Superconducting Toroid Design at Ft. Worth SSC Detector Conference, October 1990.

T. Kirk

Program Chairman, IISSC '91.
Institutional Board Chairman, SDC.
Vice-Chair, Director's Ad Hoc Committee on ATLAS Safety.
Chairman, SDC Panel on Magnet Type Selection.

E. May

Member, HEPNET Technical Coordinating Committee.

L. Nodulman

Subgroup Leader for Top Quark, Snowmass.

L. Price

Executive Committee of Users Organization of the SSC (Secretary).
SSC Detector R&D Committee.
SSC Computer Policy Committee.
SSC Computer Acquisition Committee.
ESNET Steering Committee.
SDC Executive Board (Vice Chair).
SDC Computing Technical Steering Committee (Co-Chair).
SDC Physics and Detector Performance Technical Steering Committee (Co-Chair).

D. Sivers

Co-organizer, ANL Nuclear and Particle Theory Workshop with H. Lee (Physics).
Advisory Committee - Polarized Collider Workshop.

H. Spinka

LAMPF board of Directors.
Session Organizer for 4th Conference on the Intersection between Particle and Nuclear Physics.

B. Wicklund

Physics in Collision Conference (1991).
DPF Meeting at Fermilab (1992).

A. Yokosawa

Advisory Committee, Polarized Collider Workshop at Penn State University.

X. HIGH ENERGY PHYSICS RESEARCH PERSONNEL

Accelerator Physicists

S. Mtingwa
J. Norem
J. Rosenzweig
M. Rosing
P. Schoessow
J. Simpson

Experimental Physicists

D. Ayres
R. Blair
M. Derrick
T. Fields
A. Gabutti
R. Garnett
M. Goodman
W. Gai
D. Grosnick
R. Hagstrom
P. Job
S. Kuhlmann
F. Lopez
D. Lopiano
E. May
B. Musgrave
L. Nodulman
Y. Ohashi
L. Price
J. Proudfoot
J. Repond
T. Shima
H. Spinka
R. Stanek
K. Sugano
R. Talaga
J. Thron
H.-J. Trost
D. Underwood
R. Wagner
A. B. Wicklund
A. Yokosawa

Theoretical Physicists

P. Arnold
E. Berger
G. Bodwin
R. Kauffman
R. Meng
D. Sinclair
D. Sivers
S. Vokos
A. White
C. P. Yuan
C. Zachos

Engineers, Computer Scientists and Applied Scientists

A. Buehring
E. Chojnacki
J. Dawson
D. Hill
N. Hill
R. Noland
H. Rhude
J. Schlereth
A. Stevens
W. Wang

Technical Support Staff

I. Ambats
L. Balka
J. Biggs
H. Blair
W. Haberichter
D. Jankowski
T. Kasprzyk
R. Konecny
R. Laird
R. Miller
R. Rezmer
J. Sheppard

Laboratory Graduate Participants

W. Graves
C. Ho
D. Keubel
M. Pundurs
F. Ukegawa